Separation Science and Technology
Publication details, including instructions for authors and subscription information:
http://www.informaworld.com/smpp/title~content=t713708471

State-of-the-art Adsorption and Membrane Separation Processes for Carbon Dioxide Production from Carbon Dioxide Emitting Industries

Armin D. Ebner[a]; James A. Ritter[a]
[a] Department of Chemical Engineering, Swearingen Engineering Center, University of South Carolina, Columbia, SC, USA

To cite this Article Ebner, Armin D. and Ritter, James A.(2009) 'State-of-the-art Adsorption and Membrane Separation Processes for Carbon Dioxide Production from Carbon Dioxide Emitting Industries', Separation Science and Technology, 44: 6, 1273 — 1421
To link to this Article: DOI: 10.1080/01496390902733314
URL: http://dx.doi.org/10.1080/01496390902733314

Separation Science and Technology, 44: 1273–1421, 2009

ISSN: 0149-6395 print/1520-5754 online
DOI: 10.1080/01496390902733314

Taylor & Francis
Taylor & Francis Group

State-of-the-Art Adsorption and Membrane Separation Processes for Carbon Dioxide Production from Carbon Dioxide Emitting Industries

Armin D. Ebner and James A. Ritter
Department of Chemical Engineering, Swearingen Engineering Center, University of South Carolina, Columbia, SC, USA

Abstract: With the growing concern about global warming placing greater demands on improving energy efficiency and reducing CO_2 emissions, the need for improving the energy intensive, separation processes involving CO_2 is well recognized. The US Department of Energy estimates that the separation of CO_2 represents 75% of the cost associated with its separation, storage, transport, and sequestration operations. Hence, energy efficient, CO_2 separation technologies with improved economics are needed for industrial processing and for future options to capture and concentrate CO_2 for reuse or sequestration. The overall goal of this review is to foster the development of new adsorption and membrane technologies to improve manufacturing efficiency and reduce CO_2 emissions. This study focuses on the power, petrochemical, and other CO_2 emitting industries, and provides a detailed review of the current commercial CO_2 separation technologies, i.e., absorption, adsorption, membrane, and cryogenic, an overview of the emerging adsorption and membrane technologies for CO_2 separation, and both near and long term recommendations for future research on adsorption and membrane technologies. Flow sheets of the principal CO_2 producing processes are provided for guidance and new conceptual flow sheets with ideas on the placement of CO_2 separations technologies have also been devised.

Received 1 September 2008; accepted 22 October 2008.
Address correspondence to James A. Ritter, Department of Chemical Engineering, Swearingen Engineering Center, University of South Carolina, Columbia, SC 29208, USA. Tel.: (803) 777-3590; Fax: (803) 777-8265. E-mail: ritter@cec.sc.edu

Keywords: Absorption processes, adsorbents, adsorption processes, carbon dioxide capture, chemical process industries, cryogenic processes, gas separation, membrane processes, membranes

INTRODUCTION

Carbon dioxide production and emissions are ubiquitous with combustion, energy generation, and manufacturing. Some CO_2 is produced as a byproduct of chemical manufacturing, while most is produced in the generation of power through the combustion of fossil fuels. The growing concern about global warming is placing greater demands on improving the energy efficiency of processes and on reducing CO_2 emissions. The US Department of Energy has shown that the separation of CO_2 represents 75% of the cost associated with its separation, storage, transport, and sequestration operations. Hence, the underlying economic and environmental drivers are encouraging the development of more energy efficient CO_2 separation technologies. With both adsorption and membrane technologies classified as low energy separation processes, the overall goal of this review is to foster the development of new adsorption and membrane processes for CO_2 separation.

While reading this reveiw, it is recommended to keep in mind the following questions: What are the generic technologies with the most promise? What are the high level technical issues to be overcome to commercialize a new CO_2 separation technology, e.g., a new membrane process (such as costs and sulfur tolerance, etc.)? What is the estimated time of development for a new commercial application without additional action? What will it take to deliver a new commercial application in 3–5 years? What will it take to accelerate these developments? What breakthroughs, if any, are needed to accelerate these developments? These questions or guidelines provide for overall focus and direction. However, direct answers to these questions are not offered here, as they depend on specific applications. Instead, this review provides specific recommendations for improving adsorption and membrane technologies for CO_2 separation to meet the CO_2 separation challenge.

The objective of this review, while focusing exclusively on the CO_2 emitting industries, is to provide a detailed review of the current commercial CO_2 separation technologies, i.e., absorption, adsorption, membrane, and cryogenic, an overview of the emerging adsorption and membrane technologies for CO_2 separation, and both near and long term recommendations for future research on adsorption and membrane technologies. Flow sheets of the principal CO_2 producing processes are also provided for guidance, and new conceptual flow sheets with ideas on the placement of CO_2 separations technologies have been devised.

CURRENT COMMERCIAL PRACTICES

This section provides an overview of the CO_2 production processes. More details on these processes are also provided in the appendix. This section also reviews the four most widely used commercial CO_2 removal processes, i.e., absorption, adsorption, membrane, and cryogenic processes.

There are three incentives to remove CO_2 from a process stream. First, and in most cases, CO_2 is being removed from a valuable product gas, such as H_2, where it is eventually emitted to the atmosphere as a waste by-product. Second, CO_2 is recovered from a process gas, such as in ethanol production, as a saleable product. However, only a modest fraction of the CO_2 produced is marketed as a saleable product; and much of this CO_2 finds its way to the atmosphere because the end use does not consume the CO_2. Third, CO_2 is recovered simply to prevent it from being released into the atmosphere; but, this necessarily requires sequestration of the recovered CO_2. To date, there is little if any use of commercially available CO_2 capture processes for this purpose. At the moment these processes are simply too expensive to use, and in most cases there is no place to put the CO_2 once it is captured.

Processes to remove CO_2 from gas streams vary from a simple once-through wash or treatment operation to complex multistep recycle systems. Most of these processes were developed for natural gas sweetening or H_2 recovery from syngas. Recently, interest has built on the capture of CO_2 from flue gas, and even landfill gas and coal bed methane gas. Natural gas, flue gas, landfill gas, and coal bed methane gas systems are more complex than the typical H_2 system. Along with CO_2, other contaminants generally must be removed or handled. Among these are particulates, H_2O, N_2, H_2S, C_{2+} hydrocarbons, and trace elements in various oxidation states. In addition, flue gas, coal bed methane, and some landfill gases contain O_2 that can interfere with certain CO_2 separation systems. This complication is generally not present in natural gas, most landfill gas, or H_2 systems. For these reasons, commercial CO_2 gas treatment plants are usually integrated gas processing systems; few are designed simply for CO_2 removal.

Four different CO_2 removal technologies are widely practiced in industry. These include

1. absorption, both chemical and physical,
2. adsorption,
3. membranes, and
4. cryogenic processes (1).

Tables 1 and 2 provide information on CO_2 removal technologies in terms of the number of patents and/or peer-reviewed articles published by a company or research team from 1995 to 2005, and then from 2002 to 2005 to determine more recent activity. Table 3 lists the licensors of CO_2 separation processes as of 2004 (2).

Absorption Processes

The overwhelming majority of CO_2 removal processes in the CO_2 emitting industries take place by absorption in the petrochemical industry (see Table 3). The chemical process industries (CPIs) remove CO_2 to meet process or product requirements, e.g., the production of natural gas requires the removal of CO_2 in order to be effectively utilized. Other examples include the removal of CO_2 from the circulating gas stream in ammonia manufacture or ethylene oxide manufacture.

A variety of liquid absorbents are being used to remove CO_2 from gas streams. Absorption processes generally can be divided into two categories. Processes where the solvent chemically reacts with the dissolved gas are referred to as chemical absorption processes. For these applications alkanolamines are commonly used as reactive absorbents.

Physical absorption processes are processes where the solvent only interacts physically with the dissolved gas. Here a solvent is used as an absorbent with thermodynamic properties such that the relative absorption of CO_2 is favored over the other components of the gas mixture. Some commonly used physical solvents are methanol (Rectisol Process) and glycol ethers (Selexol Process).

In many industrial applications, combinations of physical solvents and reactive absorbents may be used in tandem. Table 4 lists the most widely used absorbents. These include monoethanolamine (MEA), diethanolamine (DEA), diisopropanolamine (DIPA), methyldiethanolamine (MDEA), and diglycolamine (DGA). Ammonia and alkaline salt solutions are also used as absorbents for CO_2. However, in all cases solvent recycling is energy and capital intensive.

Table 4 and and also Table 5 compare key properties of some of the important alkanolamines used in acid gas treating. Ethanolamine has the highest capacity and the lowest molecular weight. It offers the highest removal capacity on either a unit weight or unit volume basis.

Table 5 also lists the major types of CO_2 and acid gas absorption processes that are commonly used in gas treating. Of the CO_2 producing processes listed above, only natural gas production, H_2, syngas, and NH_3 production, and coal gasification utilize absorption processes for removing CO_2 and or acid gases. As far as the authors are aware the use of CO_2

Table 1. Number of patents (P) and peer review manuscripts (M) per researcher or research group on CO_2 related separation processes since 1995 and since 2002 (in parentheses)

		Membrane		Membrane process		Adsorption		Absorption		Other	
Main investigator	Company or institution	P	M	P	M	P	M	P	M	P	M
Katsuki Kusakabe, Shigeharu Morooka	Kyushu Sangyo University, Japan	0(0)	35(9)								
Tai S Chung and Rong Wang	National U. of Singapore, Nanyang Technological U., Singapore	1(1)	37(29)								
William J. Koros	Georgia Institute of Technology, USA	8(8)	42(22)	2(1)	0(0)						
Ken-ichi Okamoto, Hidetoshi Kita	Yamaguchi University, Japan	1(0)	31(25)								
Richard D. Noble and John L. Falconer	University of Colorado, USA	3(0)	29(13)								
Kenji Haraya	National Institute of Advanced Industrial Science and Technology, Japan	1(0)	15(6)								
Hiroyoshi Kawakami	Tokyo Metropolitan University, Japan	1(0)	26(6)								
Akira Miyamoto, Momoji Kubo	Tohoku University, Japan	0(0)	8(1)								
Matthias Wessling	U. of Twente, the Netherlands	1(1)	23(16)								

(*Continued*)

Table 1. Continued

Main investigator	Company or institution	Membrane		Membrane process		Adsorption		Absorption		Other	
		P	M	P	M	P	M	P	M	P	M
Richard W. Baker, Ingo Pinnau	Membrane Tech. & Research, Inc., USA	7(4)	14(4)	12(5)	3(1)						
Stephen J. Miller, Curtis L. Munson, De Q. Vu	Chevron USA Inc., USA	9(9)	6(6)	2(2)	1(1)	2(2)	3(3)	3(3)	0(0)		
Benny D. Freeman	U. of Texas, USA	0(0)	43(11)								
William D. Dolan	Engelhard Corporation, USA	5(5)	2(2)								
Raymond Clarke	Landec Corporation, USA	4(2)	2(1)								
John W. Simmons	L'air Liquide, France	5(5)	0(0)								
Santi Kulprathipanja	UOP LLC, USA	2(2)	1(1)								
David J. Hasse, Sudhir S. Kulkarni	L'air Liquide, France	4(4)	2(0)								
Harry W. Deckman, Donald J. Victory, Eugene R. Thomas	Exxon Mobil, USA	3(3)	0(0)			1(1)	0(0)				
Benjamin Bikson, Joice K. Nelson, Yong Ding	Praxair Technology, Inc., USA	6(2)	0(0)								
Gilles P. Robertson, Michael D. Guiver	Institute for Chemical Process and Environmental Technology, Canada	1(1)	10(8)								
Hisao Hachisuka, Tomomi Ohara, Ken-Ichi Ikeda	Nitto Denko Corporation, Japan	0(0)	5(0)								

Nikunj P. Patel, Richard J. Spontak	North Carolina State University, USA	0(0)	8(6)						
Liang Hu	Hampton University, USA	1(1)	6(4)						
Eva Marand	Virginia Polytechnic I. and State U., USA	1(1)	9(6)						
Yong S. Kang	Korea I. of Science and Tech., South Korea	3(2)	2(1)						
Shigeo T. Oyama	Virginia Polytechnic I. and State U., USA	1(1)	12(7)						
Anthony M. Sammels	Eltron Research Inc., USA	2(1)	2(2)	1(0)	2(1)				
S. Alexander Stern	Gas Research Institute, USA	0(0)	8(0)						
Shivaji Sircar, Jeffrey R. Hufton, Madhukar B. Rao	Air Products and Chemicals, Inc., USA	2(0)	0(0)	3(0)	2(0)	7(0)	5(0)		
Charles L. Anderson	L'Air Liquide, France	2(2)	0(0)						
WH Winston Ho	ExxonMobil, USA	4(0)	0(0)					9(0)	5(0)
Ravi Prasad, Frank Notaro	Praxair Technology, Inc., USA	1(1)	0(0)			4(1)	0(0)		
George P. Sakellaropoulos	Aristotle Univ Thessaloniki, Greece	1(0)	1(1)	0(0)	3(2)	0(0)	8(2)		
Kang Li, Wah K. Teo, Dongliang Wang	National University of Singapore, Singapore	1(0)	10(1)						
Takeshi Matsuura	U. of Ottawa, Canada	1(0)	19(6)						
Gilbert M. Rios, Stephane Sarrade	I. Europeen des Membranes-UM2, France	0(0)	12(6)						
Tsutomu Nakagawa	Meiji University, Japan	0(0)	21(3)						

(*Continued*)

Table 1. Continued

Main investigator	Company or institution	Membrane		Membrane process		Adsorption		Absorption		Other	
		P	M	P	M	P	M	P	M	P	M
Theodore T. Tsotsis	U. of Southern California, USA	0(0)	13(5)	0(0)	3(1)						
Antonio B. Fuertes, Teresa A. Centeno	Instituto Nacional del Carbon, Spain	0(0)	11(2)								
A. F. Ismail	U. Teknologi Malaysia, Malaysia	0(0)	9(4)								
Ho Bum Park, Young Moo Lee	Hanyang University, South Korea	0(0)	19(16)								
S. Ted Oyama	Virginia Polytechnic Institute and State University, USA	2(1)	9(5)								
Zhi Kang Xu	Zhejiang University, China	0(0)	10(4)							0(0)	2(2)[a]
Enrico Drioli	U. of Calabria, Italy	0(0)	20(12)								
Yong Soo Kang	Korea I. of Science and Tech., South Korea	5(4)	15(6)								
Ricardo AF Machado	U. Federal de Santa Catarina, Brazil	0(0)	6(5)								
Henk Verweij	U. of Twente, the Netherlands	0(0)	5(2)								
Daniele Fiaschi	U. degli Studi di Firenze, Italy	0(0)	5(4)								
Jose Sanchez	Institut Europeen des Membranes, France	0(0)	15(6)							0(0)	1(1)[a]
Kamalesh K. Sirkar	New Jersey Institute of Technology, USA			0(0)	3(1)					3(1)	14(3)[b]

Tomonori Takahashi, Hitoshi Sakai, Toshihiro Tomita	NGK insulators, Japan	4(0)	2(2)		
Paul A. Daus, Charles R. Pauley	Messer Griesheim Industries, Inc., Germany	3(0)	0(0)		
Sawas Vasileiadis	Ivatech Corporation, USA	2(1)	2(0)		
Ralph T. Yang	U. of Michigan, USA			1(0)	19(6)
Tsutomu Hirose, Monotobu Goto	Kumamoto University, Japan			0(0)	18(4)
Chang Ha Lee	Yonsei University, South Korea			0(0)	19(8)
Angel Linares, Diego Cazorla	U. de Alicante, Spain			0(0)	29(14)
Isao Mochida	Kyushu University, Japan			0(0)	12(2)
Alirio E. Rodrigues	U. de Oporto, Portugal			0(0)	16(9)
James A. Ritter	U. of South Carolina, USA			0(0)	5(1)
Jia Guo, Aik C Lua	Fudan University, China			0(0)	12(6)
Juan M. D. Tascon, Amelia Martinez, Silvia Villar Rodil	Instituto Nacional del Carbon, Spain			0(0)	30(21)
Jose Ortiga, Cristina Volzone	Centro de Tecnologia de Recursos Minerales y Ceramica, Argentina			0(0)	5(2)
F. Handan Tezel	U. of Ottawa, Canada			0(0)	10(4)
Kenzi Suzuki	Agency of Industrial Sci. & Tech, Japan			0(2)	7(0)

(*Continued*)

Table 1. Continued

Main investigator	Company or institution	Membrane		Membrane process		Adsorption		Absorption		Other	
		P	M	P	M	P	M	P	M	P	M
Martin Bulow	The BOC group, Inc., USA					3(12)	7(5)				
Ravi Kumar	The BOC group, Inc., USA					4(13)	2(1)				
Akhilesh Kapoor	The BOC group, Inc., USA					0(8)	0(0)	1(0)	0(0)		
Ravi Jain	The BOC group, Inc., USA					0(7)	0(0)				
Mohamed S. A. Baksh	Praxair Technology, Inc., USA					2(4)	0(0)				
Roger D. Whitley, Robert L. Chiang	Air Products and Chemicals, Inc., USA					4(4)	0(0)				
Norberto O. Lemcoff, Divyanshu R. Acharya	The BOC group, Inc., Canada					2(5)	3(1)				
Bowie G. Keefer	Questair Technologies, Inc., Canada					6(9)	0(0)				
Amitabh Gupta, Shrikar Chakravarti	Praxair Technology, Inc., USA					1(1)	0(0)	6(1)	0(0)		
Timothy C. Golden	Air Products and Chemicals, Inc, USA					11(28)	1(0)				
Hans H. Funkel, Dan Fraenkel	Matheson Tri-Gas, Inc., USA					6(7)	1(1)				
Richard K. Lyon	General Electric Co., USA					5(5)	4(0)				
Omar M. Yaghi	U. of Michigan, USA					4(5)	15(8)				
Robert S. Wegeng	Battelle Memorial Institute, USA					2(2)	0(0)				

Alan Mather	U. Alberta, Canada	0(0)	18(2)
SangWook Park	Korean I. of Chemical Engineers, Korea	0(0)	16(16)
Gary T. Rochelle	University of Texas, USA	2(2)	15(10)
Syamalendu S. Bandyopadhyay	Indian I. of Technology, India	0(0)	14(13)
Menghui Li	Chung Yuan Christian University, Taiwan	0(0)	13(6)
Helmuth Sigel	U Basel, Switzerland	0(0)	13(6)
Fumio Kiyono	Agency of Industrial Sci. & Tech., Japan	1(0)	5(5)
Arturo Trejo	Instituto Mexicano de Petroleo, Mexico	1(0)	9(5)
Mohamed K. Aroua	U. Malaya, Malaysia	0(0)	7(4)
Gerd Maurer	U. of Kaiserslautern, Germany	0(0)	8(5)
Orville C. Sandall	U. California Santa Barbara, USA	0(0)	8(0)
Hallvard F. Svendsen	Norwegian I. Science and Tech., Norway	0(0)	8(7)
Takayuki Saito	Nat. Institute for Res. & Environ, Japan	2(0)	8(1)
Masaki Iijima, Kazuto Kobayashi, Kazuhiro Morita, Shigeaki Mitsuoka	Mitsubishi Heavy Industries, Japan	19(10)	8(1)
Paul L. Wallace	Texaco Development Corp., USA	3(1)	0(0)

(*Continued*)

Table 1. Continued

Main investigator	Company or institution	Membrane		Membrane process		Adsorption		Absorption		Other	
		P	M	P	M	P	M	P	M	P	M
Tofik K. Khanmamedov	TKK Company, USA							3(1)	1(1)		
Guido Sartori	ExxonMobil, USA							23(0)	1(0)		
Bernt H. Torkildsen, Martin Sigmundstad, Harald Linga, Patrick Finn	Den Norske Stats Oljieselskap A.S., Norway							7(0)	0(0)		
James E. Critchfield	Hunstmann Petrochemical Corp., USA							2(0)	1(0)		
Jerry D. Blue	Alliance, USA							3(1)	0(0)		
Fabrice Lecomte	Institut Francais du Petrole, France							3(3)	3(2)		
Gary Palmer	USA							2(2)	0(0)		
John Mak	Fluor Corporation, USA							7(7)	2(2)		
Paolo Chiesa	Politecnico di Milano, Italy							0(0)	5(1)		
Masahiro Kato	Toshiba Corporation, Japan							0(0)	12(4)		
Paitoon Tontiwachwuthikul, Amornvadee Veawab Raphael Idem	U. of Regina, Canada							0(0)	30(18)		
Syamalendus S. Bandyopadhyay	Indian Institute of Technology, India							0(0)	5(2)		

ChengFang Zhang	Shanghai Jiaotong University, China	0(0)	8(4)		
Dwain F. Spencer	USA	7(1)	5(2)		
Frederic Dutil	CO_2 solution, Inc., Canada	7(7)	0(0)		
Joan F. Brennecke	U. of Notre Dame, USA	0(0)	37(14)	1(1)	0(0)[b]
Satish Reddy	Fluor Corporation, USA	0(0)	1(1)	4(2)	0(0)[c]
Geert F. Versteeg, Vishwas Y. Dindore	Institute for Kjemisk Process teknologi, Norway	1(1)	11(7)	0(0)	8(8)[a]
Robert Quinn	Air products and Chemicals, Inc., USA	0(1)	6(1)	0(0)	6(1)[b]
Hideto Matsuyama, Masaaki Teramoto	Kyoto Institute of Technology, Japan			0(0)	17(4)[a,b]
Kew-Ho Lee, You-In park	Korea Research I. of Chemical Tech., South Korea			0(0)	18(11)[a,b]
Zhi Wang	Tianjin University, China			0(0)	15(9)[b]
Paul HM Feron	TNO Institute of Environmental Sciences, The Netherlands			2(1)	16(10)[a]
Zoher M. Meratla	CDS Research Ltd.,USA			1(0)	2(0)[d]
Olav Falk-Pedersen	Kvaerner ASA, Norway			2(0)	8(4)[a]
Fawzy T. Abdelmalek	Abdelmalek & Associates, Inc., USA			4(0)	1(0)[c]

[a]Membrane contactors.
[b]Immobilized liquid and facilitated transport membranes.
[c]Autorefrigeration and liquefaction.
[d]Cryogenic separation.

Table 2. Number of patents per company on CO_2 related separation processes since 1995 and since 2002 (in parentheses)

Company	Membrane	Adsorption	Absorption
Air Products and Chemicals, Inc., USA	11(3)	51(18)	5(2)
The BOC group, Inc., USA	3(1)	49(15)	5(2)
Praxair Technology, Inc., USA	23(7)	24(9)	10(2)
ExxonMobil, USA	10(4)	2(2)	28(1)
UOP LLC, USA	7(3)	17(5)	2(0)
Membrane Technology and Research, Inc., USA	23(9)		
Mitsubishi Heavy Industries, Japan	1(1)	2(1)	19(10)
L'Air Liquide, France	11(5)	7(3)	2(0)
Chevron USA Inc., USA	9(9)	3(3)	5(5)
Shell Internationale Research, The Netherlands	4(2)	3(2)	8(7)
Battelle Memorial Institute, USA	4(3)	4(3)	4(3)
DSM N V, The Netherlands			13(8)
Fluor Corporation, USA		4(3)	8(7)
E.I. Du Pont de Nemours and Company, USA	5(0)	1(0)	5(1)
Engelhard Corporation, USA	6(6)	4(4)	
General Electric Co., USA	2(2)	5(5)	3(2)
Norsk hydro ASA, Norway	6(1)		3(0)
Questair Technologies, Inc., Canada		9(6)	
Den Norske Stats Oljieselskap A.S., Norway	2(0)		7(0)
Hamilton Sundstrand Corporation, USA	2(2)	4(4)	2(2)
Texaco Development Corp., USA	3(0)		4(1)
Kvaerner ASA, Norway	4(1)		3(0)
Matheson Tri-Gas, Inc., USA		7(6)	
DOW/Corning Corp, USA		3(0)	4(0)
Messer Griesheim Industries, Inc.	3(0)	1(0)	2(0)
Agency of Industrial Sci. & Tech, Japan	1(0)	3(0)	2(0)
Korea Institute of Science and Technology, South Korea	4(3)	2(1)	

(*Continued*)

Table 2. Continued

Company	Membrane	Adsorption	Absorption
Conoco/Phillips, USA	2(2)	2(1)	1(1)
Honeywell International Inc, USA	1(0)	3(2)	
Hunstmann Petrochemical Corporation, USA		1(2)	0(2)
BP-Amoco, UK-USA	4(2)		4(3)
Union Carbide, USA			4(1)
Institut Francais du Petrole, France		1(1)	3(3)
Landec Corporation, USA	3(2)		

scrubbers for the production of CO_2 from iron and steel, cement, lime, aluminum, and from combustion is virtually non-existent.

Natural gas is treated to remove the acid gas constituents (H_2S and CO_2) by contacting the natural gas with an alkaline liquid. The most commonly used treating solutions are aqueous solutions of the ethanolamines or alkali carbonates, although a considerable number of other treating agents have been developed in recent years, as illustrated in Tables 3 to 5. Most of the newer treating agents rely on a combination of physical absorption and chemical reaction. When only CO_2 is to be removed in large quantities, or when only partial removal is necessary, a hot carbonate solution or one of the physical solvents is economical preferred.

MEA has good thermal stability, but reacts irreversibly with COS and CS_2. In addition to the main desired, readily reversible product, ammonium bicarbonate, MEA also reacts with CO_2 to give a series of products that lead to slow losses of this alkanolamine. More serious is the MEA loss by evaporation. Its vapor pressure is much higher that those of the other compounds in Table 4. Thus, using MEA to meet pipeline specifications for H_2S may be difficult.

Diethanolamine has a lower capacity than MEA and it reacts more slowly. Although its reactions with COS and CS_2 are slower, they lead to different products that cause fewer filtration and plugging problems. Triethanolamine has been almost completely replaced in sour gas treating because of its low reactivity toward H_2S. Diglycolamine has the same reactivity and capacity as DEA, with a lower vapor pressure and lower evaporation losses.

Diisopropanolamine (DIPA) is used in the Sulfinol and Shell Adip processes to treat gas to pipeline specifications. DIPA can remove COS

Table 3. Licensors of CO_2 separation processes, type of process, production rate, and number of plants worldwide (467)

Licensor	System	Primary goal		CO_2 in tailgas	Capacity/unit	Plants worldwide
Linde AG	PSA-H_2	H_2	(P)	30–60%	1–100 MMscfd	250
Technip	PSA-H_2	H_2	(P)	30–60%	–	240
Uhde	PSA-H_2	H_2	(P)	30–60%	−110 MMscfd	60
Haldor Topsøe A/S	PSA-H_2	H_2	(P)	30–60%	−20 MMscfd	31
UOP LLC (Polybed)	PSA-H_2	H_2	(P)	30–60%	−200 MMscfd	700
CB & I Howe-Baker	PSA-H_2	H_2	(P)	30–60%	1–280 MMscfd	170
Foster Wheeler	PSA-H_2	H_2	(P)	30–60%	1–95 MMscfd	100
Lurgi Oel-Gas-Chemie GmbH	PSA-H_2	H_2	(P)	30–60%	1–200 MMscfd	105
Air Products (PRISM)	PSA-H_2	H_2	(P)	30–60%	15–120 MMscfd	50
Linde AG	PSA-NH_3	H_2	(P)	30–60%	230–1350 mtpd	3
Uhde Gmbh	PSA-NH_3	H_2	(P)	30–60%	500–1800 mtpd	14
Haldor Topsøe	PSA-NH_3	H_2	(P)	30–60%	650–2050 mtpd	60
Kellogg Brown & Root, Inc	PSA-NH_3	H_2	(P)	30–60%	−1850 mtpd	200
Engelhard Corp. (Molecular Gate^{TM})	Adsorption	CO_2, H_2O	(R)	1–98%	2–10 MMscfd	2
Axens	Adsorption	GC+CO_2	(R)	1–98%	–	60
ProPure As (CAP-compact)	Scrub (MDEA)	H_2S	(R)	–	–	2
Shell Global Solutions International B.V (ADIP)	Scrub (MDEA, DIPA)	AG	(R)	1–98%	–	400
Shell Global Solutions International B.V (ADIP-X)	Scrub (MDEA)	AG	(R)	1–98%	–	1
Prosernat-IFP Group Tech. (Advanced Amines)	Scrub (DEA, MDEA)	AG	(R)	1–98%	0.3–25.2 Nm^3/d	120
BASF AG (aMDEA)	Scrub (MDEA)	AG	(R)	1–98%	3.5–700 MMscfd	230
UOP LLC (Amine Guard FS)	Scrub (amine)	AG	(R)	1–98%	−500 MMscfd	500

Prosernat IFP & Titan SNC Lavalin (ifpex-2)	Scrub (Methanol)	AG	(R)	1–98%	−350 MMscfd	–
UOP LLC (Benfield)	Scrub (DEA-K_2CO_3)	AG	(R)	1–98%	−500 MMscfd	700
Randall gas Tech, ABB Lummus Global Inc.	Scrub (MEA)	AG	(R)	1–98%	2700 mtpd	8
Exxon Mobil Research & Eng. Co. (FlEXSORB)	Scrub (amine)	AG	(R)	1–98%	–	49
Fluor Enterprises, Inc. (Econamine)	Scrub (DGA)	CO_2	(R)	+99%	3–400 MMscfd	55
Fluor Enterprises, Inc. (Econamine FG Plus)	Scrub (MEA)	CO_2	(R)	+99%	−300 mtpd	24
Fluor Enterprises, Inc. (Improved Econamine)	Scrub (DGA)	CO_2	(R)	+99%	547 MMscfd	7
Fluor Enterprises, Inc. (Fluor Solvent)	Scrub (fluor solvent+PC)	CO_2	(R)	+99%	−220 MMscfd	13
Advantica Ltd. (LRS-10)	Scrub (LRS10-K_2CO_3)	CO_2	(R)	+99%	–	30
Uhde Gmbh (Morphysorb)	Scrub (Morphysorb)	AG	(R)	1–98%	300 MMscfd	2
Lurgi Oel-Gas-Chemie GmbH (Omnisulf)	Scrub (Morphysorb)	AG	(R)	1–98%	–	1
Lurgi Oel-Gas-Chemie GmbH (Purisol)	Scrub (NMP)	AG	(R)	1–98%	–	7
Lurgi Oel-Gas-Chemie GmbH (Rectisol)	Scrub (Methanol)	AG	(R)	1–98%	–	100
UOP LLC (Selexol)	Scrub (DME, PEG)	AG	(R)	1–98%	–	55
Shell Global Solutions International B.V (Sulfinol)	Scrub (sulfolane, amine)	AG	(R)	1–98%	–	200
Fluor (CO_2LDSEP)	Liquifaction	CO_2, H_2	(R, P)	+99%	−15 MMscfd	–

(*Continued*)

Table 3. Continued

Licensor	System	Primary goal		CO_2 in tailgas	Capacity/unit	Plants worldwide
Costain Oil, Gas & Process ltd.	Liquifaction	CO_2	(P)	100%	5–1200 mtpd	7
Air Liquide (Medal)	Membrane	CO_2, H_2O	(R)	2–70%	1–1000 MMscfd	Several
NATCO Group Inc. (CYNARA)	Membrane	CO_2	(R)	−95%	5–750 MMscfd	30
UOP LLC (Separex)	Membrane	AG	(R)	–	1–1000 MMscfd	50
Merichem Chem & Refineries Services (AMINEX)	HFMC	AG	(R)	1–98%	–	10

PSA = Pressure Swing Adsorption, Mem = membrane, CEL = compression-expansion liquefaction, L = Liquefaction, HFMC = hollow fiber membrane contactor, AG = All acid gases (i.e., H_2S, COS and CO_2), P = purification, R = removal, PC = propylene carbonate, GC = Gas contaminants (Hg, As, H_2O, TBC, NH, and Sx).

Table 4. Characteristics of key alkanolamines used in gas treating (468)

Name		Chemical formula	Molecular weight	Vapor pressure (mm Hg)	Relative acid gas capacity (%)
Ethanolamine (Monoethanolamine)	MEA	$HO\text{-}CH_2CH_2\text{-}NH_2$	61	1.05	100
Diethanolamine	DEA	$(HO\text{-}CH_2CH_2)_2\text{-}NH$	105	0.058	58
Triethanolamine	TEA	$(HO\text{-}CH_2CH_2)_3\text{-}N$	148	0.0063	41
Hydroxyethanolamine (Diglycolamine)	DGA	$H\text{-}(OCH_2CH_2)_2\text{-}NH_2$	105	0.016	58
Diisopropanolamine	DIPA	$(CH_3CH(OH)CH_2)_2\text{-}NH$	133	0.01	46
Methyldiethanolamine	MDEA	$(HO\text{-}CH_2CH_2)_2\text{-}N\text{-}CH_3$	119	0.0061	51

and is selective for H_2S removal over CO_2 removal. Methyldiethanolamine (MDEA) selectively removes H_2S in the presence of CO_2, has good capacity, good reactivity, and very low vapor pressure. As a result, MDEA is a preferred solvent for gas treating.

By-product CO_2 from H_2, syngas and NH_3 production via methane steam reforming is recovered using hot carbonate absorption or MEA absorption. The hot carbonate systems used in many ammonia plants typically afford 95–97 vol% CO_2 by-product. MEA systems are generally capable of recovering a CO_2 stream that is 99.5+ vol% pure. Indeed, saleable CO_2 is being recovered from H_2, syngas, and NH_3 production plants, where absorption processes are being used. Here a high purity CO_2 product is delivered by the scrubber which requires little, if any, further purification.

Coal gasification to produce syngas (mostly $CO + H_2$) also yields some CO_2 that must generally be removed before using the syngas (e.g., for making methanol or acetic acid). If water gas shift is used to make more H_2, the by-product is additional CO_2. Also, for synthetic natural gas (SNG) production via coal gasification followed by methanation, some CO_2 is recovered. Recovery of the CO_2 requires treating a gas stream rich in CH_4 and H_2O. Absorption processes similar to those used in H_2, syngas, and NH_3 production are also used here.

Flue gas from combustion processes associated with burners, flaring, incineration, utility boilers, etc. contain significant amounts of CO_2. However, as discussed above, this CO_2 is generally of low quality, because its concentration tends to be low, the flue gas is very hot, and it contains a variety of other gaseous species and particulates that make CO_2 recovery difficult and expensive. Nevertheless, CO_2 is being recovered from flue gas for commercial use (2). A train of separation and purification equipment is used, with the CO_2 being removed via

Table 5. Major types of acid gas absorption processes (468–470)

	Chemical absorption		
	Alkanolamine	Inorganic carbonate	Physical solvent absorption
Adsorbents	MEA, DEA, DGA, MDEA, DIPA	K_2CO_3, K_2CO_3-MEA, K_2CO_3-DEA	Purisol, Selexol, Rectisol,
CO_2 & H_2S absorption mechanism	Chemical Reaction	Chemical Reaction	Physical Dissolution
	CO_2: $2RNH_2+CO_2+H_2O\leftrightarrow(RNH_3)_2CO_3$ $(RNH_3)_2CO_3+CO_2+H_2O\leftrightarrow2RNH_3HCO_3$	CO_2: $Na_2CO_3+CO_2+H_2O\leftrightarrow2NaHCO_3$	
	H_2S: $2RNH_2+H_2S\leftrightarrow(RNH_3)_2S$ $(RNH_3)_2S+H_2S\leftrightarrow2RNH_3HS$	H_2S: $Na_2CO_3+H_2S\leftrightarrow NaHS+NaHCO_3$	
Operating Pressure, psig	Insensitive to pressure	>200	250–1000
Operating Temp., °F	100–400	200–250	Ambient temperature
Stripper Gas	Steam	Steam or Air*	Steam or Air*
Absorbent Recovery	Reboiled Stripper	Stripper	Flash, Reboiler, or Steam Stripper
Swing variables (Temp. or Pressure)	Temperature principally	Both, but pressure principally	Pressure principally
Selectivity CO_2 vs. H_2S	Only MDEA selective for H_2S	May be selective for H_2S	Some selectivity for H_2S
Meets ppmv H_2S	Yes	Yes	Yes
Effect of O_2 in Feed	Amine degradation Products	None	Sulfur (S_8) precipitates at low temperatures

COS and CS_2 Removal and degradation	MEA – no removal and strong degradation; DEA – slight removal and some degradation; DGA – removes both, strong degradation; DIPA, MDEA – Removes both, no degradation	Converts both into CO_2 and H_2S, then removes both, no degradation	Removes both, no degradation
Solvent: solute concentration, wt%	H_2O: MEA, 13–25; DEA, 10–30; DGA, 40–60; MDEA, 33–55	H_2O: $K_2CO_3 < 30$	N-methyl-2-pyrrolidone (purisol); dimethyl ether of polypropylene glycol (selexol); methanol (rectisol);
Operating Problems	Solution degradation, Foaming, Corrosion, evaporation (MEA)	Column instability, Corrosion, Erosion	Absorption of heavy Hydrocarbons
Utility Cost	High	Medium	Low to Medium
Other comments	MEA limited to COS, CS_2 free streams with low CO_2 and H_2S concentrations; inhibitors used to control corrosive character of loaded alkanolamines; Performance improves: MEA < DEA < DIPA < MDEA	Rate enhancers are used to improve low adsorption rates; good for high pressure gases	Best for high pressure gases

*For streams free of sulfur compounds.

MEA absorption technology, which was developed in the 1970s and 1980s for enhanced oil recovery (1).

Fluor Enterprises Inc. has 24 Econamine flue gas plants operating worldwide and producing a saleable CO_2 product for both the chemical and food industries. Randall Gas Technologies, ABB Lummus Global Inc. has four installations of similar technology operating on coal fired boilers. Two of these plants produce chemical grade CO_2 and the other two plants produce food grade CO_2. Mitsubishi Heavy Industries Ltd. also has commercialized a flue gas CO_2 recovery process, based on their newly developed and proprietary hindered amine solvents (KS-1, KS-2 and KS-3). As of April 2005, they have agreed to license two KD CDR Process plants to a fertilizer company in India. Each plant can capture 450 metric tons per day of CO_2, making them the world's largest CO_2 recovery plants. It appears that these are the only examples of marketing flue gas CO_2 recovery technology.

With CO_2 emissions becoming more of a concern worldwide, and with absorption processes dominating CO_2 removal from industrial streams, the literature on the subject of CO_2 removal has grown substantially in the last few years. A review of the recent literature identified about 230 articles since 2000. Table 6 lists the number of papers and the corresponding absorbent that was studied. Although other reactive absorbents are represented, the family of amines is clearly dominant. It is noteworthy that a recent review article on this subject was not found during this search. Clearly, a review of the recent literature on absorption processes for the removal of CO_2 and other acid gases from process streams would be quite valuable. For more thorough reading on the subject please refer to references (1,3–5).

Table 6. Number of papers since 2000 containing in the title the indicated alkanolamine and other absorbents for CO_2 removal

Absorbent	
Methyldiethanolamine (MDEA)	73
Monoethanolamine (MEA)	55
Diethanolamine (DEA)	38
Piperazine (PZ)	33
Potassium Carbonate	7
Aminomethylpropano (AMP)	6
Triethanolamine (TEA)	5
Diglycolamine (DGA)	4
Sodium Glycinate	4
Dyethylene triamine (DETA)	3
Diisopropanolamine (DIPA)	2

Adsorption Processes

Only a few classes of adsorbents and adsorption processes are being used to remove CO_2 from gas streams. These adsorbents include aluminosilicate zeolite molecular sieves, titanosilicate molecular sieves, and activated carbons. CO_2 adsorption capacities of typical commercial adsorbents are given in Table 7. Other classic adsorbents are being used to remove contaminants from CO_2 streams destined for commercial use. In this case, the adsorbents include activated carbons for sulfur compounds and trace contaminate removal, silica gels for light hydrocarbon removal, and activated aluminas, bauxite, and silica gels for moisture removal. The adsorption processes include PSA, temperature swing adsorption (TSA), and hybrid PSA/TSA. Of the CO_2 producing processes listed above, only H_2, syngas, NH_3, fermentation ethanol, natural gas, and combustion are beginning to use adsorption processes for removing or purifying CO_2.

By-product CO_2 from H_2 production via methane stream reforming is recovered using PSA in lieu of absorption. In the early 1980s, new H_2 plants were being built with PSA units as the main H_2 purification

Table 7. Typical capacities of commercial and developmental CO_2 and CO selective adsorbents

Adsorbent	Adsorbate	T (°C)	P (torr)	Loading (mol/kg)	Mode
Act. carbon	CO_2	25	500	1.5–2.0	PSA
Act. carbon	CO_2	250–300	500	0.1–0.2	PSA
5A zeolite	CO_2	25	500	~3.0	PSA
5A zeolite	CO_2	250	500	0.2	PSA
Titanosilicates	CO_2	25–200	$760–6 \times 10^5$	Proprietary[a]	PSA
Titanosilicates	N_2	25–200	$760–6 \times 10^5$	Proprietary[a]	PSA
Titanosilicates	CH_4	25–200	$760–6 \times 10^5$	Proprietary[a]	PSA
Solid amine (supported PEI)		75	760	1.5–3.0	PSA
HTlc (K-promoted)	CO_2	300–400	200–700	0.4–0.7	PSA
Double-layer hydroxides	CO_2	375	230	1.5	PSA
Alumina (un-doped)	CO_2	400	500	0.06	PSA
Alumina (doped w/Li_2O)	CO_2	400	500	0.52	PSA
Alumina (basic)	CO_2	300	500	0.3	PSA
Li zirconate	CO_2	500	760	3.4–4.5	TSA
CaO	CO_2	500	150	4–8	TSA
CaO	CO_2	700	76	7	TSA
Cu(I) (alumina)	CO	25–30	760	0.8–1.2	PSA
Cu(I) (alumina)	CO	30	760	0.8	PSA

[a]Molecular Gate™ titanosilicates molecular sieves patented by Engelhard Corporation (7).

process. This eliminated the CO_2 scrubber, the low temperature CO shift reactor and the methanation reactor. The PSA unit offers advantages of improved H_2 product purity (99-99.99 vol% H_2, 100 ppmv CH_4, 10–50 ppmv carbon oxides, and 0.1–1.0 vol% N_2) with capital and operating costs comparable to those of wet scrubbing. PSA has also found applications in H_2 production from the coal-driven syngas industry. An example of this is the commercial gasification-based NH_3 production process in Coffeyville, KS (6).

Modern PSA plants for H_2 purification generally utilize layered beds containing 3 to 4 adsorbents (silica gel or alumina for water, activated carbon for CO_2, and 5A zeolite for CH_4, CO, and N_2 removal). Depending on the production volume requirements, from four to sixteen columns are used in tandem. The PSA unit is operated at ambient temperature with a feed pressure ranging between 20 and 60 atm. The hydrogen recovery depends on the desired purity, but ranges between 60 and 90%, with the tail gas (i.e., the desorbed gas containing H_2O, N_2, CO_2, CH_4, CO, and H_2) generally being used as fuel for the reformer.

Although PSA systems are increasingly used for H_2 recovery, they yield a by-product CO_2 stream that is only about 50 vol% pure. Low purity makes this tail gas stream less attractive as a commercial CO_2 source. PSA systems are under development to process this tail gas into H_2 and CO_2 rich streams, as discussed later in the *Emerging Literature Concepts* section.

Fermentation to produce ethanol has recently emerged as a major source of CO_2 by-product for industrial use. The crude by-product is typically 99.8% pure CO_2 on a dry basis after a simple water wash. But, the product is wet (saturated with water at ambient temperature) and not odor-free. After recovery, the CO_2 is usually washed with a simple water scrubber to remove water soluble compounds. It is then treated with activated carbon to remove traces of H_2S, SO_2, and organics. The gas is finally dried with activated alumina, bauxite, or silica gel before compression and cooling to the liquid or solid form. When destined for large-scale industrial use (urea, enhanced oil recovery, industrial inerting, etc.), the purification is not as exacting as it is for food grade CO_2.

The composition of natural gas varies widely depending on the location of the well, another source of CO_2. Since landfill gas and coal bed methane gas are somewhat similar in composition to natural gas, they are included here for convenience. The CO_2 concentration in natural gas varies between 3 and 40 vol%; but it could be as high as 80 vol%. Because of the complexity and variability of the composition of natural gas, a train of separation processes, including adsorption, absorption, cryogenic, and even membrane separation processes, may be used to process it into pipeline quality methane. CO_2 has been traditionally removed using an amine-based scrubbing process, as described in detail above.

However, PSA technology is beginning to supplant some of the absorption technology in natural gas treatment, especially in the so-called shut in natural gas wells that previously contained too much N_2 to justify processing. The Molecular Gate^{TM} adsorption technology commercialized by Engelhard Corporation uses a titanosilcate adsorbent combined with a PSA process in a vacuum swing adsorption mode to remove N_2 and/or CO_2 from natural gas streams. Two of these units are in operation (2).

To remove CO_2 from coal bed methane, Engelhard Corporation uses Molecular Gate^{TM} adsorption technology with a more traditional PSA mode with compressed feeds ranging in pressure from 80 to 800 psig (7). Ten of these units are being built and three are in operation for upgrading methane from abandoned coal mines (14). Similarly, Axens has commercialized natural gas purification technology, based on alumina and zeolite molecular sieve adsorbents and a temperature swing adsorption (TSA) regeneration mode. The alumina removes trace and bulk contaminants in the natural gas other than CO_2 through both chemisorption and physisorption mechanisms. The zeolite molecular sieve serves to remove CO_2 and other contaminants via physisorption. Axens has over 60 installations operating worldwide that treat a variety of natural gas and industrial process streams (2).

The recovery of CO_2 from flue gas by adsorption technology is not commonly practiced by industry. The only example was obtained from a recent report in the literature that indicated CO_2 is being recovered from flue gas commercially in Japan (8) using a layered PSA bed containing X and A type zeolites and activated carbon. Neither the flow sheet nor the purity of the recovered CO_2 is known; but, the CO_2 does not appear to be used for commercial applications.

Membranes Processes

In general, membrane technology for separating gas streams is attractive for many reasons (9–16). First, it does not require a separating agent nor does it involve phase changes. As a consequence, the elevated processing costs associated with regeneration and phase change are eliminated. In addition, membrane systems involve small footprints compared to other processes and require low maintenance. They are also compact and lightweight and can be positioned either horizontally or vertically, which is especially suitable for retrofitting applications. Finally, the modular aspect of membrane units allow for multi-stage operation and linear scale up costs that speed up the design time of larger scale units.

Membranes are an appealing option for CO_2 separation, mainly because of the inherent permeating properties of this species. CO_2 is a

very small gas molecule, with a smaller kinetic radius (i.e., 3.3 Å) than lighter gases, such as O_2 (3.46 Å), N_2 (3.64 Å), and CH_4 (3.8 Å). In fact, among permanent gases, only He (2.59 Å) and H_2 (2.89 Å) are smaller than CO_2. Hence, CO_2 is a fast diffusing gas in many membrane materials, such as glassy and rubbery polymers, molecular sieves, and several other inorganic materials. On the other hand, CO_2 also has a relatively high molecular weight and a large quadruple moment, enabling it to naturally adsorb more strongly to or dissolve at much higher concentrations in these membrane materials compared to many other gas species. These properties give rise to very high CO_2 permeation rates and selectivities over many other gas species, sometimes even higher than H_2 and He.

Membrane systems potentially or actually commercialized for gas separations are listed in Tables 1 and 2. The number commercialized is given in Table 3. Of the CO_2 producing processes listed above, only natural gas production, to a lesser extent landfill gas production, and H_2, syngas and NH_3 production are beginning to use membrane processes for removing or purifying CO_2.

The first commercial cellulose acetate membrane units for CO_2 removal from natural gas were implemented only a few years after the introduction in 1980 of the first commercial PRISM membrane air separation system developed by Monsanto (11,12). By the end of the 1980s companies such as Natco (Cynara), UOP (Separex), and Kvaerner (Grace Membrane Systems) were producing membrane plants for this purpose. A few years later, more selective polyimides and only recently polyaramides were slowly introduced to displace the old cellulose acetate systems. Today, commercial membrane technology for CO_2 separation is largely based on glassy polymeric materials (cellulose acetate, polyimides and polyaramides).

Currently, the membrane market devoted to CO_2 separation from natural gas is about 20%, which is only 2% of the total separations market for natural gas. Amine based absorption processes dominate this market, as shown in Table 3. Membranes are used in situations where the produced gas contains high levels of CO_2. However, a key sensitivity with these current membranes is that they must be protected from the heavier C_{5+} hydrocarbons present in wet natural gas streams. Exposure to these compounds immediately degrades performance, and can cause irreversible damage to the membranes.

Membranes for large-scale recovery of CO_2 from, e.g., natural gas, for use as a salable product are a relatively recent development. As gleaned from above, current membranes have been designed generally to remove unwanted CO_2 from a desired product, rather than to recovery CO_2 for its own value. The advent of enhanced oil recovery (EOR) projects using CO_2 has changed this situation. Natural gas fields in West

Texas now recover CO_2 that is pipelined to areas where it is needed for EOR. A variety of membranes, including ones with separating layers made of cellulose acetate, polysulfone, and polyimide, are used for this purpose. Air Products and Chemicals and Ube are marketing membrane systems for EOR and landfill gas upgrading, respectively.

Membrane units have also been commercialized for H_2 purification in reforming processes (UOP, Air Products and Chemicals). For example, membrane processes, such as the Polysep membrane systems developed by UOP and the PRISM membrane systems developed by Monsanto, and now sold by Air Products and Chemicals (2) recover H_2 from various refinery, petrochemical, and chemical process streams. Both are based on polymeric asymmetric membrane materials composed of a single polymer or layers of at least two different polymers, with the active polymer layer being a polyimide. The Prism system is based on a hollow fiber design and Polysep is a spiral wound sheet type contactor. Both are used to recover H_2 from refinery streams at purities ranging from 70 to 99 vol% and recoveries ranging from 70 to 95%. Relatively pure H_2 containing a very low concentration of CO_2 leaves these units in the low pressure permeate stream. This stream can be sent to a methanator for CO_2 removal and further purification. The high pressure retentate stream, consisting of H_2 and CO_2 with low concentrations of CO and CH_4, can be used as fuel.

Cryogenic Liquefaction Processes

Recovery of CO_2 by cold liquefaction has the advantage of enabling the direct production of very pure liquid CO_2, which can be readily transported. Liquefaction is achieved by the dual action of external refrigeration and the Joule-Thompson effect that results from the compression and adiabatic expansion of the stream. The disadvantages associated with the cryogenic separation of CO_2 are the amount of energy required in refrigeration, particularly in dilute gas streams, and the requirement to remove gases, such as water and heavy hydrocarbons, that tend to freeze and block the heat exchangers.

Liquefaction technology for CO_2 recovery is still incipient. Cryogenic CO_2 recovery is typically limited to streams that contain high concentrations of CO_2, with a lower limit of about 50 vol%, but with a preferred concentration of > 90 vol%. It is not considered to be a viable CO_2 capture technology for streams that contain low concentrations of CO_2, which includes most of the industrial sources of CO_2 emissions. Cryogenic separation of CO_2 is most applicable to high pressure gas streams, like those available in precombustion and oxyfuel combustion processes.

One exception is for the production of ethanol through fermentation. In fact, liquefaction is generally practiced in this case to produce a highly pure liquid CO_2 product. Details about this cryogenic CO_2 process are not readily available, however.

Nevertheless, cryogenic CO_2 recovery is increasingly being used commercially for purification of CO_2 from streams that already have high CO_2 concentrations (typically >90 vol%). Of the CO_2 producing processes listed above, only ethanol production and H_2, syngas and NH_3 production utilize (or are beginning to utilize) cryogenic processes for removing or purifying CO_2. Tables 1 and 3 provide some information on the cryogenic systems that are described in the literature.

Currently, Costain Oil, Gas & Process Ltd has commercialized a CO_2 liquefaction process with around seven units installed worldwide. The process is assisted by membrane technology to treat streams with CO_2 fractions greater than 90 vol%. Recently, Fluor Enterprises Inc. also developed a CO_2 liquefaction process called CO_2LDSEP. This technology exploits liquefaction to separate CO_2 from H_2 and other gases in the tail gas of a H_2 purification PSA unit. However, no commercial units of this technology have been reported.

EMERGING LITERATURE CONCEPTS

The goal of this review is to highlight research areas that impact energy usage and to improve CO_2 separation process performance and economics. To set forth recommendations for future R&D on CO_2 removal processes, key factors must be considered:

1. The large scale and conditions of industrial production,
2. materials requirements,
3. economic goals and drivers, and
4. purity demands of gases involved.

To this end, emerging literature concepts in adsorption and membrane technology for CO_2 removal are reviewed and then recommendations are set forth for future R&D.

For this review, a focus has been placed on emerging concepts in the separation sciences to overcome the limitations of current CO_2 removal processes. The potential for novel adsorbents and membranes and associated processes are outlined. Many opportunities are identified, including hybrid systems that have the potential for significant improvement in separation technology.

Adsorption

The emerging literature concepts on the use of adsorbents and adsorption processes in the industries that produce CO_2 have been focused on a few processes. These include the H_2, syngas, and NH_3 production processes, and the natural gas production processes, which include landfill gas and coal bed methane gas. Emerging literature concepts on the use of adsorbents and adsorption processes to remove CO_2 from flue gas generated from the burning of fossil fuels have also been identified. A survey of the recent literature in these areas is given below. The latest developments in PSA and TSA process refinements, sorption enhanced reaction processes (SERP) or periodic adsorptive separating reactors, and selective adsorbents for CO_2 are discussed. The concepts presented in these studies have the potential for both near term and longer term impact on adsorption technology for the removal of CO_2 from industrial process streams. Tables 7 and 8 respectively provide a list of adsorbents and PSA cycle configurations currently being investigated for CO_2 removal.

Adsorption Process Refinements

Adsorption-based CO_2 separation and capture technologies are based primarily on thermal and pressure swing regeneration processes, i.e., TSA and PSA technologies. These are well known cyclic adsorption processes with many commercialized gas separation and purification applications. The performance, cost, and reliability of the adsorbent is one of the key factors to successful commercial acceptance. Another key factor to success is matching the adsorbent with the cycle configuration, which is critical for success in both PSA and TSA processes.

Major breakthroughs in PSA technology for large-scale H_2 purification and associated CO_2 removal were realized in the early 1970s with the development of a 4-bed, multi-layer PSA process. Modifications to improve separation efficiency have included additional beds, typically 7 to 10 beds (17), as many as 16 beds (18), and tanks (19,20) for storing intermediate process streams between cycle stages. Along with these additional beds and tanks came more complex cycle sequencing to achieve higher throughputs with the same or even less volume of adsorbent distributed in the additional beds.

Each bed in a PSA plant undergoes adsorption and regeneration cycle steps. These steps include

1. pressurization,
2. high pressure feed,

Table 8. Performances of various PSA cycle configurations investigated for CO_2 concentration from flue gas, with the process performance judged primarily in terms of the CO_2 purity in the heavy product (y_{CO_2F}), with the CO_2 recovery (R_{CO_2}) and the feed throughput (θ) being secondary but also important process performance indicators

Cycle configuration	Cycle step sequence*	Ads**	P_H (atm)	P_H/P_L	y_{CO_2F} (%)	y_{CO_2HP} (%)	R_{CO_2} (%)	θ (LSTP/hr/kg)	Reference
2-bed 2-step	FP, CnD	Y	2.0	2.0	15	18	90	12,600	(471)
2-bed 4-step	FP, F, CnD, LR	13X	3.0	3.0	8.3	–	–	15	(472)
1-bed 4-step	LPP, F, CnD, LR	13X	1.7	1.9	15	24.4	9	17	(473)
2-bed 4-step	FP, F, CnD, LR	13X	1.1	17.2	10	68	50	507	(35)
1-bed 4-step	FP, F, CnD, LR	13X	14.0	15.9	15	56.4	98	908	(474)
3-bed 8-step	FP, F, CoD, LEE, HPP or HR-IP, N, CnD, LEE	AC	1.5	15	17	99.8	34	331	(475)
3-bed 7-step	FP, F, LEE, HR-IP, N, CnD, LEE	AC	2.0	20	13	99	55	156	(476)
3-bed 8-step	FP, F, LEE, HPP, HR-IP, N, CnD, LEE	13X	1.5	30	13	99.5	69	228	(477)
3-bed 8-step	FP, F, CoD, FR, N, HR-IP, CnD, N	AC	1.1	16.6	16	99	50	610	(478)
4-bed 4-step	LPP, F+ReC, HR, CnD	AC	1.2	12	17	99.9+	68	33	(479)
4-bed 8-step	LPP, N, F, HR, LEE, CnD, LR, LEE	13X	1.1	11	13	64	80	120	(480)
3-bed 5-step	FP, F, HR, CnD, LR	13X	1.1	17.2	10	83	54	338	(35)

2-bed 6-step	LEE, FP, F, LEE, CnD, LR	13X	1.1	17.2	10	82	57	477	(35)
2-bed 4-step	HPP, FP, CoD, CnD	13X	5.5	110	20	48	94	426	(480)
2-bed 5-step	LPP, FP, F, CoD, CnD	13X	5.5	110	20	43	88	426	(480)
3-bed 4-step	LPP, F, CnD, LR	13X	1.5	30	20	58	75	273	(480)
3-bed 6-step	LPP, FP, F, HR, CoD, CnD	13X	1.5	30	20	63	70	273	(480)
4-bed 4-step	LPP, F, CnD, LR	HTlc	1.4	12	15	63	75	22	(34)
4-bed 5-step	LPP, F, CoD, CnD, LR	HTlc	1.4	12	15	84	68	15	(34)
5-bed 5-step	LPP, F, CoD, CnD, LR	HTlc	1.4	12	15	65	87	12	(34)
5-bed 5-step	LPP, F, HR (from CnD), CnD, LR	HTlc	1.4	12	15	72	82	12	(34)
5-bed 5-step	LPP, F, HR (from LR), CnD, LR	HTlc	1.4	12	15	76	49	23	(34)
4-bed 4-step	LPP, F, HR (from CnD), CnD	HTlc	1.4	12	15	83	17	14	(34)
5-bed 5-step	LPP, F, HR (from LR), CnD, LR	HTlc	1.4	12	15	89	72	58	(58)
4-bed 4-step	LPP, F, HR (from CnD), CnD	HTlc	1.4	12	15	98	5	202	(58)

*CnD = countercurrent depressurization; CoD = cocurrent depressurization; FP = feed pressurization; F = high pressure feed; HPP = heavy product pressurization; HR = heavy reflux; IP = intermediate pressure; LEE = light end equalization; LPP = light product pressurization; LR = light reflux; N = null or delay; ReC = recycle.

**All processes operated at ambient temperature except for HTlc (hydrotalcite like compound), which was done at 575 K.

3. co-current depressurization,
4. counter-current depressurization,
5. counter-current purge (light reflux), and
6. several equalization (pressurization/depressurization) steps between two beds.

Improvements, not only in H_2 purification PSA plants, but also in CO_2 concentration and recovery PSA plants, can be realized by

1. further refinement of these cycle steps,
2. addition of new cycle steps, and
3. by novel refinement of the cycle sequencing to create a more effective separation process.

The evolution of H_2 PSA technology serves as a good example to illustrate how simple cycle modifications can have a significant impact on the process performance, and to show that intuition may not always be correct. As an example, Whysall et al. of UOP (18) recently demonstrated that the duration of the purge step does not have to be equal to or less than the duration of the adsorption step and by extending the purge step, the production capacity of a PSA H_2 plant, for the first time, could exceed 110 Nm^3/hr using 16 beds. Baksh et al. of Praxair Technology, Inc. (19,20) decreased the number of PSA beds with the judicious use of storage tanks to collect and reuse gas during cycle steps, to increase H_2 production per unit adsorbent. They (20) also show that the PSA process performance can be improved significantly by first removing N_2 from the feed stream using modified (via cation exchange) X-type zeolite adsorbents, which also advantageously remove CO_2. Xu et al. of Air Products and Chemicals (21) modified the pressure equalization steps by using four steps with just six beds, and decreasing the cycle time for pressure equalization between beds (22). Most of these changes are not obvious but have provided a pathway for improved separations.

Sircar and Golden (23) describe several other novel approaches to PSA cycle sequencing for both H_2 purification and simultaneous H_2 and CO_2 purification. The latter PSA cycle involves two interconnected cascades of PSA beds each operating with their own unique cycle sequence and number of beds. The complexity between the different cycle steps in a H_2 purification PSA unit has recently been reported by Waldron and Sircar (24). Many improved and novel PSA cycle sequences are anticipated for use in CO_2 recovery plants, based on continued industrial and academic research.

Another way to improve the performance of a PSA process is to decrease the cycle time, which allows more gas to be processed using less

adsorbent. This is referred to as rapid cycle PSA. For example, QuestAir has recently announced improved H_2 purification technology with a rapid cycle PSA unit with a rotary valve. This technology is planned for installation in the largest liquid H_2 plant in Asia which will be fabricated in Japan.

Rapid cycle PSA is not a new concept; however, it required major innovations in process design for handling the gas streams before commercialization became feasible. This innovation has been reported in a series of patents by Keefer et al. of QuestAir Technologies (25–27) which describe the rotary valve and multi-bed cycle sequencing approaches. The same rapid cycle PSA concepts based on a rotary valve are now being applied by QuestAir to remove CO_2 from natural gas and landfill gas.

Adsorbent attrition and intraparticle mass transfer effects still limit how rapid the cycle sequencing can be carried out. This problem has been partly alleviated with the recent development of novel structured adsorbents, incorporating very small commercially available adsorbent particles or crystals, like activated carbons and zeolites, in a support material like a sheet of paper. In this way, the effects of mass transfer and adsorbent attrition are minimized. Structured adsorbent materials are described in the recent patents by Golden et al of Air Products and Chemicals (28–30), and by Keefer et al. (31).

With the development of a very thin, paper like, structured adsorbent material by QuestAir came the development of a second generation, ultra rapid cycle PSA H_2 purification system. In this system, a rotary adsorbent bed concept has supplanted the rotary valve concept, with the rotary adsorbent bed being comprised of multiple beds within one cylindrical adsorber unit (32). This unique configuration has resulted in a very compact PSA unit that can be operated at very short cycle times and thus very high H_2 production rates. ExxonMobil recently partnered with QuestAir to design and build a rotary bed PSA plant for the recovery of H_2 from the tail gas of a conventional H_2 PSA plant (33). This rotary adsorbent bed concept is certainly applicable to CO_2 capture and concentration from a variety of process streams. However, further improvements in this technology are required for this application, including the continued development of new structured, multilayered adsorbents, with each layer containing an adsorbent that is selective to one or more of the gases to be separated.

A comprehensive review of relevant studies that deal with removing and concentrating CO_2 from simulated flue and stack gases by various PSA cycles has been given recently by Ritter and co-workers (34). Table 8 provides a summary of the performances of these various PSA cycles. All utilize a light, heavy, dual, or even a no reflux PSA cycle configuration, intermixed with various cocurrent and/or countercurrent

depressurization steps, feed, light product, and heavy product pressurization steps, and null (delay) on idle and pressure equalization steps. Note the heavy and dual (light and heavy) reflux cycle steps have been included to concentrate the heavy component like CO_2.

H_2 PSA plants, which have been designed specifically for producing a very pure light component, e.g., H_2, only include a light reflux step. This heavy reflux step, or so-called high pressure rinse step, has been introduced in several PSA patents, with only limited commercialization. Not surprisingly, the fairly complicated two cascade PSA system developed by Sircar and Golden (23) utilize a heavy reflux step in the cascade that produces the concentrated CO_2; the other cascade uses only the light reflux purge step to produce the high purity H_2.

In addition, these PSA cycles being studied for removing and concentrating CO_2 from simulated flue and stack gases also utilize

1. a vacuum swing cycle with the high pressure set just above atmospheric pressure and the low pressure set at some vacuum level, or
2. a more conventional pressure swing cycle with the purge or low pressure set at or near atmospheric pressure and the feed set at a higher pressure.

To concentrate and recover CO_2 from flue or stack gas, most PSA cycles utilize one or more commercially available adsorbents that exhibit a high capacity for CO_2 at ambient temperature and pressure, e.g., activated carbon, carbon molecular sieve, and X and Y type aluminosilicate zeolites. Some of these cycles also utilize a developmental adsorbent, i.e., a K-promoted hydrotalcite like (HTlc) adsorbent that exhibits a high capacity for CO_2 at elevated temperatures (e.g., 300 to 500°C) and ambient pressure.

It is clear from the summary in Table 8 that there are numerous designs for operating PSA processes for CO_2 capture and concentration. It also illuminates the challenge associated with choosing one PSA cycle over another one for a given application. After carefully examining the results summarized in Table 8, in most cases, it is still not clear which PSA cycle would be more advantageous. For example, it could easily be reasoned by the expert that it would be inappropriate to use a no reflux cycle or just a light reflux cycle in an attempt to concentrate a heavy component by PSA. But even in this light reflux only case, a particular PSA cycle outperformed a PSA cycle with heavy reflux, depending on many factors like the process conditions, cycle times, bed sizes, adsorbent CO_2 capacity, or even the addition of a light end equalization step (35) which are all interrelated. So, it appears that a PSA cycle with light reflux for concentrating a heavy component can be considered

for separating CO_2, especially since a light reflux only PSA cycle reduces the capital and operating costs by avoiding the use of an additional compressor for implementing a heavy reflux step.

Hence, PSA cycle configurations are difficult to predict, understand and interpret, even for an expert. A better understanding of these heavy and dual reflux cycles through R&D is clearly warranted so that more efficient PSA processes can be developed for current commercial separations and for concentrating CO_2 from stack and flue gases. This is true in regard to both the more conventional multi-bed PSA process and even the new rotary bed process described above.

TSA is also being explored for CO_2 capture and concentration from stack and flue gases. For example, Ding and Alpay (36) used K-promoted HTlc as the adsorbent in a TSA process for CO_2 removal from high temperature streams. In a TSA mode, the adsorbent bed is usually regenerated by using a hot purge gas to effect desorption of CO_2. This purge gas, e.g., steam can be any gas that does not adsorb appreciably on the adsorbent at the desorption temperature.

PSA processes are also being developed for CO_2 removal from natural gas (37–29), and even landfill gas (40,41), and coal bed methane (7,42–45). For example, Engelhard Corporation developed a PSA process to remove H_2O, CO_2 and heavier hydrocarbons from methane using their Molecular Gate^{TM} adsorbent technology. These adsorbents are comprised of titanium silicate molecular sieves that were originally developed to remove only N_2 from natural gas by kinetic separation. This class of materials was subsequently found to provide uniquely higher kinetic and adsorption selectivities for CO_2 and H_2O, exceeding those of more traditional aluminosilicate molecular sieves. A typical PSA system using the Molecular Gate^{TM} adsorbent to separate CO_2 from CH_4 rich gas streams at feed pressures between 100 and 800 psia produces a product stream containing CH_4 at concentrations of >90 vol%. This commercial technology is able to process gas streams containing up to 30 vol% CO_2 with favorable economics (37,39).

Over the past decade, academic researchers have also focused on the development, understanding, and optimization of new PSA cycle configurations for gas separation and purification. For example, Biegler and co-workers (46) are developing important optimization tools for multi-bed PSA processes, especially for H_2 purification and CO_2 recovery. Process design and fine tuning affords opportunities for significant improvements in the PSA process performance. However, this work needs to be extended to include the number of beds and all possible cycle steps for robust optimization.

Warmuzinski and coworkers (47,48), Lee and coworkers (49–51), Ritter and co-workers (52), and others are studying the design of

multi-layered adsorbent beds through mathematical simulation and bench scale experimentation. Multi-layed beds are the industrial standard; however, very little information has been published in the literature on the design and optimization of layered bed PSA processes. Most published work involving the purification of H_2 simply reports the performance of a given layered bed; they do not address optimizing the number of layers, types of adsorbents or depth of each layer. More PSA R&D is needed in this area, for recovering the heavy component like CO_2 from a gas stream.

Some very novel PSA cycles were introduced to the literature by Hirose and co-workers in Japan (53–56) and then by Ritter and co-workers (57,58). Both groups are studying PSA cycles to concentrate the heavy component, like CO_2, in gas streams. In one configuration, the feed step is maintained at low pressure and the adsorbent bed enriches the gas phase with the heavy component due to desorption (58). This kind of PSA cycle was first described by Wilson (59) and has recently appeared in two patents (60,61).

These uncommon enriching PSA cycles operate in stark contrast to common stripping PSA cycle configurations. The word "stripping" is used to denote that the feed step is carried out at the high pressure and that the adsorbent strips the heavy component from the gas phase due to selective adsorption, whereas the word "enriching" is used to denote that the feed step is carried out at the low pressure and that the adsorbent bed enriches the gas phase with the heavy component due to desorption (58). Hence, an enriching PSA cycle functions in a reversed or inverted mode compared to a stripping PSA cycle. It appears that a vast majority (>99%) of the PSA literature involves only the stripping PSA cycle concept. Hence, very little is known about the operation and performance of an enriching PSA cycle, which are effective at concentrating CO_2 from gas streams (53–56).

Another novel feature includes feeding a PSA column at intermediate position between the ends of the column. In this mode, the feed can be introduced at high (stripping) or low (enriching) pressure, and light and heavy reflux operations can be carried out simultaneously at the respective ends of the column. This type of PSA process mimics the behavior of a distillation column. Dong et al. (62) borrowed ideas from distillation and applied them to PSA by interconnecting two or more sets of twin columns through side, top, and or bottom ports for feeding, recycling, and or collecting gases. This concept was demonstrated by separating a ternary gas mixture, CO_2-CH_4-N_2, into three enriched products. In one case activated carbon was used in both sets of columns; in two other cases they used activated carbon in one set of columns, and layered 13X zeolite and carbon molecular sieve in the other set of columns. The possibility of treating complex gas streams containing

multiple components, like natural gas, landfill gas, and coal bed methane gas streams, with multiple adsorbents appears feasible with these PSA cycles. Clearly, more research needs to be done with these PSA cycles that mimic multi-component distillation operations.

Sorption Enhanced Reaction (Periodic Adsorptive Separating Reactors)

Conducting reaction and adsorptive separation in a single fixed bed reactor configuration dates back to 1987, beginning with the work of Kadlec and coworkers (63–65). The general idea is to use the adsorbent to selectively remove one or more of the products formed from an equilibrium limited reaction to shift the equilibrium in favor of increased conversion. The adsorbent is then regenerated with a pressure or temperature swing. Improved adsorbents with greater selectivity, larger working capacity, more rapid adsorption, and desorption kinetics, reduced sensitivity to moisture and other poisons are required for this approach to have commercial interest. These separation characteristics are required at the elevated process temperatures. Because the performance of most commercial adsorbents like zeolites, activated carbons, activated aluminas, or silica gels is lacking at these higher operating temperatures, which is typical of the regeneration conditions, the development of new adsorbents is needed specifically for these high temperature applications.

A team at Air Products and Chemicals has developed adsorptive separating reactors using a sorption enhanced reaction process (SERP). SERP is a fixed bed process with the reactor containing a mixture of a conventional catalyst and a selective, high temperature adsorbent. For an equilibrium limited reaction, the adsorbent shifts the equilibrium in favor of higher conversion through Le Chatlier's principal. When the adsorbent becomes saturated with the product a simple pressure swing in the bed can be used for regeneration.

In a series of patents (66–70) and three publications (71–73), this group discusses a redesign of the methane reforming operation. For this approach a high temperature CO_2 selective adsorbent is mixed with a typical reforming catalyst to conduct the steam methane reforming and water gas shift reactions in one unit at a lower temperature. Reforming can be practiced at this lower temperature because of the *in situ* removal of CO_2 (68,70). Medium purity H_2 production ($\sim$95%) was achieved by conducting this SERP process in a water gas shift reactor containing the catalyst and a CO_2 selective adsorbent. The feed for this unit was obtained from a conventional steam methane reformer (74).

In a more general patent, three uses of the SERP concept are discussed (75). In the first case steam methane reforming is driven using CO_2 and/or CO selective adsorbents. In the second case, methane reforming with CO_2 can be revamped by using CO or H_2 selective adsorbents. In the third case, H_2O selective adsorbents are used in the production of CO using a reverse water gas shift reactor. An emphasis is placed on the judicious use of these different adsorptive reactors to optimize the production of H_2, CO or syngas from the reforming of methane. There appears to be significant potential for the development of additional applications of and new adsorbents for the SERP concept, especially for CO_2 removal and concentration.

Some very recent work on the SERP concept by Hufton et al. (76) involves the development of precombustion decarbonization technology for CO_2 capture from IGCC, NGCC, or related combined cycle processes. This process is referred to as sorption enhanced water gas shift (SEWGS). It involves a multi-bed PSA process operating at high temperature with the columns again packed with catalyst and K-promoted HTlc. CO is converted to CO_2 which is quickly removed by the CO_2 selective adsorbent. This *in situ* removal of CO_2 facilitates more conversion of the CO to CO_2 through Le Chatlier's principal, as discussed above. A H_2 product free of CO_2 is produced at high pressure and temperature. This gas is burned in a high efficiency gas turbine. After a series of PSA cycle steps, including a heavy reflux step, a concentrated CO_2 product is produced at low pressure. This CO_2 product can be recovered, and either sold for industrial or commercial use or further processed for sequestration.

The success of the SERP relies on CO_2, H_2O and even H_2 selective adsorbents. The preferred CO_2 adsorbents include: K-promoted hydrotalcite (HTlc), modified double layer hydroxides, spinels and modified spinels, with metal oxides and mixed metal oxides of Mg, Mn, La and Ca, and clay minerals such as sepiolite and dolomite (68–70,73,74). The preferred H_2O adsorbents include commercially available A, X, and Y zeolites, mordenites, and aluminas and silica gel (66,67,75). The preferred H_2 adsorbents include metal hydrides such as Pd, PdAg, MgNi, FeTi, and LaNi (75). The preferred CO adsorbents include Cu(I) or Ag(I) on silica-alumina (75). Clearly, a wide range of commercially available and developmental adsorbent materials can be used in the SERP concept.

Harrison and co-workers (77–79) have been researching SERP for the steam reforming of methane in a single unit using a TSA cycle to remove CO_2 reversibly from the reaction product gas with CaO. Rodrigues and co-workers (76–85), and also Alpay and co-workers (86,87), have been studying the performance of the SERP for the steam reforming of methane in a single unit using a PSA cycle to remove

CO_2 reversibly from the reaction product gas using a K-promoted HTlc. The continued experimental validation of modeling analyses, coupled with the study of various PSA cycle sequences, should contribute to the understanding of this type of adsorptive reactor system, and to optimizing its performance.

It is clear that these SERPs allow steam methane reforming, water gas shift, and/or reverse water gas shift reactors to operate at reduced temperatures or pressures. They can reduce or eliminate downstream separation and purification units currently associated with the production of high purity H_2, CO, or syngas and for removing CO_2 for recovery or sequestration. Although the SERP concept seems to work well, industrial acceptance of this technology has been limited. Again, further implementation of this SERP would be fostered with the development of improved adsorbents, especially high temperature adsorbents.

Selective Adsorbents

New selective adsorbents can play a key role in CO_2 separation. A recent review on CO_2 absorbents by Yong et al. (88) covered activated carbons, aliminosilicate zeolites, metal oxides, and hydrotalcite like compounds (HTlcs) for reversible adsorption. The overall conclusion is that activated carbons and zeolites are superior to metal oxides and HTlcs for ambient temperature applications; but, for high temperature applications metal oxides and HTlcs are preferred over activated carbons and zeolites. As shown in Table 7, typical activated carbons exhibit 1.5 to 2.0 mol/kg CO_2 adsorption at 25°C and 500 torr, which decreases to 0.1 to 0.2 mol/kg at 250 to 300°C and 500 torr. Similarly, 5A zeolite exhibits ~3.0 mol/kg at 25°C and 500 torr, and 0.2 mol/kg at 250°C and 500 torr. The capacities of these materials would be less than 0.1 mol/kg at the temperatures associated with the steam methane reforming, water gas shift, and reverse water gas shift reactive adsorbers.

The recent work by Engelhard Corporation involves the development of novel adsorbent materials for CO_2 separation from natural gas streams. The Molecular Gate™ technology, which was originally targeted for kinetic separation of N_2 from natural gas, was also found to be uniquely attractive for CO_2 and H_2O separation from natural gas. Based on titanium silicate molecular sieves, the Molecular Gate™ process takes advantage of the unique ability to adjust pore size opening of the material within an accuracy of 0.1 angstrom. Despite the small differences of kinetic radius between N_2 and CH_4, the material pore size of 3.7 angstroms is effective at excluding CH_4 from its pores while accepting N_2 and other smaller and far more adsorbing molecules such as CO_2 and

H_2O into its pores (7). The CO_2, N_2, CH_4, and H_2O capacities of theses various Molecular Gate^{TM} adsorbents are proprietary.

For selective adsorbents, the K-promoted hydrotalcite (HTlc) materials exhibit a high and pressure-reversible CO_2 capacity at temperatures compatible with steam methane reforming, water gas shift, and reverse water gas shift applications (89,90). Mayorga et al. (90) of Air Products and Chemicals report synthesis procedures and operational capacities for both HTlcs and double layer hydroxides. Rodriques and co-workers (91,92) have characterized HTlcs for CO_2 adsorption at ambient and elevated temperatures, as has Alpay and co-workers (86,87). Overall, the reversible CO_2 capacities typically range between 0.4 and 0.7 mol/kg at 300 and 400°C and 200 and 700 torr, even in the presence of steam. This performance is highly dependent on the synthesis and pretreatment conditions (93). Double layer hydroxides exhibit even higher reversible capacities in the presence of steam, typically of around 1.5 mol/kg at 375°C and 230 torr (90). These adsorbents are attractive not only for SERPs, but also for high temperature PSA processes, as shown recently by Ritter and co-workers (58,94). Table 7 compares the capacities of these developmental CO_2 selective adsorbents to established commercial materials.

Several teams are also exploring alumina as a high temperature and pressure-reversible CO_2 adsorbent for use in a PSA cycle (88,95). The CO_2 capacity of aluminas undoped and doped with metal oxides and carbonates ranges from 0.06 (undoped) to 0.52 (doped with 9 wt% Li_2O) mol/kg at 400°C and 500 Torr (95), which is similar to that reported by Yong et al. (88) for commercially available basic aluminas, i.e., ~0.3 mol/kg at 300°C and 500 torr (see Table 7).

Lithium zirconate and CaO can function as high-temperature, selective CO_2 adsorbents with temperature-reversibility. Lin and coworkers are exploring the zirconates (96–98), as is Nair et al. (99) in Japan. Typical CO_2 adsorption capacities are high at 3.4 to 4.5 mol/kg at 500°C and 760 torr, with reasonable regeneration rates exhibited at 780°C that improve with CO_2 free purge gas (97) (see Table 7). The sensitivity of these materials to H_2O vapor has not been reported.

CaO adsorbents are being investigating by Fan (100–102), Harrison (77–89), Kuramoto et al. (103) in Japan, and Abanades (104) in Spain. These materials are also showing high CO_2 capacities at high temperatures with reasonable regeneration rates. For example, typical reversible CO_2 capacities range between 4 and 8 mol/kg at 500°C and 150 torr, with regeneration carried out at 900°C in N_2 (103). A similarly high CO_2 capacity of 7 mol/kg resulted for a CaO exposed to 76 torr of CO_2 and cycled over 50 times at 700°C using N_2 for purge. This is a large reversible CO_2 capacity (see Table 7). These CaO adsorbents are very sensitive to sulfur, but the sensitivity to H_2O vapor has not been reported (100).

The operating temperature range of this material may be too high for most SMR, WGS, and RWGS reactors, however.

United Technologies working with NASA in the mid to late 1990s developed novel low temperature solid amine based CO_2 adsorbents that are pressure and/or temperature regenerable (105,106). One variant of this novel material consists of a liquid amine, e.g., polyethyleneimine (PEI), chemically bonded to polymethyl methacrylate with poly(ethyleneglycol), a second liquid phase, used to enhance mass transfer (107). This solid amine adsorbent has a reversible CO_2 capacity of around 0.9 mol/kg at 25°C and 15.2 torr of CO_2, it can be regenerated using PSA at a moderate vacuum of 1 torr, and its capacity markedly improves in the presence of water vapor (107).

More recently, Song and co-workers at Pennsylvania State University, in a series of works (108–110), have been developing a similar reversible solid amine based adsorbent for CO_2 using MCM-41 as the support and PEI as the CO_2 active amine. Depending on the Si/Al ratio of the MCM-41 and the loading of PEI ranging from 30 to 75 wt%, typical CO_2 adsorption capacities range from 1.5 to 3.0 mol/kg at 75°C and 1 atm of CO_2, with complete reversibility achieved simply by purging with pure N_2 at 75°C (109). However, the adsorption and desorption kinetics are generally quite slow with 150 min required in each case. Most recently they investigated its effectiveness for treating simulated flue gas comprised of 14.9, 4.25, and 80.85 vol% CO_2, O_2 and N_2, respectively (110). The results at 75°C were encouraging with CO_2/N_2 selectivites of over 1000 and CO_2/O_2 selectivites of over 180. This supported solid amine based adsorbent has limited applications, however, as it is unstable at 100°C.

MEMBRANES

A wide variety of membrane materials and membrane gas contactors are being developed for gas separation and purification applications involving CO_2. A survey of the recent literature is given below. The latest developments in polymeric, facilitated transport, inorganic, and hybrid organic/inorganic membranes are reviewed. This is followed by a brief assessment of hollow fiber gas-liquid contactors. Ideas presented in these studies have the potential for both near term and longer term impact of membrane applications on the removal of CO_2 from process streams, including flue gas or combustion gas streams. Tables 9–11, respectively, provide the permeability and permeance of membrane materials used for CO_2 separation, the permeability and permeance of membrane materials for facilitated transport, and the trans-membrane flux data

for different capillary hollow fiber membrane contactors reported in the literature.

Polymeric Membranes

Polymeric membranes are attractive because they can be manufactured into units with very high surface areas, either in the form of hollow fibers arranged in the shell and tube configuration (85% of the market) or in the form of flat sheets packaged as spiral-wound modules, with less area but more resilience against adverse conditions (11,12,16). There are two types of polymeric membranes. Those that are referred to as glassy polymeric membranes have a glass transition temperature that is higher than room temperature. In contrast, those that have a glass transition temperature that is well below room temperature are referred to as rubbery polymeric membranes. Table 9 summarizes the permeability and permeance obtained with these kinds of membrane materials when used for CO_2 separation.

Most commercial membrane systems in gas separations are based on glassy polymeric materials as opposed to their rubbery counterparts, because of their superior mechanical properties and overall permeability-selectivity tradeoffs (111–113). Common glassy polymeric materials include polysulfones (114–124), polyimides (113,125–147), polyaramides and polycarbonates (148–151), polyphenylene oxides (PPO) (152–160), and cellulose derivatives (161–165). Although there are less than 10 commercial membrane processes available today (11,12), these glassy polymeric membranes are still receiving significant attention in the literature (166–173).

As indicated earlier, the selectivity of a large fraction of glassy polymeric membranes depends largely on their ability to discriminate gas species by size and diffusivities through the membrane structure. Such ability is for a large group of glassy polymeric membranes consistent with the solution-diffusion model (11–16,174–177). In the solution-diffusion model the transport of molecules is regulated mainly by thermal oscillations of the semi-rigid polymer structure that allows diffusion selectivities based upon subtle changes in size. However, there is a small fraction of stiff glassy polymeric materials (described below), where the diffusion selectivity is governed by a size selection mechanism similar to that found in inorganic molecular sieves (175–184).

Because the performance of most glassy polymers is structure dependent, physical or chemical attacks upon it can lead to a significant deterioration of performance. Glassy membranes that become overexposed for extended periods of time to large concentrations of CO_2 or even traces

Table 9. Permeabilities and permeances of membrane materials used for CO_2 separations

	*	T (°C)	Units	Permeances and permeabilities						Selectivities				Reference
				He	H_2	N_2	O_2	CH_4	CO_2	CO_2/He	CO_2/H_2	CO_2/N_2	CO_2/CH_4	
ORGANIC MEMBRANES														
Polyacetylenes														
R groups														
$R = H$; $R' = C(CH_3)_4$	S	25	Barrer	180	300	43	130	85	560	3.11	1.87	13.02	6.59	(227)
$R = CH_3$; $R' = CH(CH_3)_2$ (PMP)	S	25	Barrer	2630	5800	1330	2700	2900	10700	4.07	1.84	8.05	3.69	(227)
$R = CH_3$; $R' = CH(CH_3)_2$ (PMP)	S	35	Barrer	2650	5640	1250	2460	2690	9090	3.43	1.61	7.27	3.38	(216)
$R = CH_3$; $R' = CH_2CH(CH_3)_2$ (P5M2H)	S	35	Barrer	460	750	93	245	190	900	1.96	1.20	9.68	4.74	(216)
$R = CH_3$; $R' = CH_2CH_2CH(CH_3)_2$(P6M2H)	S	35	Barrer	240	370	51	130	112	390	1.63	1.05	7.65	3.48	(216)
$R = CH_3$; $R' = SiMe_3$ (PTMSP)	S	25	Barrer		18000	7000	11000		41000		2.28	5.86		(228)
$R = CH_3$; $R' = SiMe_3$ (PTMSP)	M	23	Barrer		11800	5700			18200		1.54	3.19		(219)
$R = CH_3$; $R' = SiMe_3$ (PTMSP)	S	35	Barrer	5080		4970	7730	13000	28000	5.51		5.63	2.15	(113)
$R = CH_3$; $R' = SiMe_3$ (PTMSP)	S	25	Barrer	2200	5200	1800	3000	4300	19000	8.64	3.65	10.56	4.42	(113)
$R = H$; $R' =$ t-Bu	S	25	Barrer	180	300	43	130	85	560	3.11	1.87	13.02	6.59	(113)
$R = H$; $R' = CH_3$; 'Poly(cis-isoprene)	S	35	Barrer	100		35.9	91	150	520	5.20		14.48	3.47	(113)
$R = CH_3$; $R' = Si(CH_3)_2CH_2Si(CH_3)_3$	S	25	Barrer	180	270	21	75	45	310	1.72	1.15	14.76	6.89	(113)

(*Continued*)

Table 9. Continued

				Permeances and permeabilities						Selectivities				
	*	T (°C)	Units	He	H_2	N_2	O_2	CH_4	CO_2	CO_2/He	CO_2/H_2	CO_2/N_2	CO_2/CH_4	Reference
R = H; R′ = o-$C_6H_4Si(CH_3)_3$	S	25	Barrer	170	290	24	78	38	290	1.71	1.00	12.08	7.63	(113)
R = CH_3; R′ = n-C_5H_{11}	S	35	Barrer		150	21	57	51	200		1.33	9.52	3.92	(215)
R = CH_3; R′ = n-C_6H_{13}	S	35	Barrer		140	23	60	64	230		1.64	10.00	3.59	(215)
R = CH_3; R′ = n-C_7H_{15}	S	35	Barrer		150	29	74	84	290		1.93	10.00	3.45	(215)
R = CH_3; R′ = n-C_8H_{17}	S	35	Barrer		140	29	71	83	290		2.07	10.00	3.49	(215)
R = CH_3; R′ = n-C_7H_{15}	S	25	Barrer	48	76	14	35	40	130	2.71	1.71	9.29	3.25	(213)
R = Cl; R′ = n-C_6H_{13}	S	25	Barrer	43	76	16	47	46	170	3.95	2.24	10.63	3.70	(213)
R = Cl; R′ = n-C_4H_9	S	25	Barrer	41	66	11	32	33	130	3.17	1.97	11.82	3.94	(213)
R = Cl; R′ = n-C_8H_{19}	S	25	Barrer	59	100	10	35	30	180	3.05	1.80	18.00	6.00	(213)
R = H; R′ = CH(n-C_5H_{11})$Si(CH_3)_3$	S	25	Barrer	60	84	8	27	21	120	2.00	1.43	15.00	5.71	(213)
R = H; R′ = CH(n-C_3H_7)$Si(CH_3)_2$-n-C_6H_{13}	S	25	Barrer	58	42	6.3	19	17	70	1.21	1.67	11.11	4.12	(213)
R = Ph; R′ = n-C_6H_{13}	S	25	Barrer	30	45	5.5	14	14	48	1.60	1.07	8.73	3.43	(213)
R = H; R′ = CH(n-C_3H_7)$Si(CH_3)_2$Ph	S	25	Barrer	25	29	2.5	9.5	7	54	2.16	1.86	21.60	7.71	(213)
R = CH_3; R′ = $Si(CH_3)_2$-$CH_2CH_2Si(CH_3)_3$	S	25	Barrer	130	180	14	50	28	150	1.15	0.83	10.71	5.36	(213)
R = CH_3; R′ = n-C_3H_7	S	35	Barrer		160	12	39	21	120		0.75	10.00	5.71	(215)
R = H; R′ = o-$C_6H_4CF_3$	S	25	Barrer	130	140	7.3	25	6.6	130	1.00	0.93	17.81	19.70	(213)
R = Ph; R′ = (CH_3) (PPP)	S	25	Barrer	30	43	2.2	6.3	2.8	25	0.83	0.58	11.36	8.93	(213)
R = Ph; R′ = Et	S	25	Barrer	40	57	4.5	12	4.4	40	1.00	0.70	8.89	9.09	(213)
R = Ph; R′ = Cl	S	25	Barrer	23	29	1	5.1	1.3	23	1.00	0.79	23.00	17.69	(213)
R = H; R′ = o-$C_6H_4(CH_3)$	S	25	Barrer	29	39	3	8.1	3	15	0.52	0.38	5.00	5.00	(213)
R = (CH_3); R′ = Ph (PPP)	S	25	Barrer		280	20	58		260		0.93	13.00		(228)

Polyolefins														
Polystyrene	S	35	Barrer	22.4		0.52	2.9	0.78	12.4	0.55		23.85	15.90	(113)
Polytetrafluoroethylene (PTFE)	M	25	Barrer		9.8				11.7		1.19			(481)
Polyethylene	S	30	Barrer		17.3	4.2	6.3	7.7	17.9		1.03	4.26	2.32	(250)
Polystyrene	S	30	Barrer		23.8	0.6	2.4	0.8	10.4		0.44	17.33	13.00	(250)
Polybenzylmethacrylate	S	30	Barrer		11			1.4	7.9		0.72		5.64	(250)
Polymethylmethacrylate	S	30	Barrer		2.4	1.2	3.3	0.6	0.6		0.25	0.50	1.00	(250)
Polyvinylacetate	S	30	Barrer		15.1	1.3	2.3	0.9	13.1		0.87	10.08	14.56	(250)
Polyethylene: Polyvinylalcohol	S	30	Barrer		0.5	0.3	0.2	0.2	0.2		0.40	0.67	1.00	(250)
Polyvinylidenefluoride	S	30	Barrer		2.4	0.7	1.4	1.3	1.2		0.50	1.71	0.92	(250)
Polyvinyltrimethylsilane (PVTMS)	S	25	Barrer		200	11	44	14	200		1.00	18.18	14.29	(113)
Poly(ethyl methacrylate)	S	35	Barrer	23.8		0.33	1.9	0.35	7.01	0.29		21.24	20.03	(113)
Poly(methyl methacrylate)	S	35	Barrer	8.4		0.02	0.14	0.0052	0.62	0.07		31.00	119.23	(113)
PVTMS	S	20–25	GPU	762		138		156	746	0.98		5.41	4.78	(482)
PVTMS (silicone coated)	S	20–25	GPU	473		52		90	450	0.95		8.65	5.00	(482)
PVTMS (silicone coated & fluorinated)	S	20–25	GPU	120		3.4		1	110	0.92		32.35	110.00	(482)
Poly(2-hydroxyethyl methacrylate)/alumina	S	Room	Barrer	15	23	7.9	7.2	10.6	7	0.47	0.30	0.89	0.66	(249)
Polydienes														
Polychloroprene	M	25	Barrer		13.6				25.8		1.90			(481)
Polybutadiene	M	25	Barrer		42				138		3.29			(481)
Silicones														
Poly(dimethylsiloxane)	M	23	Barrer		950	380		850	3200		3.37	8.42	3.76	(219)
Poly(dimethylsiloxane)	S	30	Barrer		375	299	540	600	1300		3.47	4.35	2.17	(250)
PDMS	S	23	Barrer		890	400	800	1200	3800		4.27	9.50	3.17	(364)
Poly(dimethylsiloxane) (PDMS)	S	35	Barrer	590		351	781	1430	4550	7.71		12.96	3.18	(113)

(*Continued*)

Table 9. Continued

				Permeances and permeabilities						Selectivities				
	*	T (°C)	Units	He	H_2	N_2	O_2	CH_4	CO_2	CO_2/He	CO_2/H_2	CO_2/N_2	CO_2/CH_4	Reference
Poly(methylpropylsiloxane)	S	35	Barrer					531	1520				2.86	(113)
Poly(methyloctylsiloxane)	S	35	Barrer					314	917				2.92	(113)
Poly(trifluoropropyl-methylsiloxane)	S	35	Barrer					201	1210				6.02	(113)
Poly(benzilmethylsiloxane)	S	35	Barrer					36.3	226				6.23	(113)
$[(CH_3)_2Si(CH_2)_6$-$Si(CH_3)_2O]_x$	S	35	Barrer					395	1310				3.32	(113)
$[(CH_3)_2SiCH_2]_x$	S	35	Barrer					130	542				4.17	(113)
$[(CH_3)_2Si$-p-C_6H_4Si-$(CH_3)_2O]_x$	S	35	Barrer					10.4	52.3				5.03	(113)
Polyethers														
Pol(ethylene oxide) PEO	S	25	Barrer		0.81	0.07	0.26	0.19	9.5		11.73	135.71	50.00	(174)
Pol(ethylene oxide) PEO	S	35	Barrer		1.8	0.24	0.68	0.7	17		9.44	70.83	24.29	(174)
PEO	S	35	Barrer		10	2			100		10.00	50.00		(255)
Poly (phenylene oxide) (PPO)	S	Room	Barrer			3.52	16.71	4.59	80.1			22.76	17.45	(256)
PPO 20% brominated	S	Room	Barrer			3.62	18.24	3.98	88.69			24.50	22.28	(256)
PPO 40% brominated	S	Room	Barrer			5.03	23.13	5.33	118.42			23.54	22.22	(256)
PPO 60% brominated	S	Room	Barrer			4.88	24.57	5.7	139.3			28.55	24.44	(256)
Sulfonated PPO	S	Room	Barrer				4.1		33.6					(256)
Sulfonated PPO 20% brominated	S	Room	Barrer			1.53	9.09	0.67	39.8			26.01	59.40	(256)
Sulfonated PPO 40% brominated	S	Room	Barrer			0.79	5.17	0.53	27.22			34.46	51.36	(256)
Sulfonated PPO 60% brominated	S	Room	Barrer			2.92	15.96	3.83	112.5			38.53	29.37	(256)

Polysulfones													
Bisphenol-A polysulfone (PSf)	S	35	Barrer		14	1.4			5.6		0.40	4.00	(256)
PSf	S	30	Barrer		12.1	0.8	1.7	0.4	6.1		0.50	7.63	15.25	(251)
PSf	S	35	Barrer	10.8		0.19	1.2	0.18	4.6	0.43		24.21	25.56	(113)
PSf	S	25	Barrer					5.3–8.8	23.7–68.7				5.00–8.00	(118)
PSf	S	25	Barrer					0.95–1.4	38.1–58.1				40.00	(118)
PSf	S	25	Barrer					0.36–1.06	13.7–35.7				35.00	(118)
PSf	S	25	Barrer					0.38–0.81	20.8–43.4				55.00	(118)
PSf	S	22	Barrer		5.8–23.8				3.6–8.5		0.65			(124)
PSf aldehyde (PSFCHO)	S	22	Barrer		6.7–8.2				3.8–4.3		0.55			(124)
PSFCHO/3A zeolite	S	22	Barrer		14.2–136				5.0–10.7		0.35			(124)
PSFCHO/5A zeolite	S	22	Barrer		32.6				11.9		0.37			(124)
Polyaryleneethers														
6FPT-6FBPA	S	35	Barrer		41.9	2.18	6.96	1.58	25.29		0.60	11.60	16.01	(169)
6FPT-BPA	S	35	Barrer		28.8	1.37	4.76	1.41	18.53		0.64	13.53	13.14	(169)
6FPPy-6FBPA	S	35	Barrer		50.1	2.39	7.9	1.92	29.46		0.59	12.33	15.34	(169)
6FPPy-BPA	S	35	Barrer		41.2	1.7	5.6	1.78	21.44		0.52	12.61	12.04	(169)
Polyesters														
BisA w/High KOH conc.	M	Room	GPU	5.5				0.545	12.00	2.18			22.00	(483)
DHBP w/High KOH conc.	M	Room	GPU	2				0.075	2.40	1.20			32.00	(483)
DHDPE w/High KOH conc.	M	Room	GPU	4.3				0.390	8.20	1.91			21.00	(483)
TBBA w/High KOH conc.	M	Room	GPU	3				0.480	12.00	4.00			25.00	(483)
TCHFBA w/High KOH conc.	M	Room	GPU	69				10.952	230.00	3.33			21.00	(483)
TDP w/High KOH conc.	M	Room	GPU	4.3				0.319	8.60	2.00			27.00	(483)
TMBA w/High KOH conc.	M	Room	GPU	6.8				0.486	17.00	2.50			35.00	(483)
BisF w/Low KOH conc.	M	Room	GPU	32				31.667	38.00	1.19			1.20	(483)
BisA w/Low KOH conc.	M	Room	GPU	2.8				0.061	2.00	0.71			33.00	(483)
DHBP w/Low KOH conc.	M	Room	GPU	2				0.034	1.80	0.90			53.00	(483)
DHDPE w/Low KOH conc.	M	Room	GPU	22				17.500	21.00	0.95			1.20	(483)

(*Continued*)

Table 9. Continued

				Permeances and permeabilities						Selectivities				
	*	T (°C)	Units	He	H_2	N_2	O_2	CH_4	CO_2	CO_2/He	CO_2/H_2	CO_2/N_2	CO_2/CH_4	Reference
BHPF w/High KOH conc.	M	Room	GPU	1.9				0.072	1.80	0.95			25.00	(483)
TBBA w/Low KOH conc.	M	Room	GPU	1.9				0.038	1.80	0.95			48.00	(483)
TDP w/Low KOH conc.	M	Room	GPU	4.2				0.065	2.00	0.48			31.00	(483)
TMBA w/Low KOH conc.	M	Room	GPU	2.2				0.067	1.00	0.45			15.00	(483)
SDP w/Low KOH conc.	M	Room	GPU	11				3.296	8.9	0.81			2.70	(483)
Polycarbonates														
Bisphenol-A polycarbonate	S	35	Barrer	13		0.38	1.6	0.36	6.8	0.52		17.89	18.89	(113)
Polysilmethylenes														
Poly(dimethyl silmethylene)	S	35	Barrer	43.4		14.5	37.5	47.4	191	4.40		13.17	4.03	(113)
Cellulose based														
Ethyl cellulose	S	35	Barrer	39.8		3.4	12.4	6.8	75	1.88		22.06	11.03	(113)
Cellulose acetate	M	25	Barrer		3.5				22.7		6.49			(481)
Cellulose acetate	M	−20	Barrer		3.5				22.6		6.46			(481)
Cellulose acetate	S	35	Barrer	16		0.15	0.82	0.15	4.75	0.30		31.67	31.67	(113)
Polyimides														
PI-1/PTMSP	S	25	GPU		30.1	4.2	11.9		60.9		2.02	14.50		(484)
PI-1/PTMSP	S	25	GPU		7.2	0.64	2.27		12.3		1.71	19.22		(484)
PI-2/PTMSP	S	25	GPU		2.76	0.28	0.91		5.02		1.82	17.93		(484)
PI-3/PTMSP	S	25	GPU		2.39	0.25	0.84		4.35		1.82	17.40		(484)
BDCDA-MPD	S	30	Barrer		15.4	0.13	1	0.1	3.7		0.24	28.46	37.00	(140)
BDCDA-DDSO	S	30	Barrer		12.9	0.14	0.93	0.12	4.2		0.33	30.00	35.00	(140)
HDCDA-6 F	S	30	Barrer		23.1	0.12	1.06	0.1	4.1		0.18	34.17	41.00	(140)
PDCDA-6 F	S	30	Barrer		25	0.18	1.2	0.16	5		0.20	27.78	31.25	(140)
BDCDA-6 F	S	30	Barrer		41.5	0.64	3.8	0.4	15.6		0.38	24.38	39.00	(140)
PMDA-ODA	S	35	Barrer	8		0.1	0.61	0.059	2.71	0.34		27.10	45.93	(113)
PMDA-MDA	S	35	Barrer	9.4			0.98	0.1	4.03	0.43			40.30	(113)
PMDA-IPDA	S	35	Barrer	37.1			7.1	0.9	26.8	0.72			29.78	(113)

6FDA-ODA	S	35	Barrer	51.5			4.34	0.38	23	0.45			60.53	(113)
6FDA-MDA	S	35	Barrer	50			4.6	0.43	24.2	0.48			56.28	(113)
6FDA-IPDA	S	35	Barrer	71.2			7.53	0.7	30	0.42			42.86	(113)
6FDA-DAF	S	35	Barrer	98.5			7.85		32.2	0.33				(113)
PMDA-m′pODA	S	35	Barrer		5.92	0.045	0.31	0.0258	1.18		0.20	25.99	45.74	(113)
PMDA-p′pODA	S	35	Barrer		10.6	0.145	0.825	0.0937	3.55		0.33	24.48	37.89	(113)
PMDA-BAPHF	S	35	Barrer		34.3	0.943	4.98	0.638	17.6		0.51	18.66	27.59	(113)
PMDA-BATPHF	S	35	Barrer		50.4	1.5	7.06	0.937	24.6		0.49	16.40	26.25	(113)
BPDA-p′pODA	S	35	Barrer		3.68			0.0099	0.642		0.17		64.85	(113)
BPDA-BAPHF	S	35	Barrer		17.3	0.245	1.54	0.145	4.96		0.29	20.24	34.21	(113)
BPDA-BATPHF	S	35	Barrer		30.6	0.563	3.11	0.279	9.15		0.30	16.25	32.80	(113)
BPDA-BAHF	S	35	Barrer		59.1	1.39	7.1	0.78	27.7		0.47	19.93	35.51	(113)
BTDA-p′pODA	S	35	Barrer		4.79	0.024	0.191	0.0109	0.625		0.13	26.48	57.34	(113)
BTDA-BAPHF	S	35	Barrer		16.1	0.195	1.14	0.105	4.37		0.27	22.41	41.62	(113)
BTDA-BATPHF	S	35	Barrer		24.6	0.37	2.17	0.189	6.94		0.28	18.76	36.72	(113)
BTDA-BAHF	S	35	Barrer		30.8	0.45	2.5	0.226	10.1		0.33	22.44	44.69	(113)
6FDA-m′pODA	S	35	Barrer		23.7	0.259	1.57	0.125	6.11		0.26	23.59	48.88	(113)
6FDA-APAP	S	35	Barrer		38.2	0.473	2.89	0.217	10.7		0.28	22.62	49.31	(113)
6FDA-p′pODA	S	35	Barrer		40.7	0.733	3.88	0.341	16.7		0.41	22.78	48.97	(113)
6FDA-BAPHF	S	35	Barrer		47.4	0.981	5.13	0.52	19.1		0.40	19.47	36.73	(113)
6FDA-BATPHF	S	35	Barrer		55.4	1.3	6.5	0.703	22.8		0.41	17.54	32.43	(113)
6FDA-BAHF	S	35	Barrer		108	3.11	14.2	1.34	51.2		0.47	16.46	38.21	(113)
6FDA-TADPO (polypyrrolone)	S	35	Barrer	89			4.34		23	0.26				
6FDA-HAB	S	35	Barrer					0.071	7.83				110.28	(146)
6FDA-durene	S	35	Barrer	490	786	55.4	186	45.1	612	1.25	0.78	11.05	13.57	(129)
6FDA-6FpDA-8%–DABA	S	30	Barrer	178		10	36	6	84	0.47		8.40	14.00	(129)
6FDA-6FpDA-8%–DABA:Aluminophoshate (95:5)	S	30	Barrer	148		6.2	24	3.6	66	0.45		10.65	18.33	(129)
6FDA-6FpDA-8%–DABA:Aluminophoshate (90:10),1	S	30	Barrer	94.4		2.1	18.5	1.3	51	0.54		24.29	39.23	(129)

(*Continued*)

Table 9. Continued

				Permeances and permeabilities						Selectivities				
	*	T (°C)	Units	He	H_2	N_2	O_2	CH_4	CO_2	CO_2/He	CO_2/H_2	CO_2/N_2	CO_2/CH_4	Reference
6FDA-6FpDA-8%–DABA:Aluminophoshate (90:10),2	S	30	Barrer	67.5		1.2	9.3	0.7	28.3	0.42		23.58	40.43	(129)
Matrimid 5218	S	35	Barrer			0.32	2.12	0.28	10			31.25	35.71	(312)
Matrimid 5218	M	20–25	GPU	83.2				0.57	28.5	0.34			50.00	(482)
Matrimid 5218 (Fluorinated)	M	20–25	GPU	77				0.2	18.7	0.24			93.50	(482)
Polyphosphotens														
Pendant groups: 2-(2-methoxyethoxy)ethanol: 4Methoxyphenol: 2-Allylphenol														
6:75:19	S	30	Barrer	4.7	4.2	0.3	1.7	1.4	9.3	1.98	2.21	31.00	6.64	(265)
23:72:5	S	30	Barrer	9.7	13.4	1.8	4.8	3.6	38.9	4.01	2.90	21.61	10.81	(265)
25:59:16	S	30	Barrer	15.1	19.4	2.8	7.7	7.1	81.9	5.42	4.22	29.25	11.54	(265)
38:46:16	S	30	Barrer	16.8	25.6	3.9	10.2	13.9	107.7	6.41	4.21	27.62	7.75	(265)
48:48:4	S	30	Barrer	16.6	23.7	8.3	14.8	16	115.9	6.98	4.89	13.96	7.24	(265)
74:24:2	S	30	Barrer	21.9	28.8	10.2	18	19.2	226.7	10.35	7.87	22.23	11.81	(265)
100:0:0	S	30	Barrer	17	25	4	7	11	250	14.71	10.00	62.50	22.73	(265)
R Group														
PPOP	S	30	Barrer		7.5	1.3	2.1	1.2	4.8		0.64	3.69	4.00	(238)
PTBP	S	30	Barrer		23	2.4	8.2	1.7	17		0.74	7.08	10.00	(238)
PBTBP:Cl (20:80)	S	30	Barrer		75	3	11	5	27		0.36	9.00	5.40	(238)
Other Polymers														
Cytop	S	35	Barrer	1270	620	34	130	11	300	0.24	0.48	8.82	27.27	(147)
Poly(3-(2-acetoxyethyl) thiophene) (P3AcET)	S	20	Barrer			22	111	36	668			30.36	18.56	(147)

Poly(3-(2-hydroxyethyl) thiophene) (P3AcET),1	S	20	Barrer			5	63	14	281			56.20	20.07	(147)
Poly(3-(2-hydroxyethyl) thiophene) (P3AcET),2	S	20	Barrer			5	60	8	336			67.20	42.00	(147)
Copymers														
Ether-Olefin														
Poly(propylene glycol) diacrylate (PPGDA) 540	S	23	Barrer		15	2	5		30		2.00	15.00		(239)
PPGDA900	S	23	Barrer		33	7	15		110		3.33	15.71		(239)
Poly(ethylene glycol) diacrylate (PEGDA) 575	S	23	Barrer		7.2		1.8	0.73	39		5.42		53.42	(239)
PEGDA575 + 10 wt% fumed silica	S	23	Barrer		5.3		1.4	0.6	32		6.04		53.33	(239)
PEGDA700	S	23	Barrer		8.5		3	1	72		8.47		72.00	(239)
PEGDA700+10 wt% fumed silica	S	23	Barrer		7.2		3.1	0.9	68		9.44		75.56	(239)
PEGDMA/alumina	S	Room	Barrer	6.7	7.5	1	1.5	1.1	19	2.84	2.53	19.00	17.27	(249)
poly(tetramethylene oxide) (PTMEO):nylon (PEA)12 (80:20)	S	35	Barrer		59.73	9.44			221		3.70	23.40		(253)
PTMEO:PEA12 (53:47)	S	35	Barrer		32.29	5.54			113		3.50	20.40		(253)
PEO:PA6 (55:45)	S	35	Barrer		12.24	2.33			120		9.80	51.40		(253)
PEO:PA12 (57:43)	S	35	Barrer		8.46	1.17			66		7.80	56.40		(253)
Methoxy PEG acrylate (MePEGA)0/Polyacrylonitrile (PAN)	S	30	GPU			0.658			6.45			9.80		(252)
MePEGA2/PAN	S	30	GPU			0.186			6.14			33.00		(252)
MePEGA4/PAN	S	30	GPU			0.159			5.4			34.00		(252)
MePEGA6/PAN	S	30	GPU			0.174			5.65			32.40		(252)

(*Continued*)

Table 9. Continued

				Permeances and permeabilities						Selectivities				
	*	T (°C)	Units	He	H_2	N_2	O_2	CH_4	CO_2	CO_2/He	CO_2/H_2	CO_2/N_2	CO_2/CH_4	Reference
MePEGA8/PAN	S	30	GPU			0.180			5.87			32.60		(252)
MePEGA10/PAN	S	30	GPU			0.206			6.36			30.90		(252)
MePEGA12/PAN	S	30	GPU			0.239			7.06			29.50		(252)
MePEGA14/PAN	S	30	GPU			0.684			7.52			11.00		(252)
MePEGA16/PAN	S	30	GPU			1.532			9.04			5.90		(252)
MePEGA18/PAN	S	30	GPU			3.570			9.64			2.70		(252)
PEGDA/Poly(ethylene glycol) methyl ether acrylate (PEGMEA) (100:0)	S	35	Barrer			2.15			112			52.00		(234)
PEGDA/PEGMEA (80:20)	S	35	Barrer			2.59			150			58.00		(234)
PEGDA/PEGMEA (50:50)	S	35	Barrer			6.10			250			41.00		(234)
PEGDA/PEGMEA (30:70)	S	35	Barrer			6.81			320			47.00		(234)
PEGDA/PEGMEA (9:91)	S	35	Barrer			12.68			520			41.00		(234)
PEGDA/PEGMEA (1:99)	S	35	Barrer			13.90			570			41.00		(234)
PEG dimethacrylate(DM) 14:PEG methyl ether methacrylate (MM)9 (100:0)	S	35	Barrer			1.23			65			53.00		(254)
DM14:MM9 (90:10)	S	35	Barrer			1.57			85			54.00		(254)
DM14:MM9 (70:30)	S	35	Barrer			2.53			129			51.00		(254)
DM14:MM9 (50:50)	S	35	Barrer			3.70			185			50.00		(254)
DM14:MM9 (30:70)	S	35	Barrer			5.42			260			48.00		(254)
DM9:MM9 (90:10)	S	35	Barrer			0.53			28			53.00		(254)
DM23:MM9 (90:10)	S	35	Barrer			3.73			194			52.00		(254)
2,2-bis(4-methacryloxy polyethoxy phenyl)propane (DB) 30:MM9 (100:0)	S	35	Barrer			2.61			128			49.00		(254)

DB30:MM9 (90:10)	S	35	Barrer		2.80	140		50.00	(254)
DB30:MM9 (70:30)	S	35	Barrer		3.63	185		51.00	(254)
DB30:MM9 (50:50)	S	35	Barrer		4.81	231		48.00	(254)
DB30:MM9 (30:70)	S	35	Barrer		6.55	308		47.00	(254)
DB10:MM9 (90:10)	S	35	Barrer		0.25	12		48.00	(254)
Ether-Ether									
EO:2-(2-methoxyethoxy) ethyl glycidyl ether (EM-2):allyl glycidyl ether (AGE) (94:4:2)	S	35	Barrer	20	4	250	12.50	62.50	(255)
Ethylene oxide (EO):propylene oxide (PO):AGE (83:16:1)	S	35	Barrer	30	5	220	7.33	44.00	(255)
EO:epichlorohydrin (EP):AGE (56:39:5)	S	35	Barrer	30	6	260	8.67	43.33	(255)
PO:EP:3-glycidoxy-propyltrimethoxysilane (GPTMS) (35:63:2)	S	35	Barrer	30	6	270	9.00	45.00	(255)
EO:AGE (92:8)	S	35	Barrer	30	5	350	11.67	70.00	(255)
EP:AGE (94:6)	S	35	Barrer	20	6	250	12.50	41.67	(255)
EO:GPTMS (95:5)	S	35	Barrer	40	6	380	9.50	63.33	(255)
EO:PO (90:10)	S	35	Barrer	45	6	400	8.89	66.67	(255)
EO:EM-2 (78:22)	S	35	Barrer	38	7	610	16.05	87.14	(255)
Ester-Ether									
PEG-1500: 1,4-butanediol:DMT	S	35	Barrer	28.2		262	9.29		(173)
PEG-1500:1,4-butanediol: 2,6 DMN	S	33	Barrer	30.6		333	10.88		(173)
PEG-1500:1,3-propanediol:DMCH	S	33.5	Barrer	35.8		353	9.86		(173)

(*Continued*)

Table 9. Continued

	*	T (°C)	Units	Permeances and permeabilities						Selectivities				Reference
				He	H_2	N_2	O_2	CH_4	CO_2	CO_2/He	CO_2/H_2	CO_2/N_2	CO_2/CH_4	
PEG-1500:1,3-propanediol:SBMB	S	36	Barrer		23.1				237		10.26			(173)
PEG-1500:1,3-propanediol:DMBPD	S	33	Barrer		45.3				322		7.11			(173)
PEG-2000:1,2-ethyleneglycol:2,6-DMN	S	33	Barrer		5.6				59.3		10.59			(173)
Diene-Olefin														
Poly(butadiene-styrene)	S	35	Barrer	32.9		10.3	32.9	34.2	171	5.20		16.60	5.00	(113)
Polyvinyl-butadiene	S	30	Barrer		7.9	1.8	0.6	2.5	15.3		1.94	8.50	6.12	(250)
Poly(acrylonitrile-butadiene)	M	25	Barrer		25.2				63.1		2.50			(481)
Ether-Urethane														
PU1	M	35	Barrer					8.1–11.2	77.5–55.8				5.0–9.	(172)
PU3	M	35	Barrer					4.7–5.1	58.8–62.2				12.2–12.5	(172)
Ether-Urethane urea														
PU2	M	35	Barrer					32.5–34.7	195–197				5.6–6.0	(172)
PU4	M	35	Barrer					2.7–3.4	44.7–50.8				15.0–16.6	(172)
Copolyimides														
Teflon AF2400 (Hyflon AD87)	S	25	Barrer	3600	3400	780	1600	600	3900	1.08	1.15	5.00	6.50	(485)
BTDA-TDI/MDI (80:20) (P84)	S	25	Barrer	7.2		0.024	0.24	0.0246	0.99	0.14		41.25	40.24	(131)
Hyflon AD60	S	35	Barrer	1360	790	52	180	17.6	433	0.32	0.55	8.33	24.60	(150)
Hyflon AD60	S	22	Barrer					27	460				17.04	(150)
Hyflon AD80	S	22	Barrer					125	1620				12.96	(150)
Polysulfone:poly	S	25	GPU		140	1.3	8.1	0.77	40		0.29	30.77	51.95	(123)

(4-vinylpyridine):Silcon Rubber (25:0.1:3)												
Polysulfone:poly (4-vinylpyridine):Silcon Rubber (25:0.2:3)	S	25	GPU	90	0.92	6.7	0.48	40	0.44	43.48	83.33	(123)
Polysulfone:poly (4-vinylpyridine):Silcon Rubber (25:0.5:3)	S	25	GPU	74	0.65	4.9	0.44	24	0.32	36.92	54.55	(123)
Polysulfone:poly (4-vinylpyridine):Silcon Rubber (25:1.0:3)	S	25	GPU	54	0.59	3.4	0.36	16	0.30	27.12	44.44	(123)
Polysulfone:poly (4-vinylpyridine):Silcon Rubber (23:0.2:3)	S	25	GPU	132	1.3	8.6	0.87	51	0.39	39.23	58.62	(123)
Polysulfone:poly (4-vinylpyridine):Silcon Rubber (21:0.5:3)	S	25	GPU	96	1.6	7.5	1.8	40	0.42	25.00	22.22	(123)
Polysulfone:poly (4-vinylpyridine):Silcon Rubber (21:1.0:3)	S	25	GPU	81	1.1	5.3	0.99	28	0.35	25.45	28.28	(123)
Polysulfone:poly (4-vinylpyridine):Silcon Rubber (21:2.0:3)	S	25	GPU	20	0.4	2.1	0.26	8.8	0.44	22.00	33.85	(123)
Polysulfone:poly (4-vinylpyridine):Silcon Rubber (17:2.0:3)	S	25	GPU	54	3	5.2	1.9	16	0.30	5.33	8.42	(123)
INORGANIC MEMBRANES												
Zeolites												
Fau-type,1	S	50	GPU		717.44			567.97		0.79		(321)
Fau-type,2	S	50	GPU		777.23			627.76		0.81		(321)
Fau-type,3	S	50	GPU		161.42			388.61		2.41		(321)
Fau-type,4	S	50	GPU		47.83			358.72		7.50		(321)
Fau-type,5	S	50	GPU		14.65			233.17		15.92		(321)

(*Continued*)

Table 9. Continued

				Permeances and permeabilities						Selectivities				
	*	T (°C)	Units	He	H_2	N_2	O_2	CH_4	CO_2	CO_2/He	CO_2/H_2	CO_2/N_2	CO_2/CH_4	Reference
Fau-type,6	S	50	GPU			5.98			116.58			19.50		(321)
Fau-type,7	S	50	GPU			38.86			275.02			7.08		(321)
Fau-type,8	S	50	GPU			23.62			230.18			9.75		(321)
ZSM-5	S	25	GPU			2.27			104.63			46.00		(315)
ZSM-5	S	25	GPU			30.45			1644.13			54.00		(315)
Na-Y	M	30	GPU			4.48			448.40			100.00		(330)
K-Y	M	40	GPU			177.58			5380.80			30.30		(328)
Silicalite	M	180	GPU			2.54			50.82			20.00		(335)
Silicalite	M	30	GPU			38.05			209.25			5.50		(331)
K-ZSM-5	M	50	GPU			67.26			134.52			2.00		(334)
B-ZSM-5	M	27	GPU			45.08			567.97			12.60		(323)
Na-ZSM-5	M	27	GPU			567.32			7772.27			13.70		(326)
Sapo-34,1	S	24	GPU					12.26	328.83				26.83	(316)
Sapo-34,2	S	24	GPU					7.47	418.51				56.00	(316)
Sapo-34,3	S	24	GPU					4.78	418.51				87.50	(316)
Sapo-34	M	22	GPU					15.51	573.95				37.00	(317)
Sapo-34	M	22	GPU					17.58	298.93				17.00	(317)
Carbon-Silicalite composite	S	27	GPU	22.12		0.54	1.91		32.88	1.49		61.11		(322)
Sapo-34,1	S	25	GPU		203.27	37.37		110.61	179.36		0.88	4.80	1.62	(326)
Sapo-34,2	S	25	GPU		179.36	32.88		50.82	158.43		0.88	4.82	3.12	(326)
Silicas														
Silica,1	S	20	GPU			0.38			6.40			17		(318)
Silica,2	S	20	GPU			0.54			3.89			7.2		(318)
Aminosilicate,1	S	22	GPU			5.83			304.82			52.3		(319)
Aminosilicate,2	S	22	GPU			1.16			72.37			62.6		(319)
Aminosilicate,3	S	22	GPU			3.76			225.88			60.1		(319)
Aminosilicate,4	S	22	GPU			0.64			63.60			100		(319)
Aminosilicate,5	S	22	GPU			2.75			212.72			77.3		(319)

Aminosilicate,6	S	22	GPU			1.23			50.44			41		(319)
Aminosilicate,7	S	22	GPU			2.33			116.23			49.9		(319)
Aminosilicate,8	S	22	GPU			1.19			83.33			70.2		(319)
Aminosilicate,9	S	22	GPU			0.40			30.70			76.8		(319)
Aminosilicate,10	S	22	GPU			1.33			70.18			52.9		(319)
Microporous Silica	S	50	GPU	8968	14049	2989	419		10164	1.13	0.72	3.40		(319)
Microporous Silica	S	50	GPU	5381	5380	1494	50.8		2391	0.44	0.44	1.60		(486)
Carbon Molecular Sieves (precursors)														(486)
BTDA-TDI/MDI	S	25	GPU	400	1250	120	400	80	2000	5.00	1.60	16.67	25.00	(309)
BTDA-TDI/MDI (80:20) (P84)	S	25	Barrer	58.5		2.8	3		3.3	0.06		1.18		(307)
BTDA-TDI/MDI (80:20) (P84):AgSPEEK (95:5)	S	25	Barrer	161		4.6	27.5		83.3	0.52		18.11		(307)
BTDA-TDI/MDI (80:20) (P84):AgSPEEK (90.9:9.1)	S	25	Barrer	465		10.3	91.8		366	0.79		35.53		(307)
BTDA-TDI/MDI (80:20) (P84):AgSPEEK (83.3:16.7)	S	25	Barrer	361		3.9	52.7		191	0.53		48.97		(307)
BTDA-TDI/MDI (80:20) (P84):$AgNO_3$ (94:6)	S	25	Barrer	169		0.19	3		12.4	0.07		65.26		(307)
Matrimid 5218	S	35	Barrer			1.65	22	0.22	44			26.67	200.00	(390)
Matrimid 5218,1	S	25	Barrer	18		0.8	4.5	0.37	12	0.67		15.00	32.43	(145)
Matrimid 5218,2	S	25	Barrer	70		2.5	7.5	2	10	0.14		4.00	5.00	(145)
Matrimid 5218,3	S	25	Barrer	22		0.72	3.1	0.72	8.5	0.39		11.81	11.81	(145)
Kapton	S	25	Barrer	9		0.15	1.15	0.15	2	0.22		13.33	13.33	(145)
PMDA-ODA-PDM (Poly(imide-siloxane:PIS),1	S	25	Barrer	315		0.3	8		21	0.07		70.00		(305)
PMDA-ODA-PDM (Poly(imide-siloxane:PIS),2	S	25	Barrer	3416	8216	27	326		1068	0.31	0.13	39.56		(305)
PMDA-ODA-PDM (Poly(imide-siloxane:PIS),3	S	25	Barrer	610		1.4	30		84	0.14		60.00		(305)

(*Continued*)

Table 9. Continued

				Permeances and permeabilities						Selectivities				
	*	T (°C)	Units	He	H_2	N_2	O_2	CH_4	CO_2	CO_2/He	CO_2/H_2	CO_2/N_2	CO_2/CH_4	Reference
PMDA-ODA-PDM (Poly(imide-siloxane:PIS),4	S	25	Barrer	4245	9518	40	399		1509	0.36	0.16	37.73		(305)
PMDA-ODA-PDM (Poly(imide-siloxane:PIS),5	S	25	Barrer	1258		8.5	111		386	0.31		45.41		(305)
PMDA-ODA-PDM (Poly(imide-siloxane:PIS),6	S	25	Barrer	7319	12598	69	595		2526	0.35	0.20	36.61		(305)
BTDA-ODA (PI)-(PVP) blend (10:10:0),1	S	25	Barrer	1700		47	500		1500	0.88		31.91		(303)
BTDA-ODA (PI)-(PVP) blend (10:10:0),2	S	25	Barrer	1100		9	140		350	0.32		38.89		(303)
BTDA-ODA (PI)-(PVP) blend (10:10:5),1	S	25	Barrer	2000		57	550		1800	0.90		31.58		(303)
BTDA-ODA (PI)-(PVP) blend (10:10:5),2	S	25	Barrer	1250		13	160		400	0.32		30.77		(303)
BTDA-ODA (PI)-(PVP) blend (10:10:10),1	S	25	Barrer	2200		66	640		1950	0.89		29.55		(303)
BTDA-ODA (PI)-(PVP) blend (10:10:10),2	S	25	Barrer	1700		17	230		550	0.32		32.35		(303)
Matrimid 5218	S	35	Barrer			30.3	227	10	611			20.17	200.00	(310)
Matrimid 5218, MeOH pretreat	S	35	Barrer			15.8	138	4.8	423			26.77	88.13	(310)
Matrimid 5218, EtOH pretreat	S	35	Barrer			6.3	75.4	1.1	191			30.32	173.64	(310)
Matrimid 5218, PrOH pretreat	S	35	Barrer			24.1	204	6.7	565			23.44	84.33	(310)
Matrimid 5218, BuOH pretreat	S	35	Barrer			21	186	7	547			26.05	78.14	(310)

P84	S	35	Barrer			17.8	158	5.6	499			28.03	201.00	(310)
P84, MeOH pretreat	S	35	Barrer			13.6	132	3.7	402			29.56	108.65	(310)
P84, EtOH pretreat	S	35	Barrer			9	101	2	278			30.89	139.00	(310)
P84, PrOH pretreat	S	35	Barrer			14.6	144	3.9	428			29.32	109.74	(310)
BTDA-ODA-mPDA-DBA (10:8:2:0)	S	25	Barrer	2763		24	256		829	0.30		34.54		(251)
BTDA-ODA-mPDA-DBA (10:8:0:2)	S	25	Barrer	3208		49	501		1674	0.52		34.16		(251)
BTDA-ODA-mPDA-DBA (10:8:0:5)	S	25	Barrer	4193		83	707		2863	0.68		34.49		(251)
CMSM,1	S	20	GPU		2160.00	10.40	86.27		486.67		0.23	46.79		(298,299)
CMSM,2	S	20	GPU		1680.00	7.47	63.33		288.00		0.17	38.57		(298,299)
CMSM,3	S	20	GPU		2093.33	13.33	141.33		792.00		0.38	59.40		(298,299)
CMSM,4	S	20	GPU		1893.33	8.13	97.33		530.67		0.28	65.25		(298,299)
CMSM,5	S	20	GPU		1130.67	4.40	58.53		317.33		0.28	72.12		(298,299)
Surface Flow (adsorption Selective membranes)														
Carbonized latex-graphite, MI	M	25	Barrer					350	1130				3.23	(481)
Carbonized latex-graphite, MI	M	−20	Barrer					240	1080				4.50	(481)
Carbonized latex-graphite, MII	M	25	Barrer					250	1800				7.20	(481)
Carbonized latex-graphite, MII	M	−15	Barrer					58	1500				25.86	(481)
Carbonized latex-graphite, MIIIA	S	22	Barrer	22	150			335	631	28.68	4.21		1.88	(481)
Carbonized latex-graphite, MIIIB	S	22	Barrer	31	129			663	1054	34.00	8.17		1.59	(481)
Carbonized latex-graphite, MIIIC	S	22	Barrer	28	145			551	973	34.75	6.71		1.77	(481)

(*Continued*)

Table 9. Continued

				Permeances and permeabilities						Selectivities				
	*	T (°C)	Units	He	H_2	N_2	O_2	CH_4	CO_2	CO_2/He	CO_2/H_2	CO_2/N_2	CO_2/CH_4	Reference
Carbonized phenolic resin	S	25	GPU	239		329	448	836	1195	5.00		3.64	1.43	(357)
HDFS in Vycor	S	20	GPU	1.01	0.52	0.34		0.56	2.1	2.07	4.03	6.12	3.74	(352)
ODS in g-Alumina	S	20	GPU		38	11		17	60		1.58	5.45	3.53	(359)
$C_nH_{2n+1}(CH_3)_2SiCl$ in porous glass, n = 18	S	25	GPU	0.051		0.028			0.284	5.59		10.00		(263)
$C_nH_{2n+1}(CH_3)_2SiCl$ in porous glass, n = 8	S	25	GPU	0.358		0.299			0.538	1.50		1.80		(263)
$C_nH_{2n+1}(CH_3)_2SiCl$ in porous glass, n = 3	S	25	GPU	3.58		2.09			2.69	0.75		1.29		(263)
$C_nH_{2n+1}(CH_3)_2SiCl$ in porous glass, n = 1	S	25	GPU	5.38		2.99			3.88	0.72		1.30		(263)
Novolak-phenolic resin-N-methyl-2-pyrrolidone,1	S	25	GPU		151.86	39.04		68.51	335.70		2.21	8.60	4.90	(357)
Novolak-phenolic resin-N-methyl-2-pyrrolidone,1	S	25	GPU		216.73	311.05		677.00	1150.89		5.31	3.70	1.70	(357)
Novolak-phenolic resin-N-methyl-2-pyrrolidone,1	S	25	GPU		70.25	47.10		150.02	405.05		5.77	8.60	2.70	(357)
Novolak-phenolic resin-N-methyl-2-pyrrolidone,1	S	25	GPU		248.11	83.93		134.64	646.29		2.60	7.70	4.80	(357)
Novolak-phenolic resin-N-methyl-2-pyrrolidone,1	S	25	GPU		322.55	55.98		48.87	615.80		1.91	11	12.6	(357)
Zeolite-T	S	35	GPU	10.46	23.91	5.38		0.42	89.68	8.57	3.75	16.67	214.29	(353,354)

DDR-zeolite	S	18	GPU	29.89	119.57	14.95	26.90	0.34	239.15	8.00	2.00	16.00	703.37	(356)
Sapo-34,3	S	25	GPU	119.57	248.11	65.77		20.93	448.40	3.75	1.81	6.82	21.43	(326)
SSZ-13 Zeolite,1	S	25	GPU		403.56	89.68		44.84	478.29		1.19	5.33	10.67	(358)
SSZ-13 Zeolite,2	S	25	GPU		388.61	134.52		80.71	627.76		1.62	4.67	7.78	(358)
SSZ-13 Zeolite,3	S	25	GPU		553.03	107.62		113.59	702.49		1.27	6.53	6.18	(358)
SSZ-13 Zeolite,4	S	25	GPU		463.35	134.52		89.68	553.03		1.19	4.11	6.17	(358)
SSZ-13 Zeolite,5	S	25	GPU		463.35	134.52		74.73	702.49		1.52	5.22	9.40	(358)
HYBRID ORGANIC-INORGANIC MEMBRANES														
Poly(amide-6-b ethylene oxide) (PEBAX)-Silica														(204)
PEBAX:Silica (100:0)	S	25	Barrer	18.6		1.71	5.84		122	6.56		71.35		(204)
PEBAX:Silica (90:10)	S	25	Barrer	21.4		2.13	6.82		154	7.20		72.30		(204)
PEBAX:Silica (81:19)	S	25	Barrer	25.5		1.73	8.74		205	8.04		118.50		(204)
PEBAX:Silica (73:27)	S	25	Barrer	32.2		3.52	11.3		277	8.60		78.69		(204)
PDMS-pentaerythrithol triacrylate (PETA)-Silica														(364)
PDMS:PETA:Silica (11:89:0)	S	23	Barrer		479	206	441	648	1154		2.41	5.60	1.78	(364)
PDMS:PETA:Silica (10:85:5)	S	23	Barrer		647	381	665	1246	4511		6.97	11.84	3.62	(364)
PDMS:PETA:Silica (10:80:10)	S	23	Barrer		285	156	341	466	1422		4.99	9.12	3.05	(364)
Poly(ethylene glycol)(PEG)-Silica														(363)
PEG600:Silica	S	30	Barrer			0.52	1.51	1.48	23.92			46.00	16.16	(363)
PEG1000:Silica	S	30	Barrer			1.16	2.68	3.12	49.3			42.50	15.80	(363)
PEG2000:Silica	S	30	Barrer			2.46	5.56	6.01	94.2			38.29	15.67	(363)
Poly(propylene glycol) (PPG)-Silica														(363)
PPG600:Silica	S	30	Barrer			1.69	5	4.99	33.91			20.07	6.80	(363)
PPG1000:Silica	S	30	Barrer			2.54	6.73	7.3	48.37			19.04	6.63	(363)
PPG2000:Silica	S	30	Barrer			3.81	9.24	10.95	72.26			18.97	6.60	(363)

(*Continued*)

Table 9. Continued

				Permeances and permeabilities						Selectivities				
	*	T (°C)	Units	He	H_2	N_2	O_2	CH_4	CO_2	CO_2/He	CO_2/H_2	CO_2/N_2	CO_2/CH_4	Reference
(PEG-PPG-PEG) (PEPG)-Silica														(363)
PEPG2000:Silica	S	30	Barrer			3.2	8.1	10.1	83.64			26.14	8.28	(363)
PEPG2700:Silica	S	30	Barrer			4.39	10.6	13.6	110			25.06	8.09	(363)
PEPG3300:Silica	S	30	Barrer			6.59	15.76	20.18	132.3			20.08	6.56	(363)
Acrylonitrile-butadiene-sturene (ABS)/ Activated carbon 1(AC1)	S	20	Barrer					0.162–0.315	4.31–10.81				26.6–34.3	(393)
ABS/AC2	S	20	Barrer					0.264–0.406	7.49–20.50				28.4–50.5	(393)
6FDA-TAPOB hyperbranched polyimide (HBPI)-Silica														(203)
HBPI-Silica (100:0)	S	25	Barrer			0.22	1.5	0.098	7.4			26.67	75.51	(203)
HBPI-Silica (90:10)	S	25	Barrer			0.31	2	0.092	10			32.26	108.70	(203)
HBPI-Silica (80:20)	S	25	Barrer			0.32	2.1	0.08	12			37.50	150.00	(203)
HBPI-Silica (100:30)	S	25	Barrer			0.46	3	0.08	19			41.30	237.50	(203)
Polysulfone (PSF)-Carbon Black (CB)														
PSF:CB (100:0)	S	25	GPU			2.05	12.21	2.1	86.12			26.67	41.01	(122)
PSF:CB (98:2)	S	25	GPU			1.94	12.65	2.16	76.25			39.30	35.30	(122)
PSF:CB (95:5)	S	25	GPU			2.81	12.78	4.77	68.72			24.46	14.41	(122)
PSF:CB (90:10)	S	25	GPU			2.25	11.89	2.44	75.13			33.39	30.79	(122)

PSF-Vapor grown carbon fibers (VGVF)	S	25	GPU	3.95	12.63	5.52	57.12	26.67	10.35	(122)
PSF-Titania	S	25	GPU	3.17	14.7	3.67	89.56	28.25	24.40	(122)
Matrimid® 5218-Carbon molecular sieve (CMS)										
Matrimid® 5218:CMS (100:0)	S	35	Barrer	0.32	2.12	0.28	10	26.67	35.71	(390,391)
Matrimid® 5218:CMS (83:17)	S	35	Barrer	0.29	2.08	0.23	10.3	35.52	44.78	(390,391)
Matrimid® 5218:CMS (81:19)	S	35	Barrer	0.35	2.41	0.23	10.6	30.29	46.09	(390,391)
Matrimid® 5218:CMS (67:33)	S	35	Barrer	0.38	2.7	0.24	11.5	30.26	47.92	(390,391)
Matrimid® 5218:CMS (64:36)	S	35	Barrer	0.38	3	0.24	12.6	33.16	52.50	(390,391)
Matrimid® 5218:CMS (0:100)	S	35	Barrer	1.65	22	0.22	44	26.67	200.00	(390,391)
Ultem® 1000-Carbon molecular sieve (CMS)										
Ultem® 1000:CMS (100:0)	S	35	Barrer	0.052	0.38	0.037	1.45	27.88	39.19	(390,391)
Ultem® 1000:CMS (84:16)	S	35	Barrer	0.071	0.56	0.058	2.51	35.35	43.28	(390,391)
Ultem® 1000:CMS (80:20)	S	35	Barrer	0.09	0.71	0.06	2.9	26.67	48.33	(390,391)
Ultem® 1000:CMS (65:35)	S	35	Barrer	0.136	1.09	0.083	4.48	32.94	53.98	(390,391)
Ultem® 1000:CMS (0:100)	S	35	Barrer	1.65	22	0.22	44	26.67	200.00	(390,391)

*S: Data based on single gas experiments; M: Data based on mix-gas experiments; Barrer; 10^{-10} cm^3 (STP) cm cm^{-2} s^{-1} $cmHg^{-1}$; GPU; 10^{-6} cm^3 (STP) cm^{-2} s^{-1} $cmHg^{-1}$. To convert values in GPU into mol m^{-2} s^{-1} Pa^{-1} multiply the value by 5.95×10^{-4}.

Table 10. Permeabilities and permeances of facilitated transport membranes used for CO_2 separations

	*	T (°C)	Units	Permeances and Permeabilities					Selectivities			Reference
				H_2	N_2	O_2	CH_4	CO_2	$CO_2/H2$	CO_2/N_2	CO_2/CH_4	
FACILITATED TRANSPORT												
Solid-Polyelectrolyte												
Polyvinylpyrrolidone (hydrolyzed)/polysulfone	S	26	GPU				0.3–3.5	25–800				(296,297)
PVBTAF:poly(diallyldimethyl-ammonium fluoride)	M	23	Barrer	0.276			0.0417	7.51	27.21		180.10	(282)
Poly(vinylbenzyltrimethyl-ammonium fluoride) (PVBTAF)	M	23	GPU	0.0751			0.0128	3.57	47.54		278.91	(282)
PVBTAF/poly(diallyldimethyl-ammonium fluoride)	M	23	GPU	0.0443			0.00636	4.83	109.03		759.43	(282)
PVBTAF-nCesiumFluoride, n = 4	M	23	GPU	0.20–0.3			0.035–0.044	13–25.7	43–126		371–587	(278)
PVBTAF-nCesiumFluoride-1cholineFluoride, n = 3	M	23	GPU				0.109–0.061	19.31–24.39			178–400	(278)
PDMS/poly(diallyl-dimethylammoniumfluoride) (PDADMAF)/PDMS	M	23	GPU	0.016–0.023			0.007	0.87–1.83	53–81		120–239	(280)
PTMSP/PDADMAF/PTMSP	M	23	GPU	0.065			0.007	1.1–2.84	17–44		150–380	(280)
PTMSP/PDADMAF/ microporous polymer	M	23	GPU	0.112–0.163			0.023–0.025	1.96–2.69	12–24		78–118	(280)
PTMSP/PVBTAF/ microporous polymer	M	23	GPU	0.006			0.068	2.88–6.02	490–10000		43–87	(280)
poly(vyvilbenzyltrimethyl-ammonium fluoride) PVBTAF, #1	M	23	GPU	0.07–0.10			0.00586	2.88–6.02	42–64		4910–10270	(281)

poly(vyvilbenzyltrimethyl-ammonium fluoride) PVBTAF, #2	M	23	GPU	0.011	0.026–0.022		7.17–9.02	629–835	(281)
Polyvinylamine (PVAm)/ poly(ether sulfone)	S	25	GPU			0.221	1.437	6.50	(289)
Polyvinylamine (PVAm)/polyacrylonitrile	S	25	GPU			2.375	12.111	5.10	(289)
Polyvinylamine (PVAm)/ celullose acetate	S	25	GPU			2.119	36.67	17.31	(289)
Polyvinylamine (PVAm)/ polysulfone	S	25	GPU			0.003–0.087	2.33–3.1	36–778	(289)
Inmobilized Liquid									
Glycerol-Na_2CO_3 in poly(vinylidine fluoride) (PVDF) (dry)	M	23	Barrer			1.24	2.79	2.25	(273)
Glycerol-Na_2CO_3 in PVDF (100 RH)	M	23	Barrer			1.56	1770	1135	(273)
Glycerol carbonate in PVDF (dry)	M	23	Barrer			1.1	100	90.91	(275)
Glycerol carbonate in PVDF (humid)	M	23	Barrer			3.7	320	86.49	(275)
Glycerol carbonate in Celgard 2500 (dry)	M	23	Barrer			4.4	260	59.09	(275)
Glycerol carbonate in Celgard 2500 (humid)	M	23	Barrer			3.5	160	45.71	(275)
44% dendrimer (generation 0) in glycerol in PVDF (dry)	M	23	Barrer			7.54	17	2.25	(276)
44% dendrimer (generation 0)	M	23	Barrer			0.94	900	957	(276)

(*Continued*)

Table 10. Continued

	*	T (°C)	Units	Permeances and Permeabilities					Selectivities			Reference
				H_2	N_2	O_2	CH_4	CO_2	$CO_2/H2$	CO_2/N_2	CO_2/CH_4	
in glycerol in PVDF (humid)												
75% dendrimer (generation 0) in glycerol in PVDF (dry)	M	23	Barrer				860	5800			6.74	(276)
75% dendrimer (generation 0) in glycerol in PVDF (humid)	M	23	Barrer				0.19	3200			16842	(276)
Pure dendrimer in PVDF by impregnation (dry)	M	23	Barrer				930	4700			5.05	(276)
Pure dendrimer in PVDF by impregnation (humid)	M	23	Barrer				0.17	3600			21176	(276)

Table 11. Trans-membrane flux (mmol/m^{2}s) for different capillary hollow fiber membrane contactors reported in the literature. The parameters reported include number, internal diameter, length and surface area of the fibers (i.e., No, d_i, L, a), concentration of absorbent (wt%), and feed temperature, pressure, concentration and flow (i.e., T_F, P_F, y_{CO_2}, F_{CO_2})

	Membrane						Conditions					CO_2		
Authors	Mat.	No	d_i (mm)	L (cm)	a (m^2/m^3)	Solvent (Conc., loading[a])	T_F (°C)	P_F (kPa)	y_{CO_2} (%)[e]	V_L (cm/s)	F_{CO_2} (SLPM)	Flux (mmol/m^2 s)	Eff. (%)	Stability[b]
(418)	PTFE	28	3.00	43.0	416	MEA (30 wt%)	40	NA	1.5*	1.68	NA[c]	1.910	NA	NA
							40	NA	7.5*	1.68	NA	3.360	NA	
						MEA (30 wt%, 0.150)	40	NA	1.0*	1.68	NA	1.180	NA	
							40	NA	9.0*	1.68	NA	2.450	NA	
						MEA (30 wt%, 0.068)	40	NA	5.0*	0.84	NA	2.270	NA	
							40	NA	5.0*	3.37	NA	2.910	NA	
						MEA (30 wt%, 0.043)	25	NA	5.0*	1.68	NA	3.180	NA	
							55	NA	5.0*	1.68	NA	2.000	NA	
(444)	PVDF	2050	0.83	52.0	1542	MEA (5 wt%) + TEA (5 wt%)	40	NA	11.0	0.90	2.200	0.580	99	+80 h
							40	NA	11.0	0.90	3.300	0.760	86	
							40	NA	11.0	2.70	2.750	0.730	100	
							40	NA	11.0	2.70	4.400	1.120	95	
(442)	PVDF	130	0.83	23.0	1391	Piperazine (PZ) (5 wt%)	40	NA	20.0	0.47	0.010	0.100	100	<2 h
							40	NA	20.0	0.47	0.070	0.230	35	
						TEA (5 wt%)	40	NA	20.0	0.47	0.070	0.670	100	
							40	NA	20.0	0.47	0.090	0.750	88	
						PZ (5 wt%) + TEA (5 wt%)	40	NA	20.0	0.47	0.080	0.760	100	+50 h
							40	NA	20.0	0.47	0.120	1.090	95	

(*Continued*)

Table 11. Continued

	Membrane						Conditions					CO_2		
Authors	Mat.	No	d_i (mm)	L (cm)	a (m^2/m^3)	Solvent (Conc., loading[a])	T_F (°C)	P_F (kPa)	y_{CO_2} (%)[c]	V_L (cm/s)	F_{CO_2} (SLPM)	Flux (mmol/m^2 s)	Eff. (%)	Stability[b]
(429)	PP	4900	0.60	10.0	924	Pure water	22	137.8	30.0	1.20	4.212	0.044	1	NA
							22	137.8	30.0	8.30	4.212	0.212	6	
							22	115.5	70.0	1.20	14.190	0.313	3	
							22	115.5	70.0	8.30	14.190	0.765	7	
	PP	400	0.60	10.0	471	Pure water	20	116.5	2.5	6.60	0.017	0.030	17	NA
							20	116.5	2.5	9.60	0.017	0.034	19	
							22	119.6	30.0	1.00	0.125	0.086	7	
							22	119.6	30.0	10.00	0.125	0.255	20	
							22	144.9	87.5	0.50	0.417	0.354	8	
							22	144.9	87.5	8.50	0.417	1.133	27	
(443)	PVDF	139	0.83	23.0	1488	MEA (5 wt%)	40	NA	25.0	0.27	0.110	0.530	55	NA
							40	NA	25.0	0.55	0.110	0.950	100	
	PTFE	70	1.00	23.0	1340	MEA (5 wt%)	40	NA	25.0	0.36	0.045	0.450	66	NA
							40	NA	25.0	0.76	0.045	0.680	100	
(422)	PP	1	0.60	15.0	–	Propylene Carbonate	20	172.3	100.0	2.50	NA	1.700	NA	Short
							20	172.3	100.0	9.00	NA	3.000	NA	
							20	202.7	100.0	4.00	NA	2.700	NA	
							20	202.7	100.0	14.50	NA	4.200	NA	

	PP	1	0.60	13.0	–	Propylene Carbonate	25	425.6	100.0	0.50	NA	2.200	NA	
							25	425.6	100.0	9.50	NA	9.300	NA	
							25	810.6	100.0	2.00	NA	9.200	NA	
							25	810.6	100.0	8.50	NA	17.000	NA	
	PP	1	0.60	11.5	–	Propylene Carbonate	25	1013.3	100.0	1.50	NA	11.000	NA	
							25	1013.3	100.0	9.00	NA	24.000	NA	
	PP	1	0.60	13.5	–	Propylene Carbonate	25	1519.9	100.0	3.00	NA	20.000	NA	
							25	1519.9	100.0	12.00	NA	38.000	NA	
							25	2026.5	100.0	3.00	NA	25.000	NA	
							25	2026.5	100.0	13.00	NA	56.000	NA	
	PP	1	0.60	13.0	–	Propylene Carbonate	25	405.6	10.3	2.00	NA	0.500	NA	
							25	405.6	10.3	10.00	NA	0.950	NA	
							25	405.6	22.5	2.00	NA	1.000	NA	
							25	405.6	22.5	8.00	NA	2.050	NA	
							25	810.6	8.6	2.00	NA	0.800	NA	
							25	810.6	8.6	10.00	NA	1.500	NA	
(422)	PP	400	0.60	10.0	471	K_2CO_3 (0.25 M)	24	101.3	32.6	1.00	14.90	0.540	NA	NA
							24	101.3	32.6	10.00	14.90	0.760	NA	
						K_2CO_3 (0.50 M)	24	101.3	32.6	1.00	19.50	0.640	NA	
							24	101.3	32.6	10.00	19.50	0.920	NA	

[a]Loading is shown in some results and is evaluated as mol of CO_2 absorbed per mol of active absorbent (water excluded).
[b]NA: not available or cannot be elucidated from data provided.

of vapors from organic solvents may lead to undesirable compaction, swelling and plasticization that irreversibly change the morphology, and hence may lead to reduced membrane performance (10–16,125–127, 132,139,141,142,185–201). Plasma and thermal treatment (i.e., annealing) (132,185,187,197,199,201) and chemical cross-linking methods (125–1274,139,141,142,190–196,198,200), which improve the membrane resistance by increasing the polymer rigidity, are the most frequently used strategies to improve durability.

Thermal treatments of polymeric material for membranes with cross-linking agents improve resistance to plasticization and other attacks. Thermally induced densified structures are being investigated with charge transfer complexes (CTCs) (191–195,199), diols (125–127,190–195), and diamines (126,139,141,142,190,200). The improved resistance against structural modification is realized via covalent bonding of neighboring polymeric strands. These approaches lead to reductions in permeability, sometimes with improvements in selectivity. Others have observed further success by attempting a mixed approach of both techniques (191–195). Thermal annealing, for example, can further drive cross-linking reactions to stabilize the polymer properties.

The addition of inorganic materials can also lead to further stabilization of the membrane. In this regard, polymers crosslinked with inorganic monomers (202–206), typically alkoxy-silanes, improve stability, and also improve performance. These materials belong to a different class of materials normally regarded as organic-inorganic hybrid materials and are discussed later.

Glassy polymers, characterized by a very rigid ultramicroporus structure, possess pores sufficiently small for gas separation (175,176). Molecule diffusion in these polymer molecular sieves is similar to that in inorganic molecular sieves. Examples of these materials are polypyrrolone copolymers (175–177,181–184) and the recently developed intrinsic microporous polymers (178–180,207). In general, these polymeric membranes are very attractive because they display performances normally above the upper bound for conventional polymeric materials and enhanced stability (175,176).

Another type of glassy polymer is that of di-substituted acetylene-based polymers (113,208–228). Disubstituted polyacetylenes are known for their unique gas transport properties, characterized mainly by enormous gas permeability, high fractional free volumes (typically $>20\%$) and unusually high vapor/gas selectivities (113,214,217,218,227,228). Within polyacetylenes, poly(1-trimethylsilyl-1-propyne) (PTMSP) displays the largest gas permeability of all known polymers (113). It is believed that the large permeability associated with these polymers is due mainly to a concerted action of the rigid double bonds of the

polymeric backbone and the bulky side groups, hindering chain segmental motion and restraining polymer chains from packing efficiently (212). The resulting effect is a polymeric matrix with large, possibly interconnected, free volume that provides a very efficient permeation pathway for transporting molecules.

Also, unlike the rest of the glassy polymers, polyacetylenes do not discriminate permeates based on diffusivity but rather on solubility, which provides them with the ability to permeate heavier and more soluble organic molecules and CO_2 over smaller gases. Due to this reason, polyacetylenes such as PTMSP (poly(1-trimethylsilyl-1-propyne) (213,214,217–219,221,222,226,227), PMP (Poly(1-methyl-1-pentyne)) (214–216,227,228) have been investigated as potential materials for the separation of light hydrocarbon gases and vapors (C_{3+}) from natural gas and off-gas streams containing H_2 (e.g., from fluidized catalytic crackers) in refineries.

As a result of their selectivity towards CO_2 over H_2, polyacetylenes have also found potential use in hydrogen/syngas production processes (e.g., reforming). However, the CO_2/H_2 selectivities so far displayed by these polymers (i.e., <6) are still only moderate. This limitation, due mainly to the prohibitive losses of high-pressure H_2 in the low-pressure permeate, reduces the commercial potential for these polymer membranes.

Another major concern behind polyacetylenes is their lack of chemical resistance and performance loss over time (212,221,222). Polyacetylenes tend to incur irreversible structural changes and degraded performance with long exposures to these gases. Several approaches have been attempted to overcome these problems with some success and sometimes with loss of performance. These approaches include the addition of silica fillers (220,229–231) to manipulate the molecular polymer chain packing. They also include the addition, preparation, or use of other polyacetylenes more resistant to aggressive feeds, such as poly(4-methyl-2-pentyne) (PMP) (227), poly(1-phenyl-1-propyne) (PPP) (228), and diphenylacetylene (PDPA) (212). Chemical treatments, such as fluorination and desilylation (208–212) have also been explored.

The increasing demands for purer and cheaper H_2 has fostered the development of technologies that selectively remove CO_2 from H_2/syngas under high pressure from reforming, coal, and waste gasification and partial oxidation and other similar processes. In this regard, rubbery polymeric materials allow membrane technology to be a viable option for this industrial application. In general, rubbery polymers tend to display lower performance than their glassy counterparts; but, they possess the unique ability to be selective towards CO_2 over H_2.

The transport of molecules in rubbery polymers can also be explained by the solution-diffusion model. However, in this case the selectivity of rubbery polymers relies upon the physical interactions (i.e., solubility) between gas penetrants and the polymeric phase. Thus, given relatively low temperatures, it is possible for rubbery polymeric materials to be more selective towards heavier gases such as CO_2 or H_2S over smaller molecules such as H_2 or He (10,172,232–256).

The fact that rubbery polymers do not rely on diffusion selectivity makes their performance much less likely to be affected by swelling, plasticization and other adverse attacks than their glassy counterparts (10,232–236). In the past, semi-organic rubbery polymers, such as silicone membranes, in particular, poly(dimethylsiloxane) (PDMS), have received considerable attention for their high intrinsic permeabilities (113,257–264). However, because these materials have suffered from reduced selectivities, particularly for the CO_2/H_2 system, their further study as possible membrane materials is somewhat discouraged.

Today, polyphosphazenes (237,238,265,266) and polyethers (172,232–236,239–255) are the rubbery polymers receiving the greatest attention. These materials display the largest CO_2/H_2 selectivities (i.e., 6–10) and show significantly higher CO_2/N_2 or CO_2/CH_4 selectivities (40–60) than commercially available glassy membranes. It is believed that polar groups in the polymer backbone, particularly ether oxygen atoms, are largely responsible for the enhanced selectivity for CO_2.

Despite the large selectivities, rubbery polymers suffer from modest permeabilities, principally as a consequence of the large degree of crystallinity associated with them (228–235,237,238,265,266). However, several approaches have been implemented to minimize the existence of crystalline phases within these polymers, including the addition of hydrophobic pendant groups (237,238,265,266), the preparation of block copolymers containing low molecular weight rubbery polymer segments, and glassy polymers such as nylons (172,248,253,267,268), polyimides (268–270), and others (155,156,246–248). The utilization of cross linking agents that keep rubbery polymer segments small has also been investigated (232–235,239–244,254). Cross linking improves the mechanical consistency that is normally lacking in rubbery polymers. Despite all these challenges, rubbery polymers seem to offer significant room for improvement with a great potential for future commercial use.

Facilitated Transport Membranes

Facilitated transport membranes (FTMs) have received considerable attention because of their extremely hign selectivities and relatively high

fluxes (14). Table 10 summarizes the permeabilities and permeances obtained with these kinds of membrane materials when used for CO_2 separation. The high selectivity in FTMs is achieved through the existence of carriers within the membrane that selectively interact with given molecules and facilitate their transport through the membranes. FTMs that are selective towards CO_2 can have a great impact on reducing processing costs or improving equilibrium driven processes, where CO_2 is to be removed, even if present in low concentrations. Such processes include natural gas sweetening, reforming and coal gasification, and flue gas treatment.

FTMs, however, are widely known for their stability problems, mainly as a result of the evaporation of the carrier medium. This problem is particularly acute in immobilized liquid membranes (ILMs) (271). Several approaches have been attempted with moderate success to control evaporation. In some FTMs, evaporation losses have been reduced by alternatively using non-volatile solvents such as carbonate-glycerol (272) glycine-Na-glycerol (273,274), dendrimers (275,276), and more successfully glycerol carbonate (271,275). Similarly, in polyelectrolyte membranes (PEM) (277–282), which are also ionic liquid membranes (ILMs), the evaporation is reduced by using non-volatile polyelectrolytes as molten salts or salt hydrates as solvents.

Membranes where the carriers are tightly bound to the polymer have also been developed to counteract degradation. In ionic exchange membranes (IEMs) (283–288), the carrier is ionic and physically binds to the ion exchange membrane via attractive electrostatic forces. In water-swollen membranes (WSMs) (289–291), which are a particular type of IEM, where water serves as the carrier, the membrane physically interacts and retains water, causing swelling which improves the transport of the solute.

The most successful facilitated transport membranes are the so called fixed carrier membranes (FCMs) (292–294). In FCMs the carrier consists of secondary amines or carbonates that are chemically bonded to the backbone of the membrane. Clearly, the chemically bound carrier alleviates the evaporation and migration problems associated with the free liquid FTMs.

Despite all this work on FTMs, and with the exception of some ILMs and FCMs, most FTMs still require feed preconditioning, particularly with water, to sustain their uniquely high selectivity. Otherwise, their selectivity severely deteriorates. However, FTMs may overcome these problems in applications where humidification preconditioning is not a requirement, such as in reforming, where H_2O actively participates.

Another problem, perhaps a minor one, of most FTMs is their characteristically strong decay of permeability as the partial pressure of

the favored molecule increases (275–278,281–283,289,293,294). This behavior limits their use to feeds with low partial pressures of this species. At partial pressures over 0.5 atm most carriers rapidly approach saturation and the permeation rates become severely limited.

A particularly novel approach to FTM technology is that associated with the "bulk flow liquid membrane" (BFLM) concept, which was introduced by the group of Teramoto (295–297). In BLFMs, stability problems due to evaporation of the carrier solution, observed with traditional FTMs, are avoided. The carrier solution is forced to permeate through the membrane and then is continuously recycled to the feed side.

Briefly, with BFLMs the carrier solution is continuously mixed with the feed gas and the carrier selectively reacts with the solute. Once inside the membrane unit the carrier permeates the membrane with the dissolved solute from the feed side (high-pressure side) to the receiving side (low-pressure side). Upon leaving the unit the absorbed CO_2 is released and the regenerated carrier is recycled back to the feed for reuse. Any small amount of carrier solution that does not permeate the membrane is later separated from the treated gas and returned through the receiving side of the membrane to join the carrier that is permeating through the membrane.

Because the membrane is always wetted with the carrier solution, the membrane remains highly selective while devoid of any open pores, i.e., pores unfilled with liquid through which the gas may flow unselectively. Also, BFLM units do not require the use of special membranes. The flexibility of this process is such that both microporous and capillary membranes can be successfully used. In addition, thick and porous membranes with sufficient mechanical strength and durability can be used as long as they do not severely restrict the transport of the carrier. Teramoto et al. (295,296) showed CO_2/N_2 selectivities over 500 and permeances and greater than 300 GPUs for a wide variety of BFLMs containing capillary polyethersulfone membranes 250 micron thick.

Inorganic Membranes

Inorganic membranes are very attractive not only because they have significantly better performances in terms of permeability and selectivity over organic membranes, but also because they are more resistant against high temperatures and pressures, fouling, aggressive feeds, and regeneration treatments. Table 9 summarizes the permeabilities and permeances obtained with these kinds of membrane materials when used for CO_2 separation. Materials typically used as membrane materials include carbon molecular sieves from a wide variety of organic polymeric

precursors (131,132,135,145,251,298–306,307–314), zeolites (315–337), and silicas (338–342). To improve their productivity, these membranes must be deposited as thin layers upon the surface of other, non-selective inorganic materials, such as aluminas, zirconias, or porous stainless steel that also provide structural consistency.

Most inorganic membranes exploit diffusion selectivity as the main factor for gas separation. An extreme case of diffusion selective membranes is that of molecular sieves, where the molecular spacing within the pores of the membrane is so restricted that the transport of some larger molecules become severely impeded. Most of the literature regarding inorganic membranes that rely on diffusion selectivity for CO_2 separation has been focused on the CO_2/N_2 or CO_2/CH_4 systems.

In other materials adsorption and condensation play an additional role. For example, in so-called selective surface flow (SSF) membranes, condensation is so important that even the smaller and faster diffusing species becomes the less permeable one, sometimes to the point of becoming totally excluded. The first SSF membranes were developed by Air Products and Chemicals and have been extensively studied (68,343–351). However, the CO_2/H_2 selectivities of these membranes (<5) (see Table 9) so far are too low to be of any economic value. Recently others (263,326,352–359) have reported new types of membranes with SSF characteristics.

Despite all their appealing properties, inorganic membranes are not commercially used for CO_2 separation. It is doubtful that this will change in the near future. Their inherent brittleness and the elevated manufacturing costs associated with making crack free and large surface area modules are still serious issues that limit their utility.

Hybrid Membranes

In the past two decades there has been much interest in the development of hybrid membranes consisting of mixtures of organic and inorganic phases. Table 9 summarizes the permeabilities and permeances obtained with these kinds of membrane materials when used for CO_2 separation. Polymeric membranes have shown little progress since Robeson set the permeability-selectivity trade-off upper limit in 1991 (360). So-called hybrid organic–inorganic membranes seem to offer potential to overcome this limitation. In these membranes, the inorganic phase, which is normally in dispersed form, consists of diverse types of silicas (134,170, 202–206,361–387), titanias (122,388), carbon materials (175,176,389–395), and zeolites (396–409). The organic or polymeric phase serves as the host (390–392). These membranes are attractive because they

synergistically exploit the desired properties of both phases, improving the mechanical (e.g., by increasing bursting pressures) and thermal properties of the inorganic phase and providing the manufacturing flexibility and ductility associated with the organic phase (204,361–364,390–392).

In addition, there has been an abundance of literature reporting that organic-inorganic hybrid membranes can improve the performance of the organic phase, potentially addressing many of the current needs of the membrane industry (171,172,198–201,358–361,371,372,385,386-394,387,398). Hybrid membranes have been shown to significantly increase the selectivity of the polymer, while keeping and sometimes also increasing their permeability (171,172,385,386–391). It has also been reported that hybrid membranes exhibit higher stability against aggressive environments (386).

Organic-inorganic hybrid membranes can be generally classified into two types. In the first type the inorganic phase consists of either preformed submicron particles (fillers) (118,171,172,381–384,385,386–391,393–405,) or in the form sol-gel precursors that are subsequently incorporated into the organic phase (130,361,373–379,385). In the second type both organic and inorganic phases become intermingled at the molecular level via chemical reactions between monomers of both phases (166,198–201,202,358–360,362,367,371,372). In the first type the mixing is realized in a slurry that contains both phases dispersed in a solvent that is later removed. In the second type the membrane is typically formed via a sol-gel process, whereby hydroxyls of the inorganic monomers (e.g., alkoxy silanes) become covalently bonded to the backbone of the organic monomer via organic functional groups.

There are two main reasons for the enhanced performance observed in hybrid membranes (200). The first one is due to the particular interactions that the inorganic phase establishes with the favored gas species. In this case, the inorganic phase may act as a molecular sieve, delaying the transport of the less selective species, or as a SSF material, where due to an improved condensation selectivity in favor of the heavier species, retards the flow of the smaller, more diffusing species. The second reason for the improved performance is a consequence of morphological changes that take place in the polymer structure as a result of the strong interactions now existing between the two phases. A strongly interacting inorganic phase can inhibit chain or backbone mobility (i.e., increase stiffness) and open inter-chain packing (i.e., backbone inter-distance), improving simultaneously both the selectivity and permeability of the organic phase, respectively.

Perhaps, the most critical decision in making a hybrid membrane with improved performance lies in the correct selection of the membrane materials (204,391,392). Both selected phases should facilitate the

transport of the more selective gas species, while the transport of the less selective species is delayed. In this regard, matching the permeabilities of the favored gas species in both phases is an important consideration. A polymeric phase that is otherwise too permeable or too impermeable may lead to undesirable gas bypassing (i.e., low selectivity) or poor membrane productivity (i.e., low permeability), respectively.

It is also imperative that the phases display good adhesion at the interface. Defects at the interface and phase separation lead to gas bypassing, which reduces selectivity. The simplest approach to insure interfacial adhesion is to select phases that are physically and chemically compatible with each other, so that the interfacial surface tension is minimized. For example, interacting mixtures containing zeolites and rubbery polymers (401,402), or carbon based materials with glassy polymers (175,176,389–395) have led to better performing membranes, in some cases significantly better. Limited or no success has been achieved where phase separation occurs, e.g., with mixtures of silicas or zeolites and glassy polymers (390–392).

Alternative approaches have been attempted to improve adhesion of poorly interacting phases. The use of polymeric compatibilizers (170,206,379,410) to reduce surface tension has been demonstrated. Some success has been achieved by using coupling agents and sol-gel techniques with organic polymers functionalized with, e.g., trialkoxysilane groups or alkoxysilane monomers containing functional groups (134,367,380, 382,399–402,411). The same bonding concept has been successfully exploited with the *in situ* prepared hybrid membranes, where bonding reactions result in the formation of nano-microcomposites (170,202–206,361–364,366,371,375,376).

At present, hybrid membranes are used only to improve the mechanical strength of membranes for liquid separations (i.e., ultrafiltration, reverse osmosis, ion exchange, etc.) (412,413). In the gas separation industry, hybrid membranes are currently not being used.

Hollow Fiber Gas-Liquid Contactors

The concept of using a hollow fiber membrane unit to serve as a gas-liquid contactor for absorption was first introduced by Zhang and Cussler (414,415). Currently, a handful of companies including Kvaerner Oil & Gas, W.L Associates GmbH, and TNO Environment Energy and Process Innovation have successfully developed larger scale units (416–418). However, commercialization is looming. Nevertheless, because of the inherent high selectivity and relatively large flows, hollow fiber contactors may be very attractive for CO_2 separations in processes

such as reforming and gas sweetening. Table 11 provides a summary of the trans-membrane flux being achieved for different capillary hollow fiber membrane contactors reported in the literature.

The process basically uses a non-selective membrane that serves only as a physical barrier between the gas and the liquid phase. The non-wetted pores in the membrane are such that the membrane does not offer any selectivity over the gas species; the liquid absorbent assumes this role (416–425). Thus, the membrane must only allow the solute to diffuse through the membrane with little resistance before reaching the absorbent. The pores of the membrane must be kept completely gas filled. The presence of stagnant liquid within the pores (i.e., wetting) decreases the overall mass transfer coefficient of the process.

Because of its advantages over conventional absorption towers, a great deal of research has been conducted on gas-liquid contactors in acid gas sweetening of natural gas and flue gas streams (416–418, 421–425,426–445). Hollow fiber gas-liquid contactors are flexible and can be operated over a wider range of conditions, as they are not subject to the common limitations observed in packed beds, such as flooding, foaming, channeling, and liquid entrainment (418). Superficial velocities in these membrane processes can easily exceed 2 cm/s, which is a limit in their packed bed counterparts.

The larger surface area in these contactors is perhaps the most attractive advantage. Depending on the diameter and thickness of the hollow fibers, membrane contactors may display trans-membrane surface areas between 500–3000 m^2/m^3, which is significantly higher than the typical 100–500 m^2/m^3 observed in packed bed systems. The result of having a large surface area is that despite the typically lower mass transfer coefficients associated with the laminar regime of the liquid phase in these membrane contactors, the volumetric mass transfer coefficient (i.e., k_La) can still be larger than that attained in a packed bed (441–443). Furthermore, unlike packed bed systems, the contacting area is fixed and does not vary with process conditions, and the particular modularity of the membrane contactors allows their design to be simple and scaled linearly. All these facts could lead to significant operational and capital cost savings.

These membrane contactors also offer advantages over selective membranes. The performance of hollow fiber membrane contactors depends almost exclusively on the liquid absorbent, and unlike dense or selective membranes, it is not significantly affected by plasticization and other structural attacks. Also, the extremely high selectivity towards CO_2 that can be achieved with these membrane contactors limits their loss of primary gases such hydrogen, methane or other hydrocarbons through the permeate, particularly in feeds with low CO_2 concentrations.

In spite of some many attributes, hollow fiber gas-liquid contactors are unable to sustain processing conditions for prolonged periods of time. This problem has significantly limited commercial interest. The initial high resistance against liquid penetration into the membrane pores tends to break down with time, as a result of combined mechanisms that include surface wetting, surface modification and reaction, clogging, and swelling of the polymer (317,418). Membrane wetting largely depends on an adequate selection of membrane and liquid absorbent. The ability to stop a liquid from wetting or penetrating into the pores of the membrane depends directly on the surface tension of the liquid and inversely on the size of the membrane pores. With higher surface tension and smaller pores, the less likely the membrane can be wetted. In general, the use of hydrophobic membranes, such as inexpensive polyolefin membranes, in combination with aqueous based absorbents, such as suspensions of alkanolamines or carbonates, ensures large surface tensions. However, surface tension may also vary with the absorbent concentration and CO_2 loading. In alkanolamines, for example, the interfacial surface tension tends to decrease considerably with increasing alkanolamine concentration, but then recovers as the CO_2 loading increases (418).

In addition, the selected solvent must be compatible with the membrane to ensure long-term stability. For example, alkanolamines tend to physically interact and breakdown the hydrophobicity of polyolefin membranes. More hydrophobic membranes, such as PTFE, have been developed to resolve this problem. However, PTFE is expensive and the PTFE membrane contactors exhibit only limited contacting areas. Amino acid salts made from glycine, alanine, diethyl or di-methyl glycine, which offer similar absorption characteristics to aqueous alkanolamines and do not degrade polyolefin membranes, can be used but are more expensive.

Recently, Yeon et al. (441,442) have shown that adding significant concentrations of TEA into the absorbent can also improve membrane stability against wetting. Membranes containing this alkanolamine displayed stable performances for over 3000 hrs. TEA offers a lower absorption rate than the alkanolamines; but, it requires less energy consumption and does not react with CO_2. Korikov and Sirkar (433) showed that aqueous solutions containing polyamidoamine dendrimers as absorbents may also improve membrane stability.

Another way to restrict membrane wetting is by reducing the pore size. Pores, however, cannot be so small that they restrict the flow of solute across the membrane. Below the lowest limit, which corresponds to the mean free path and is equivalent to 70 nm for CO_2, the membrane becomes selective.

Another significant problem associated with these gas-liquid contactors is pore blocking, which is related to solvent stability. Alkanolamines, in particular MEA, and some amino acid salts, for example, tend to react with the CO_2 and form precipitates that eventually cause pore clogging and fouling.

Most recent efforts are directed towards developing cross-flow membrane contactors, which improve the lower mass transfer coefficients of the traditional contactors (416,417). A summary on membrane contactors can be found in the reviews of Li and Chen (445), Drioli et al. (425), and Klaassen et al. (419,420).

RECOMMENDATIONS FOR FUTURE RESEARCH AND DEVELOPMENT

The adsorption and membrane technology survey given above identified several areas where major improvements or breakthroughs may be achieved in CO_2 removal with the judicious use of adsorption and membrane processes. In several other areas the path forward is potentially blocked by fundamental material limitations. In this next section, recommendations are presented for future work on promising adsorption and membrane technologies. It is anticipated that breakthroughs in adsorption and membrane technologies will lead to significant reductions in energy consumption, environmental impact, and feedstock requirements, and thereby provide considerable improvements in process economics.

Recommendations are set-forth for future CO_2 separation research and development needs based on this technology and industrial assessment. These recommendations are set-forth for both the near term time frame of 1 to 5 years, and for longer range research and development efforts of 7 to 15 years. The near term developments in CO_2 separations technology are divided into three categories: Near Term Adsorbent Development; Near Term Membrane Development; and Near Term Adsorption Process Development. The long range developments in CO_2 separations technology are also divided into three categories: Long Term Flow Sheet Augmentation with Adsorption and Membrane Processes; Long Term Advanced Adsorbent Materials and Process Development for CO_2 Removal; and Long Term Advanced Membrane Materials for CO_2 Removal. It must be emphasized that streams containing CO_2 tend to be dirty and contain many different contaminants, as mentioned throughout this review. This fact is very important and provides the basis for a crosscutting recommendation for adsorption and membrane materials and process development.

Crosscutting Recommendations

Develop pre-cleaning technologies to remove a wide variety of contaminants from CO_2 streams, as they may be critical to the successful development and implementation of any or most membrane and some adsorption processes.

Near Term Adsorbent Development

Overarching Goal. Develop high capacity CO_2 selective adsorbents with rapid adsorption-desorption kinetics, improved selectivity and operational stability.

The classes of adsorbent materials being studied today include low temperature activated carbons, carbon molecular sieves, and zeolites; high temperature hydrotalcites, CaOs, and zirconates; and structured adsorbents for rapid PSA, or PSA/TSA processes, e.g., carbon fiber molecular sieves.

In general, these materials have a potential for commercial use in CO_2 capture. However, they all suffer from one or more of the following deficiencies: too expensive; insufficient working capacity and selectivity; slow adsorption or desorption (or mass transfer) kinetics; moisture sensitivity and vulnerability to poisons like CO or S; too rectangular of an adsorption isotherm shape making regeneration difficult with pressure; too strong of a physiochemical interaction requiring regeneration with relatively high temperature instead of pressure; and limited rapid cycling capability because commercial pellet materials tend to crumble if the cycling is too fast. Table 7 provides some insight into the CO_2 capacities now being achieved. Any improvement in these capacities will be highly desirable.

The following specific goal is recommended

To develop high capacity CO_2 selective adsorbents that can operate at elevated temperatures in the presence of sulfur bearing compounds and possibly steam. Working capacities at elevated temperatures in the range of 3-4 mol/kg are desirable, which is similar to commercial low temperature adsorbents like 5A zeolite for CO_2. The operating pressures should be in the range that corresponds to this working capacity range, e.g., 1 to 40 atm.

Near Term Membrane Development

Overarching Goal. Develop low and high temperature membranes that are selective only to CO_2, that exhibit high permeability, are robust

and resistant to fouling and degradation, and that exhibit good mechanical stability under high differential pressures.

The general classes of membrane materials being studied today include polymeric membranes including glassy and rubbery membrane materials; facilitated transport membranes including immobilized liquid membranes, ionic exchange membranes, fixed carrier membranes, water swollen membranes, and polyelectrolyte membranes; inorganic membranes including molecular sieves and selective surface flow membranes, hybrid mixed matrix membranes including inorganic-organic hybrid materials, and hollow fiber membrane contactors that operate with absorbents.

In general, these types of membranes or membrane contactors show commercial potential with energy saving impact on CO_2 capture. However, they all suffer from one or more of the following deficiencies: polymeric glassy membranes generally suffer from chemical attack by CO_2, sulfur bearing compounds, and organic solvents; polymeric rubbery membranes generally suffer from low permeabilities and low selectivities towards CO_2 over H_2, H_2S and other sulfur bearing compounds; facilitated transport membranes suffer from being too dependent on the presence of moisture to maintain selectivity; inorganic membranes tend to be brittle and have low surface areas; selective surface flow membranes tend to have low selectivities; hybrid mixed matrix membranes suffer from phase separation; and hollow fiber membrane contactors suffer from plasticization and tend to lose their resistance to wettability with time. Tables 9 through 11 provide some insight into the properties of these various membranes towards selective CO_2 separations. Any improvement in these properties will be highly desirable.

The following specific goals are recommended

1. Develop a CO_2 permselective polymeric glassy or rubbery membrane with CO_2/H_2 selectivity of >15–20, with at least 2 times higher CO_2 flux than current commercial membranes, and with higher stability to syngas production conditions of 200°C or higher.
2. Develop a polymeric glassy or rubbery membrane for CO_2/CH_4 that has selectivity larger than 50, double the current commercial membrane CO_2 flux, resists plasticizing, and is stable to heavy oil.
3. Develop a CO_2 permselective facilitated transport membrane that can operate in the absence of water for long periods of time, avoid vapor conditioning, control or eliminate carrier evaporation, and minimize the strong dependence between CO_2 permeance and partial pressure as often observed in these materials.

4. Develop a CO_2 permselective inorganic membrane with selectivity of 15–20 or higher as this type of membrane may provide the desirable temperature stability.
5. Develop s CO_2 permselective selective surface flow membrane with a much higher CO_2 selectivity toward gases such as H_2, N_2, CH_4, etc.
6. Develop a CO_2 permselective hybrid mixed matrix membrane with improved selectivity and permeance, stability against phase separation, bypassing, plasticization for the case with matrices made of glassy polymer, etc.
7. Develop a CO_2 permselective hollow fiber membrane contactor with improved permeance and prolonged stability against solvent dissolution, wetting and pore blocking.

Near Term Adsorption Process Development

Overarching Goal. Develop new or modify existing adsorption process technology that offers increased energy savings, lower capital, and operating costs, affords higher reliability and reduces footprint and environmental impact.

As a guide, the adsorption process technology being studied today includes various pressure swing adsorption cycles at ambient and elevated temperatures; temperature swing adsoprtion for some CO_2 separations; and sorption enhanced reaction processes mainly for H_2 production.

In general, state-of-the-art cyclic adsorption processes suffer from the following: CO_2 is typically the heavy component and discarded in the tail gas of a PSA unit; the enrichment of CO_2 in typical PSA units is poor; TSA is limited to long cycle times and hence low feed throughputs; PSA is generally limited to ambient or near ambient temperature operation; PSA feed pressures tend to be very high; and PSA and TSA beds tend to be very large. Table 8 provides some insight into the performances of PSA processes for the recovery of CO_2 from stack and flue gas. Any improvement in these performances will be highly desirable. To date, no attempt has been made to recover CO_2 from the tail gas of H_2 PSA plants.

The following specific goals are recommended

1. Develop new PSA cycle designs that take advantage of new or even existing CO_2 selective adsorbents; possibly TSA or PSA/TSA hybrid cycle designs could be envisioned. Some ideas for improvement include rethinking the use of the tail gas or heavy product from PSA processes; revamping existing PSA plants through cycle modification;

using lower or even higher purge gas pressure; replacing one or more of the adsorbents with more efficient ones; decreasing the number of adsorbent vessels; adding storage tanks to replace some of the adsorbent beds; developing new PSA cycles that take advantage of the heavy reflux concept, where a pure heavy product like CO_2 is more desirable than a pure light product like H_2; and fostering a clear understanding of the design of such a PSA cycle, which appears to be lacking compared to the commercial light reflux PSA processes; hence, the application of the heavy reflux PSA concept for H_2 production is a desirable near term target. Some existing adsorbents with potential include molecular sieve zeolites, Molecular Gate^{TM} silicotitanates, and activated carbons. Some new adsorbents with potential include hydrotalcites, CaO, and zirconates.

2. Improve the efficiency for thermal management in the design of TSA and PSA/TSA hybrid cycles. Some ideas for improvement include rethinking bed designs for rapid heating and cooling because the long times required to heat conventional beds for regeneration and then to cool them to the feed temperature give rise to long cycle times and thus exceedingly large columns; and taking advantage of the many heat sources that are available throughout some of the CO_2 producing plants that may lend themselves to a TSA or a PSA/TSA hybrid cycle configuration for selective CO_2 removal from a process stream.

Long Term Flow Sheet Augmentation with Adsorption and Membrane Processes

Overarching Goal. Develop new adsorption and membrane process technology that offers lower capital and operating costs and affords higher reliability on stream with improved energy savings.

The following specific goals are recommended

1. Develop hybrid technology for H_2 production, e.g., develop a multifunctional hybrid reactor for steam methane reforming by combining the reactor with a CO_2 selective adsorbent and a H_2 permeable membrane. Driving equilibrium processes in this way can greatly improve manufacturing process efficiencies. This design would not only shift the equilibrium favorably in the reforming reaction, but it would also facilitate the water gas shift reaction. The recommended approach involves the development of new adsorbent and membrane separation materials. It appears that highly selective and highly permeable membranes will always be very difficult to fabricate. However, with hybrid

multi-reactor, multi-separator designs, the criteria for selectivity or permeability may be relaxed, so a less selective membrane with a high flux may suffice.
2. Develop new CO_2 adsorbent and membrane technologies that are amenable to IGCC and related power and chemical production technologies with CO_2 sequestration as a potential long term objective.
3. Develop hybrid technology, possibly coupled with adsorption or membranes processes, that removes CO_2 by chemical reaction in the chemical process.

Long Term Advanced Adsorbent Materials and Process Development for CO_2 Removal

Overarching Goal. Develop new adsorbent materials and CO_2 process technology that offers increased energy savings, lower capital and operating costs, affords higher reliability and reduces footprint and environmental impact.

The following specific goals are recommended

1. Develop advanced structured adsorbent materials for use in rapid cycle PSA. These adsorbents should have comparable working capacity under operational conditions for the current and new non-structured adsorbents mentioned above.
2. Further develop the design of rapid cycle PSA for CO_2 capture and concentration. In particular, this includes exploring rapid cycle PSA with the incorporation of both heavy and dual reflux cycle steps.
3. Minimize the cycle time in rapid PSA to improve its throughput and hence efficiency by investigating the limiting relationship between adsorbent particle size, surface properties, and accelerated cycle times. In particular, the mass transfer limitations associated with ultra fast cycling need to be quantified.
4. Develop TSA and or PSA/TSA hybrid cycles with improved materials for use in CO_2 separation technologies. In particular, a deeper understanding of the PSA/TSA hybrid cycle is needed to quantify the effect on the cycle time and bed sizes when adding a forced temperature swing to a PSA cycle.
5. Develop improved CO_2 separations with sorption enhanced reaction processes using pressure swing, thermal swing, or even hybrid pressure and thermal swing regeneration methods.

Long Term Advanced Membrane Materials for CO_2 Removal

Overarching Goal. Develop new membrane materials that offer increased energy savings, lower capital and operating costs, affords higher reliability and reduces footprint and environmental impact.

The following specific goal is recommended

To develop next generation membrane materials that offer very high selectivity for CO_2 (greater than 100), that resist fouling and cracking or embrittlement, and that withstand high temperatures and pressures that could save substantial energy associated with operation by replacing existing CO_2 and acid gas removal equipment.

APPENDIX: SUPPORTIVE INFORMATION ON ENVIRONMENTAL CO_2 EMISSIONS

In this supportive section, the main sources of industrial CO_2 emissions are reviewed. Ten industrial sources are disclosed in order of decreasing impact on CO_2 emissions. The emphasis is placed on where the CO_2 is produced from each flowsheet, the process capacity, and the condition and composition of various streams within the flow sheet. These existing flow sheets, and corresponding stream compositions and conditions, should be helpful in defining performance and operating condition requirements for the near and far term developments of new adsorption and membrane processes for CO_2 capture from industrial sources.

Main Sources of Industrial CO_2 Emissions

Brief descriptions of the processes most responsible for producing industrial CO_2 emissions are discussed below. Listed in order of decreasing CO_2 generation, these industrial processes include

1. combustion, including burners, flaring, incineration, and utility boilers;
2. coal gasification;
3. steel manufacture;
4. lime and cement production;
5. H_2, syngas, and NH_3 production;
6. natural gas production;
7. aluminum manufacture;
8. Claus/SCOT processes;

9. municipal solid waste landfills; and
10. fermentation to produce ethanol.

The flowsheets associated with each of these industrial CO_2 producers is provided in Figs. 1–11. The corresponding stream compositions and conditions for each of these flow sheets are given in Table 12. Typical process capacities and gas flow rates for these CO_2 producing industries are given in Table 13. Note that with the exception of some of the combustion and gasification processes, these flowsheets are concerned with CO_2 emissions resulting only from the chemical and petrochemical and other manufacturing processes.

Combustion Processes (446–449)

This section considers the carbon dioxide generated from all types of industrial combustion processes, including those that generate power from the burning of fossil fuels to simple burners, flares, incinerators, and boilers. Fossil fuel power plants, as well as many chemical, petrochemical, and other manufacturing plants, utilize burners, utility boilers, incinerators, and/or flares to generate heat, energy, steam, or to get rid of a waste product. All of these processes produce CO_2 as a by-product in the burning or combustion of various fuel sources, such as coal, solid waste, natural gas or some other type of fossil fuel. A typical flow sheet for a carbon-based combustion process that could be associated with a burner, flare, incinerator, or utility boiler is given in Fig. 1. The corresponding stream compositions are given in Table 12, and capacity and flow rate information is given in Table 13.

The carbon-based fuel enters a chamber where it is combusted in the presence of air at a temperature of up to 1100°C. In power plants and utility boilers, the generated heat is used to generate electricity from steam turbines. In some plants, such as IGCC or NGCC power plants, gas turbines are also used in addition to steam turbines. In the case of solid fuels, the chamber is designed to cope with the removal of ash from the bottom; and at the flue gas exit cyclones or other devices are used for gas phase particulate removal. Also, because of the ever increasing concerns over reducing the emissions of SO_2, VOCs, NO_x and other contaminants from the flue gas, more recent designs include a train of gas phase cleanup processes.

In general the cleanup of the exiting flue gas starts with the electrostatic precipitation of particles (fly ash) that could not be removed by the particle separators. This process is carried out continuously at 250°C and removes nearly 100% of the fly ash. The gas is then fed into an absorption

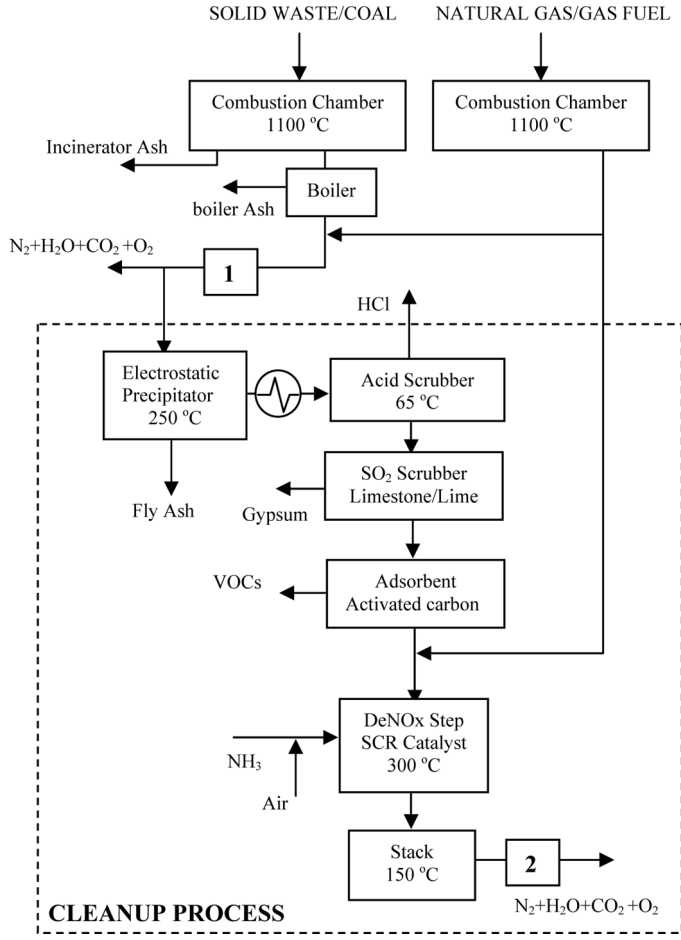

Figure 1. Flow sheet of a typical, state-of-the-art, combustion process that includes burners, incinerators, flaring, utility boilers, etc. Flaring does not necessarily take place in a chamber. Combustion processes that use coal or waste as fuel may require an elaborate cleanup process to remove ash, HCl, SO_2, volatile organics and NO_x. Combustion steps with gas fuels and natural gas may only require an NO_x removal step. The compositions of the numbered streams are shown in Table 12.

process for the subsequent removal of HCl and SO_2. In the latter case, the gas is passed through an aqueous suspension of lime that leads to the formation of $CaSO_4$ (gypsum). Next, the gas is sent to an adsorption process where activated carbon removes the VOCs. The cleanup of the flue gas is finished after a deNO_x step. In this step, the NO_x is catalytically

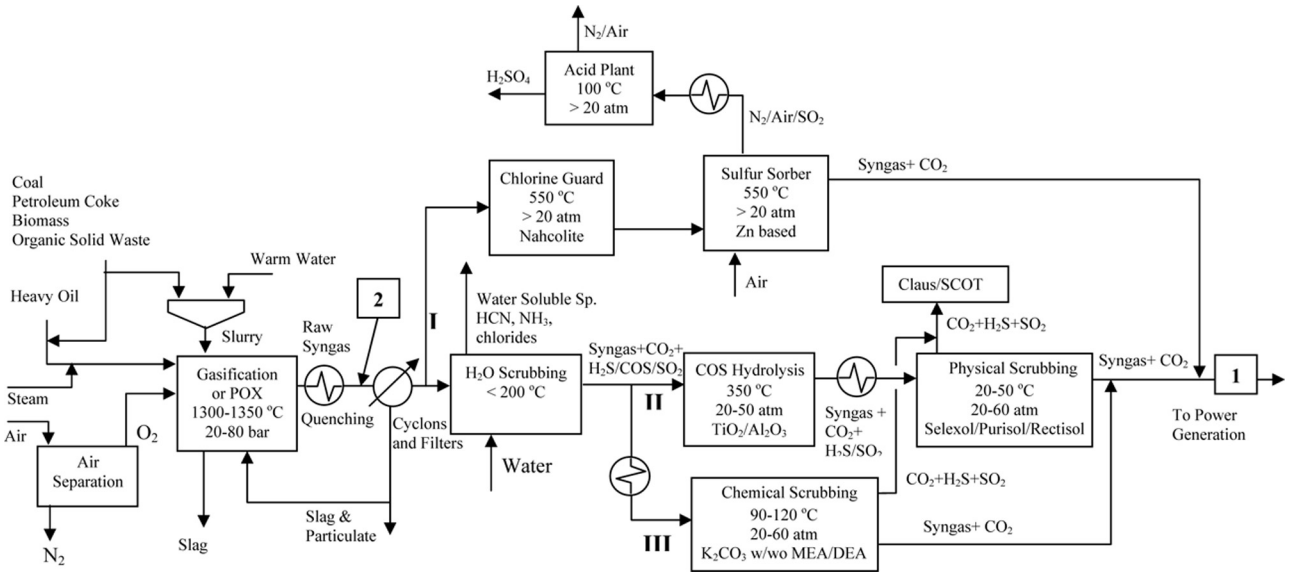

Figure 2. Flow sheet of typical, state-of-the-art, coal gasification (also referred to as integrated gasification combined cycle, IGCC) plant for power generation/syngas production. After a fuel (mostly coal) gasification step that is similar to reforming of CH_4, cleanup of acid syngas takes place either through hot (I) or cold sweetening paths (II or III). In the hot path, sulfur compunds are converted into SO_2, which is then used to produce sulfuric acid. In the cold path, acid syngas may be treated via physical scrubbing following a COS hydrolysis step (II). Alternatively, syngas may not need COS hydrolysis, if the syngas is sweetened by chemical scrubbing with K_2CO_3 (Benfield) (III). Tail gas from the cold scrubbing steps is sent to a Claus/Scott process for sulfur production. The compositions of the numbered streams are shown in Table 12.

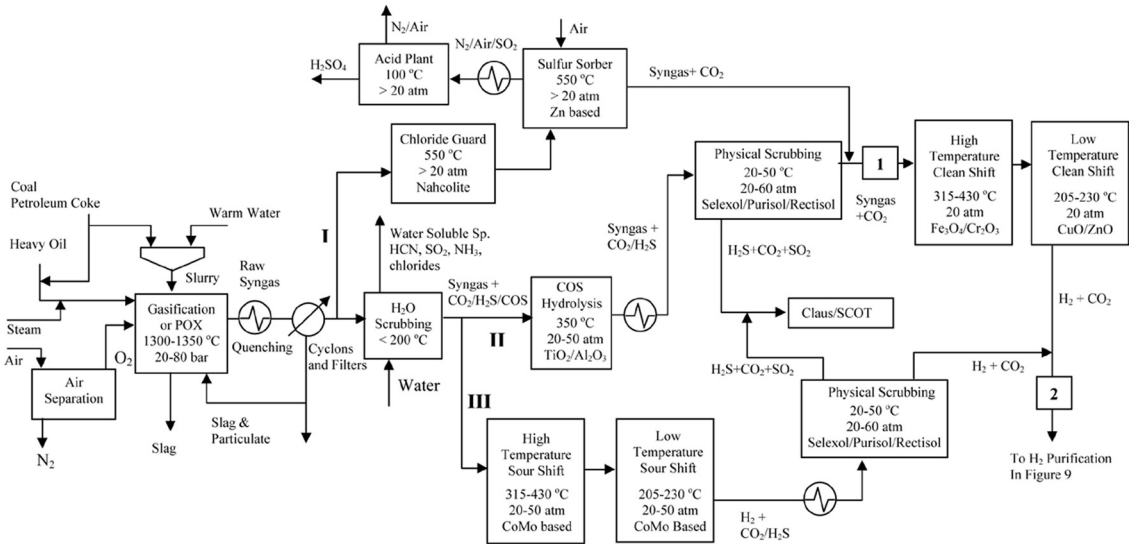

Figure 3. Flow sheet of typical, state-of-the-art, coal gasification (also referred to as integrated gasification combined cycle, IGCC) plant for power generation/H_2 production. The process is similar to that shown in Fig. 2 except that the syngas gas is further shifted for both H_2 production and pre-combustion capture of CO_2. In the case of the hot sweetening path (see Fig. 2), syngas is shifted after sweetening through two water gas shift steps (i.e, sweet shift) identical to those in ammonia production (see Fig. 6). In the case of the cold sweetening path (see Fig. 2), the acid syngas may be sweetened before (II) or after (III) shift reactions. In the first case, i.e., path II, the sweetening step is just like those shown in paths II and III in Fig. 2 (only that of path II is shown here) before going through two sweet shifts steps. In the second case, i.e., path III, sweetening takes place via physical scrubbing after two sour shift reactions that are specially prepared to deal with sulfur bearing species while chemically converting them into H_2S. The compositions of the numbered streams are shown in Table 12.

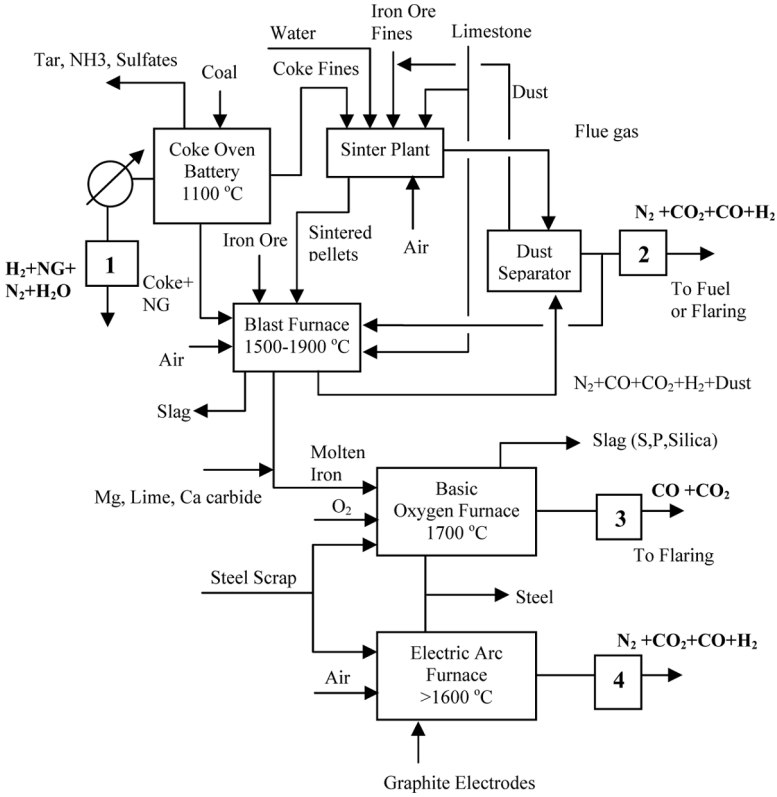

Figure 4. Flow sheet of a typical, state-of-the-art, stainless steel production plant consisting of a coke oven, sinter plant, blast furnace, basic oxygen furnace (BOF) and electric arc furnace (EAF). CO_2 and CO are produced out of the burning of methane, coal-coke and carbon removal from pig iron through all steps. The compositions of the numbered streams are shown in Table 12.

converted into N_2 and H_2O using a mixture of air and ammonia at a temperature of about 300°C. Currently, CO_2 is generally not recovered from flue gas; hence, it is released into the atmosphere in copious amounts.

Coal Gasification (4,5,446,450–452)

The increasing need to more efficiently and more cleanly utilize the energy contained within coal motivated the development of coal gasification processes to replace old coal fired power plants. Typical flow sheets of coal gasification plants are given in Figs. 2 and 3. The corresponding stream compositions are given in Table 12, and capacity and flow rate

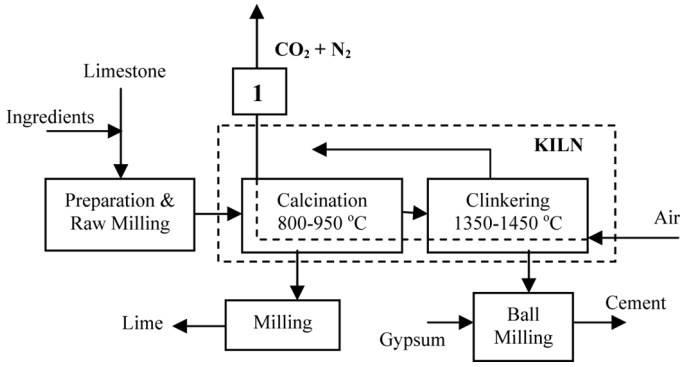

Figure 5. Flow sheet of a typical, state-of-the-art, process for the manufacture of lime and cement. After a preparation and raw milling step, lime is produced through calcination within a kiln. Cement is produced in a further clinkering step and much more elevated temperatures. CO_2 is produced from the decomposition of carbonates and burning of kiln fuel. Final products are obtained following fine milling steps. The composition of the numbered stream is shown in Table 12.

information is given in Table 13. In general, the term gasification refers to the first step of a gasification plant, in which the effluent gas is a net reducing environment consisting mostly of syngas. In a second stage, this gas is later sent through a combustion process to generate power. Coal gasification, not only can be used for power generation, but also it can be used for H_2, syngas, NH_3, and even other chemical production. When it is used to generate only power, it falls under the category of combustion. When it is designed to produce both chemicals and power, i.e., polygeneration, gasification can be incorporated into an integrated gasification combined cycle (IGCC). In IGCCs power is generated by the dual action of hot combustion gas turbines (Brayton cycle) and steam turbines (Rankine cycle) that use the steam that is generated by the hot exhaust gases leaving the gas turbines. In the act of producing power or chemicals, coal gasification processes unavoidably produce large amounts of CO_2 that, for the most part, are emitted to the atmosphere.

The coal or fuel in the gasification unit is exposed to a controlled atmosphere (>20 atm and 1300°C) of both steam and oxygen to produce syngas (i.e., $CO + H_2$), while minimizing the fraction of fully combusted carbon. The existence of these combustion and shift reactions leads to the formation of copious amounts of CO_2 that eventually makes its way into the atmosphere. The fuel is normally a solid, such as coal, petroleum coke, biomass, and even organic solid waste. It can be fed to the gasifier dry or it can be injected in the form of wet slurry. Heavy liquid oils can also be used in this process.

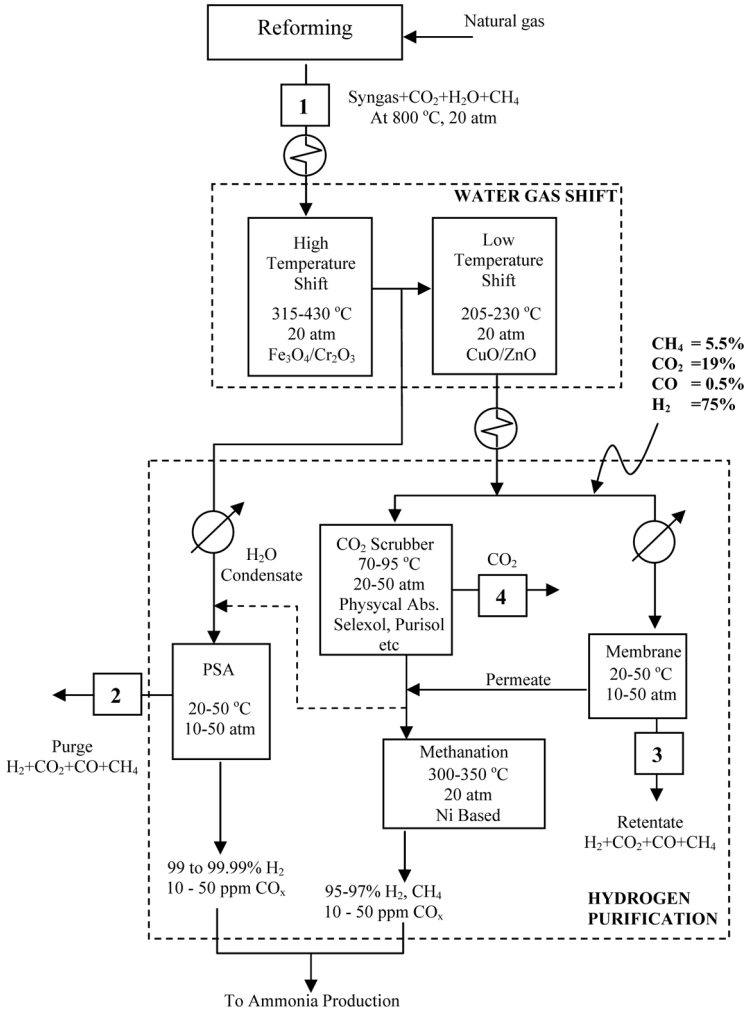

Figure 6. Flow sheet of a typical, state-of-the-art, H_2 or NH_3 production plant. Shifted syngas, which is mostly H_2, CO_2 and CH_4 with traces of CO, is purified into H_2 using either CO_2 scrubbing with physical absorbents, PSA or membranes. A methanation step may be required to convert the remaining CO into CH_4 when using scrubbing or membranes. The tail gas from the PSA or membrane unit (streams 2 and 3, respectively) are used as fuel. The compositions of the numbered streams are shown in Table 12.

Most gasifiers are provided with purified oxygen (>95 vol%) to significantly reduce the size of the unit and its operational costs (e.g., heat exchanging), with the caution not to leave any O_2 unreacted while

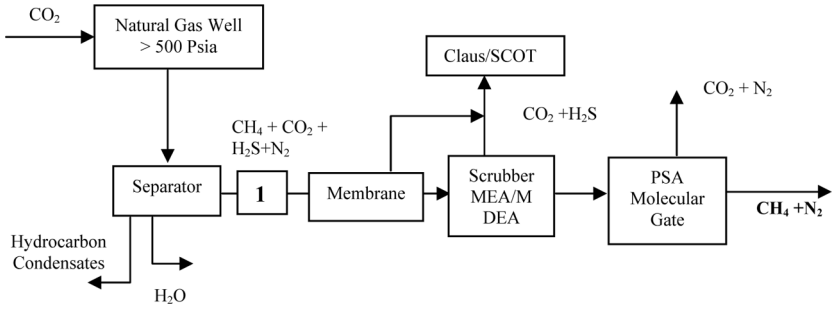

Figure 7. Flow sheet of a typical, state-of-the-art, process for the production of natural gas. After extraction from a well at elevated pressures, a series of steps are carried out to remove water and C_{3+} vapors. Traditionally, the natural gas is then sweetened by scrubbing it with alkanolamines to remover the sulfur bearing compounds and CO_2. Further steps may be required for the removal of excess N_2 or CO_2 in super sour streams. Membrane systems (with cellulose acetate, polyimide or polyaramide) are used prior to scrubbing to reduce the large concentrations of both the CO_2 and sulfur bearing compounds. Likewise, PSA systems with molecular sieves (titano silicate Molecular Gate or zeolite molecular sieves) are located downstream the scrubbing unit to remove the remaining CO_2 and excess N_2. Low pressure wells may be assisted with CO_2 injection. The Claus/Scott process (or similar processes), which is presented in Figure 9, are used to treat the tail gas from the scrubbing step to convert all the sulfur bearing compounds into solid sulfur. The composition of the numbered stream is shown in Table 12.

minimizing the fraction of fully combusted carbon. This is also done to minimize the generation of NO_x. However, due to the additional costs associated with the air separation unit, a considerable number of gasifiers operate with air.

The gasification process produces not only CO_2, but a vast quantity of thermal energy that can largely be recovered as steam. In fact, gasification itself is a large net exporter of steam, which can be used in associated chemical processes or for power generation. Such steam or power production actually avoids the same from less efficient pulverized coal or natural gas power plants or boilers.

Gasifiers also produce solids. The solid slag is easily removed from the bottom of the gasifier. The resulting gas is very hot and contains particulate matter. It is cooled by quenching and heat exchanging. The particulates are removed using cyclones and filters. The cooled and particulate free sour syngas is then sent through either a hot or cold sweetening process to be used either for power generation or H_2 (chemical) production. However, only the cold sweetening process has reached the stage of commercialization.

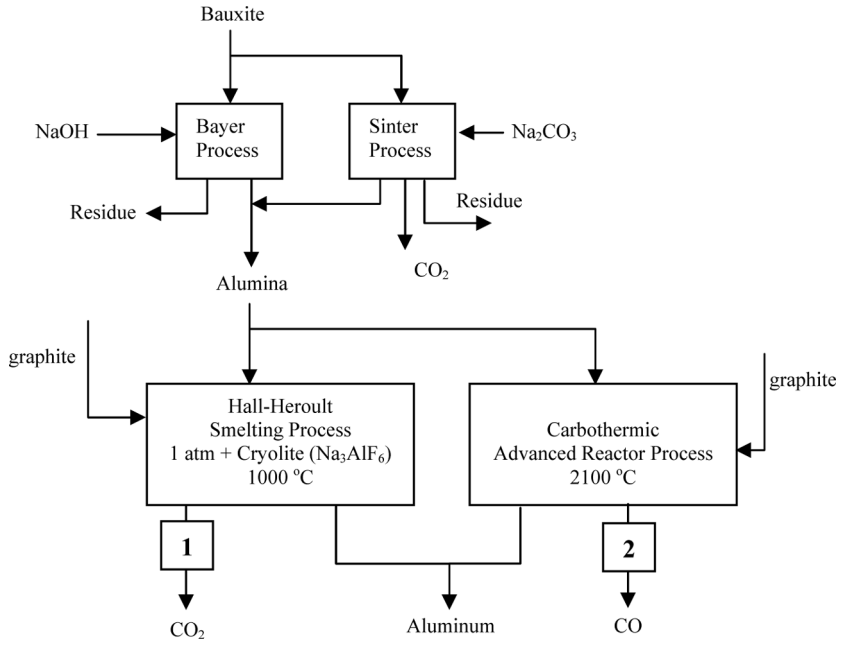

Figure 8. Flow sheet of a typical, state-of-the-art, process for the manufacture of aluminum. In the first step alumina is produced out of bauxite and other chemicals using either the Bayer process or the sinter process. Alumina is then electrochemically converted into aluminum either by the Hall-Heroult process or the more recently developed carbothermic process. CO_2 is produced out of the electrochemical decomposition of carbon made cathodes. The compositions of the numbered streams are shown in Table 12.

In hot sweetening, the gas leaves the filters at about 550°C and more than 20 atm and enters a chloride guard reactor, followed by a hot gas cleanup unit (HGCU). In the chloride guard reactor, traces of HCl are removed from the gas by reacting with sodium bicarbonate (nahcolite) in the form of pellets. The following reaction takes place:

$$HCl + NaHCO_3 \longrightarrow NaCl + H_2O + CO_2 \quad (1)$$

In the HGCU unit, the gas first goes through a column filled with a solid absorbent that contains ZnO. By simple chemical exchange, the ZnO reacts at about 550°C with all the sulfur containing compounds in the gas and converts them into ZnS. A fraction of the sweet gas produced in this step is recycled and mixed with hot air to regenerate the HGCU unit (or one that operates in parallel) once the ZnO is spent or saturated. This regeneration reaction takes place at a temperature above 750°C and the SO_2 rich

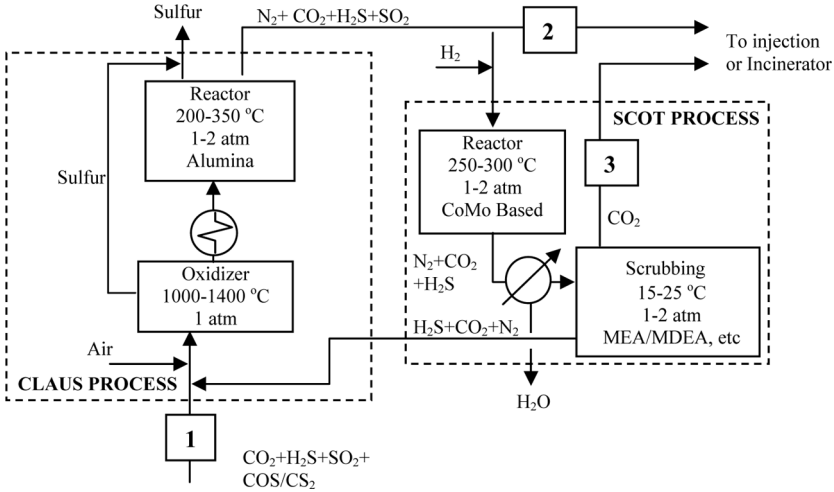

Figure 9. Flow sheet of a typical, state-of-the-art, Claus-Scott process for the production of sulfur from a stream rich in sulfur bearing compounds. In the Claus step, the gross fraction of the sulfur is removed from the stream, while leaving only H_2S and SO_2 in the processed gas as sulfur bearing species. In the Scott step, the gas is further polished by removing the remaining sulfur by first converting SO_2 into H_2S and then using a MEA/MDEA scrubbing step, the tail of which is sent back to the Claus step. The compositions of the numbered streams are shown in Table 12.

gas leaving the unit is sent to an acid plant to produce sulfuric acid. The resulting syngas is sent to a series of shift reactors and purification units that are based on the same processes used in steam reforming, as described below in the *Hydrogen, Syngas, and NH_3 Production* section.

In cold sweetening, the gas leaves the filters at a much lower temperature (350°C) and enters an acid scrubber where water is used to remove most, if not all, of the HCl, HCN, and NH_3 present in the gas stream. At this point, two different processes have evolved for producing power or H_2 (chemicals) from cold-sweetened sour syngas. In the first process, the gas is first sent to a COS hydrolysis unit (350°C), whereby a TiO_2/Al_2O_3 catalyst converts most of the COS and even CS_2 into H_2S. Then it is sent to a cold gas cleanup unit (CGCU), such as a Selexol unit or some similar process, where H_2S, SO_2, and other traces of sulfur containing gases are removed. Note that a COS-CS_2 hydrolysis unit is not always required; a chemical scrubbing unit operating as a CGCU at 90–120°C that contains K_2CO_3 has proven to be successful in hydrolyzing COS and CS_2, while simultaneously removing sulfur containing species all in one step. Alternatively, the rectisol (methanol) process is

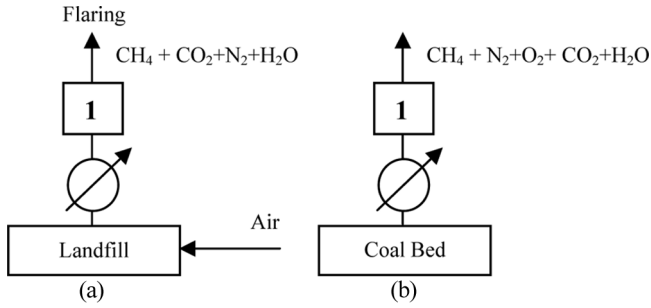

Figure 10. Flow sheet of a typical, state-of-the-art (a) solid waste landfill gas recovery process and (b) coal bed methane gas recovery process. Most of the permeating gas out of landfills consists of methane and carbon dioxide in an almost 1:1 split, which naturally vents to the atmosphere or is flared to convert methane into CO_2. In coal bed methane gas, methane splits 1:1 with N_2. Potential mechanical extraction of methane by vacuum may lead to diffusion of air into the landfill and may require separation steps similar to those of natural gas production. The same considerations are valid for coal bed methane gas, as oxygen and nitrogen may be present in considerable amounts. The compositions of the numbered streams for flow sheets (a) and (b) are shown in Table 12.

known for removing COS and can also be used. The CGCU tail gas, which contains all the sulfur compounds and a large fraction of CO_2, is sent to a sulfur recovery process, such as the Claus/SCOT process (see below), where elemental sulfur is produced. Finally, the resulting syngas is sent to a series of shift reactors and purification units that are based on the same processes used in steam reforming, as described below in the *H_2, Syngas, and NH_3 Production* section.

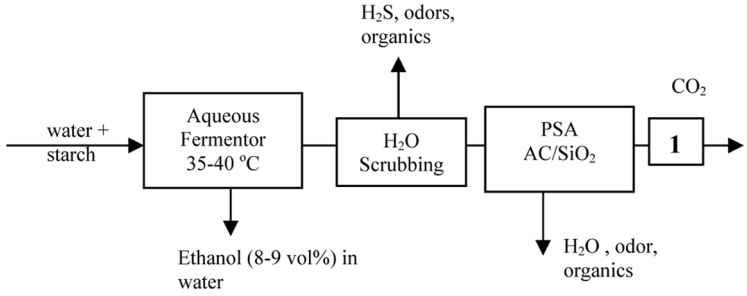

Figure 11. Flow sheet of a typical, state-of-the-art, fermentation process for the production of ethanol typically out of corn-starch. The fermented juice produced contains about 8–9 wt% ethanol; this juice is ready for distillation. CO_2 is produced as a result of a methabolic process by yeast. The composition of the numbered stream is shown in Table 12.

Table 12. Typical mole fraction concentrations in each of the streams listed in Figs. 1 to 11

Process[a]	Stream	N_2	O_2	H_2	CH_4	CO_2	CO	H_2S	SO_2	C^{2+}	H_2O	Other emissions*	Temp (°C)	Press (atm)
1	1	76	5	–	–	16	<0.05	–	<0.05	–	8	NOX,Hg,VOC,HCl	1000	1
1	2	76	5	–	–	16	–	–	–	–	–	–	<100	1
2	1	<0.5	–	38	<0.3	19	42	–	–	–	<10	–	<100	20–60
2	2	<0.5	–	38	<0.3	19	42	–	<0.05	–	20	COS,CS_2	1000	20–80
3	1	<0.5	–	38	<0.3	19	42	–	–	–	<10	–	<100	20–60
3	2	<0.5	–	58	<0.3	40	<1	–	–	–	<10	–	<100	20–60
4	1	4	–	50	30	2	8	<1	–	2	55	VOC,PAH	1000	1
4	2	51	<1	5	<1	20	22	–	~	–	7	NOX,VOC	1000	1
4	3	10	–	2	–	15	70	–	–	–	–	VOC	1000	1
4	4	55	–	4	–	12	28	–	~	–	<1	NOX,VOC	1000	1
5	1	70	9	–	–	22	–	–	<1	–	13	NOX,VOC	1000	1
6	1	–	–	72	6	12	8	–	–	–	>70	–	1000	20–30
6	2	–	–	42	15	37	7	–	–	–	–	–	20–50	20–30
6	3	–	–	39	12	48	<1	–	–	–	–	–	20–50	20–30
6	4	–	–	–	–	>99	–	–	–	–	–	–	<100	1
7	1	4	–	–	91	<1*	–	<1*	–	6	–	COS,CS_2,HCN	<100	>30
8	1	–	–	–	–	99	–	–	<0.5	–	–	PFCs,VOC	1000	1
8	2	–	–	–	–	–	99	–	~	–	–	–	1000	1
9	1	<0.5	–	–	–	36	–	60	<1.0	<2	–	COS,CS_2	<100	<1
9	2	75	–	<3	–	23	<2	<1	<0.5	<2	10	COS,CS_2	<100	1
9	3	75	–	<3	–	23	<2	<0.05	–	<2	10	–	<100	1
10a	1	<10	<1	–	45	40	–	–	–	–	<5	VOC,Sx,Clx	20–40	1
10b	1	40	7	–	50	3		<1		<1	<5			
11	1	–	–	–	–	>99.9	–	–	–	–	>0.1	–	30–40	

[a]Figure number in the text. Estimations based on dry basis. NO_X: NO_2, NO; VOC: volatile organic compounds; PAH: Polycyclic aromatic hydrocarbons; PFC: perfluorocarbons; Sx, Clx: S and Cl bearing compounds.

Table 13. Typical capacities and gas flows for processes in Figs. 1 to 11

Process[a]		Capacities	Gas production
1	Pulverized coal power plant	−7.84 t Coal/MW power −10–1000 MW plants	0.4–0.5 MMscf gas/t coal
2–3	IGCC	−7.52 t Coal/MW power −300–4000 MW plants	0.060–0.065 MMscf CO_2/t coal
4	Coke Oven Battery: 10–105 ovens, usually >45 ovens	−10–45 t coal/charge/oven −0.8 t coke/t coal –Coking time: 18–22 h –Battery capacities: 0.18–0.90 MMtpa	−9,500–11,500 scf gas/t coal
	Blast Furnace	−2,000–8,000 Mtpd of pig iron prod. −0.5 t Coke/t of pig iron prod.	−70,000–80,000 scf gas/t pig iron prod.
	Basic Oxygen Furnace	−1.00–5.50 MMtpa steel prod.	−3,200 scf gas/t steel prod.
	Electric Arc Furnace	−0.60–0.85 MMtpa steel prod.	−3,800 scf gas/t steel prod.
5	Kiln	−0.5–2.0 MMtpa per kiln	−1.0–1.2 t CO_2/t cement or lime −75,000–85,000 scf gas/t cement or lime
6	Hydrogen/Ammonia plants	1–270 MMscfd H_2 (7.5–2000 Mtpd NH_3)	1.5 t CO_2/t NH_3
7	Natural gas wells		−.05–2.5 MMscfd
8	Hall Heroult Process	−66,000–110,000 Mtpa per potline	−1.83 t CO_2/t Al
	1–3 potlines of 50–200 pots each		−33500 scf gas/t Al
9	Claus Process	3–4000 t Sulphur/day	−5–50 mol% SBC in gas steam
	Scot Process	0.3–400 t Sulphur/day	<1 mol% SBC in gas steam
10	Coal bed wells		−0.1–2.0 MMscfd
	Landfills	Sizes 1.0t–100 MMt (average 3.8 MMt; 50% 1–10 MMt)	−220 scfa gas/t landfill

(*Continued*)

Table 13. Continued

Process[a]		Capacities	Gas production
11	Fermenter	−14–15 Ga ethanol/gal of batch fermenter −20 MGa–140 MGa ethanol/plant	−0.7–1.0 t landfill/person/year −2.8 kg CO_2/gal ethanol −50 scf/gal ethanol

[a]Figure number in the text. Acronyms: Mtpa: metric tons per annum; MMtpa: million Mtpa; Mtpd: metric tons per day; Ga: gallons per annum, MGa: megagallons per annum; scf: standard cubic feet; MMscf: Million scf; scfd: scf per day; scfa: scf per annum. MW: Megawatt; SBC: sulfur bearing compounds.

In the second process, the sour syngas is sent to so a called sour shift reactor located upstream of the CGCU. This unique shift reactor contains a sulfur resistant catalyst made of Co and Mo to treat the sour syngas. It operates at high pressure (>20 atm) and in two steps: one at an intermediate temperature (315–430°C) and the other one at a lower temperature (205–230°C). Because COS and CS_2 hydrolysis takes place inside this reactor, a separate hydrolysis unit is not needed in this case.

Iron and Steel Manufacture (446,453–456)

The manufacture of steel constitutes the largest industrial producer of non-energy related CO_2. A typical flow sheet for the manufacture of steel is given in Fig. 4. The corresponding stream compositions are given in Table 12, and capacity and flow rate information is given in Table 13.

Steel manufacture starts with the coke making process, which involves the carbonization of coal at high temperature (1100°C) in an oxygen deficient atmosphere to produce coke, which is enriched in carbon relative to the raw coal. The gas leaving the coke oven is composed mainly of CH_4 and H_2 plus CO_2, CO, and heavier hydrocarbons. This flue gas is used either as fuel or it is flared.

The next step, which is carried out in a sinter plant, is a pre-treatment step in the production of iron. Fine particles of iron ore, limestone, coke, and collected dust are agglomerated by combustion with air (1200°C). These small agglomerates allow the passage of hot gases during the subsequent blast furnace operation. The result is a semi-molten mass called sinter that solidifies into porous pieces of appropriate size and strength

for feeding into the blast furnace. Large quantities of CO_2, CO, VOCs, and NO_x emissions are produced during this step.

In the blast furnace, certain proportions of coke, iron ore, sinter, and limestone are mixed together and heated to temperatures of around 1500 to 1700°C with a controlled supply of air to produce the so called pig iron. This step is where most of the CO_2 is generated that does not come from the burning of fuels. The coke as a reactant is essentially burned as a fuel to heat the furnace; and as it burns, it gives off CO, which ultimately reduces the iron oxide in both the iron ore and the sinter into metallic iron according to the following reaction:

$$Fe_2O_3 + 3CO \longrightarrow 2Fe + 3CO_2 \quad (2)$$

The limestone is used to remove the silica present in the ore in the form of fusible calcium silicate, which floats to the top of the molten metal; as such, it is easy to separate. Without limestone, iron silicate is formed, resulting in a loss of metallic iron. The pig iron produced in this step contains about 92% iron, about 4% carbon, and a balance of silicon, manganese, phosphorus, and traces of sulfur.

This step is followed by a step that utilizes a basic oxygen furnace (BOF). About 75% of the hot metal from the blast furnace is poured into a pear-shaped BOF that tilts sideways for charging and pouring. This hot metal is then mixed with 25% purchased scrap metal, along with desulfuring agents such as lime, calcium carbide, and magnesium. With a moving lance, pure oxygen is injected into the mix at various places in the BOF to combine with carbon and other unwanted elements such as silicon and phosphorus that are present in the pig iron. The heat released due to these reactions raises the furnace temperature (>1600°C) and facilitates melting of the mixture. CO is produced and leaves the reactor, while silica, calcium, and magnesium phosphates and sulfides become part of the slag that is separated from the molten steel.

Instead of a BOF, an electric arc furnace (EAF) is also used. In this furnace, energy is supplied electrically via graphite electrodes or chemically via mixing natural gas and oxygen through lances to melt the mixture. Whether the BOF or EAF are used, the steel forms in the same way, while producing CO and slag. Although it can certainly process pig iron in the feed, the EAF process has been designed more specifically for the recuperation of steel from scrap. All CO produced in this and other steps in the steel industry are utilized as a reducing agent and in the generation of heat.

Lime and Cement Production (446,457)

The manufacture of cement and lime from limestone and dolomite constitute the second and fifth largest sources of CO_2 produced in

non-energy related industrial processes. A typical flow sheet for the manufacture of cement and lime is given in Fig. 5. The corresponding stream compositions are given in Table 12, and capacity and flow rate information is given in Table 13. A review of the global cement industry and its associated CO_2 emissions has been given by Worrell et al. (458).

Cement is normally produced in three steps. After an extraction and coarse milling process, the raw limestone is mixed with mineral additives and water in proportions that lead to the formation of pellets, i.e., clinker, of uniform quality. After a preheating step, the pellets are inserted into a rotary kiln where they undergo two steps. The first step consists of a calcination step at 800–900 °C where the calcium carbonate (i.e., limestone) in the pellets undergoes decomposition with the release of CO_2 according to:

$$CaCO_3 \rightarrow CaO + CO_2 \quad (3)$$

The CO_2 is produced at around 22 vol%, with it ranging from 14 to 33 vol%. This relatively high concentration of CO_2 makes it ideal for recovery as a saleable product.

Farther down in the kiln, at temperatures between 1350 and 1450°C, additional clinkering completes the calcination stage and fuses the calcined raw mix into hard nodules (again referred to as clinker) that resemble small gray pebbles. The manufacture of cement is finished with a milling of the clinker to produce a fine grey powder. Gypsum ($CaSO_4$), which controls the rate of hydration of the cement in the cement-setting process, is blended with the ground clinker, along with other materials, to produce finished cement.

Lime is produced from limestone and dolomite in a very similar process. The major difference between them is that the rotary kiln is operated in one step to form the pellets during calcination at 800-900°C. This calcination step again produces CO_2 according to the reaction depicted in Eq. 3. The final product is then milled to produce a fine powder. This lime powder may be sold as is or it may be mixed with water to produce a milky suspension and sold as lime slurry.

Hydrogen, Syngas, and NH_3 Production (446)

The manufacture of H_2, syngas and NH_3 constitutes the third largest industrial producer of non-energy related CO_2. A typical flow sheet for the manufacture of H_2, syngas and NH_3 is given in Fig. 6. The corresponding stream compositions are given in Table 12, and capacity and flow rate information is given in Table 13. A detailed review on hydrogen, syngas and NH_3 production technologies by reforming, autothermal reforming, and partial oxidation processes has been published recently by

the authors (459). A brief overview is provided below, based on a typical reforming process.

CO_2 is produced as a by-product in the production of H_2, syngas ($H_2 + CO$) and NH_3. These important gases are all produced in a similar fashion through a chain of reforming and shift reactions. The source of the hydrogen and carbon in these gases and hence the CO_2 that is formed stems from the reforming of natural gas and other hydrocarbon feedstocks.

After leaving the reformer reactor at temperatures of over 1000°C and pressures of up to 20 atm, the resulting syngas (i.e., H_2 + CO), which is relatively rich in CO_2, is cooled down and sent to either one or two water gas shift reactors. In these reactors, H_2O is utilized to convert most of the remaining CO into CO_2 while more H_2 is generated.

Before the advent of pressure swing adsorption (PSA) for H_2 purification in the early 1980s, older H_2 production plants (still in existence) required two steps for the water gas shift reaction to achieve maximum CO conversion into H_2 using H_2O and producing more CO_2 as the by-product. The first water gas shift reactor was a high temperature shift reaction that converted most of the remaining CO into H_2 and CO_2 using a Fe-Cr catalyst at 315–430°C. This step was then followed by the second water gas shift reactor, which was operated at a lower temperature of 203–230°C. This reactor utilized a Cu-Zn catalyst to convert any remaining CO into H_2 and CO_2. The gas leaving this reactor, which contained less than 0.5 vol% CO, was sent to a high-pressure scrubbing process that removed nearly 100% of the CO_2 in the stream, typically at very high purity (>98 vol%). It was then sent to a methanator, which reduced CO by converting it back to CH_4.

With the introduction of new NH_3 plants, with PSA units replacing the CO_2 scrubbing step for the purification of H_2, new avenues for CO_2 removal came into practice. Hydrogen purification with the PSA option became less expensive because it eliminated the need for the low temperature shift reactor and a methanation step to fully eliminate CO from the hydrogen stream. But the CO_2 was not enriched as much as it was before. The PSA tail gas does not contain more than 40 vol% CO_2 and is balanced with significantly high concentrations of H_2, CH_4, and even CO. At present the PSA tail gas is used as fuel, with the resulting CO_2 typically being released to the atmosphere.

H_2 selective membrane technology is also commercially available and being used for H_2 production. This technology takes advantage of the relatively high H_2 concentration (>75 vol%) produced from the low temperature shift reactor. However, the permeate, which is rich in H_2, requires recompression and may contain significant amounts of CO_2

that forces further H_2 purification. The high pressure-reject gas, which contains H_2, CO_2, CO, and CH_4 is currently used for fuel, with the CO_2 again being released to the atmosphere.

Natural Gas Production (446,460)

Natural gas production constitutes the fourth largest producer of CO_2 as a result of natural purification. A typical flow sheet for natural gas production is given in Fig. 7. The corresponding stream compositions are given in Table 12, and capacity and flow rate information is given in Table 13.

Processed natural gas consists principally of methane, with a much smaller fraction (<5 vol%) of ethane and propane. In a raw state, it is normally extracted as an associated gas, either free or dissolved, when extracted from oil wells, or as a non-associated gas when extracted from gas and condensate wells where there is little or no crude oil. Once separated from crude oil (if present), in addition to ethane and propane, natural gas in the raw state also contains some butanes and pentanes, and it may contain considerable amounts of water vapor, H_2S, CO_2, He, N_2, and other compounds such as Hg. The CO_2 emissions result from the so-called natural gas sweetening steps that are associated with natural gas processing.

When natural gas contains H_2S, other sulfur bearing compounds, and CO_2, it is normally referred to as sour gas. After a series of dehydration steps, either with glycol absorption or adsorption with silica gel or activated alumina, and after removal of the C_2-C_5 fraction via absorption, the sour gas is sweetened through an absorption scrubbing process (typically, an ethanol-amine based process) that is followed by a desulfurization step (Claus/SCOT process), where all sulfur compounds and CO_2 are removed. Natural gas sweetening is responsible for more than 15% of the total sulfur production in the US.

In the case of natural gas streams that are rich in N_2, only those streams containing more than 10 vol% N_2 can be economically blended with more dilute streams after the sweetening step. However, the concentration of CO_2, sulfur, and N_2 in some natural gas wells can be so high that traditional steps for gas sweetening may be insufficient. It is known, for example, that in one of every 10 wells the content of CO_2 is larger than 2 vol% and that in one of every 100 wells, the CO_2 content is larger than 20 vol%. In the latter case the CO_2 concentration can even be in excess of 50 vol%. The same is true with H_2S and N_2, where concentrations may vary between 2 and 98 vol% for the former and up to 20 vol% for the latter.

Aluminum Manufacture (446,454–456,460,461)

The manufacture of aluminum constitutes the sixth largest source of non-energy related CO_2 emissions. A typical flow sheet for the manufacture of aluminum is given in Fig. 8. The corresponding stream compositions are given in Table 12, and capacity and flow rate information is given in Table 13.

The manufacture of aluminum starts with the production of alumina from bauxite. Bauxite is a mineral rich in gibbsite ($Al_2O_3 \cdot 3H_2O$) and boehmite ($Al_2O_3 \cdot 3H_2O$). It also contains significant concentrations of oxides and hydroxides of Fe, Ti, and Si. Alumina is manufactured via the Bayer process, the Sinter process, or a combination of the two processes.

In the Bayer process, which is considered economically suitable for bauxites containing 30–60% Al_2O_3 as aluminum hydroxides and less than 7% SiO_2 as clay (kaolin) minerals, the bauxite is reacted with a hot aqueous solution of NaOH (~200 g/L) to extract the aluminum in the form of an oxide (such as $Na_2O \cdot Al_2O_3$). The temperature of the digestion process varies between 150 and 250°C depending on whether the bauxite is richer in gibbsite or boehmite. Boehmite cannot be economically extracted below about 200°C. This digestion process is followed by a sedimentation and filtration step, where oxides of Fe, Ti, and Si are removed. The caustic aluminate liquor is then sent to a crystallizer (60–70°C) that forms precipitates of gibbsite. The precipitate is dried and filtered and finally undergoes a dry calcination step at 900–1100°C that leads to the formation of 99.5% pure alumina.

The Sinter process starts with a rotary kiln, wherein pellets of the bauxite and minerals of sodium carbonate and sodium hydroxide are converted into $NaAlO_2$ at a relatively high temperature of 900–1100°C. The sintered material is then converted into a very fine white alumina powder after realizing a series of steps that include water extraction, precipitation and desilication. However, because of its complexity and high energy consumption, the Sinter process is of minor commercial significance compared to the Bayer process.

The purified alumina is then fed into a Hall-Heroult smelting process, consisting of one or more (typically three) potlines of several ovens, where aluminum is produced electrochemically at about 1000°C. The process is based on the use of cryolite (Na_3AlF_3), which melts at temperatures a little under 1000°C. It is able to dissolve alumina to the extent of 15 wt% at 1030°C. Without cryolite, the temperature of the reactor would need to be over 2000°C, which is when alumina starts to melt. The electrochemical energy is provided in the form of graphite anodes and carbon cathodes placed in the upper

and lower parts of the reactor, respectively. CO_2 is evolved from the surface of the anodes and becomes the largest fraction of the off gas, while alumina reduces into aluminum when in contact with the cathode surface. The overall reaction is given by

$$2Al_2O_3 + 3C \rightarrow 4Al + 3CO_2 \quad (4)$$

Besides CO_2, the major emissions are perflurocarbons that result from the decomposition of cryolite, and SO_2 that result from sulfur impurities in the graphite.

An alternative electrochemical process to the Hall-Heroult process, recently developed for the production of aluminum out of alumina is the carbothermic advanced reactor process (CARP). CARP also uses graphite as the anode; but, it eliminates the use of cryolite so that the reactor temperature must reach 2000°C. This process has been shown to be more economically viable, and it eliminates all perflourocarbon and carbon anode baking furnace emissions. The major component of the off gas is CO instead of CO_2, which can be flared to produce CO_2 anyway.

Sulfur Recovery Processes (446,462,463)

Sulfur recovery from petroleum refineries, coke production, and natural gas sweetening is another important source of CO_2 emissions. Today, the sulfur recovery industry produces about 9 millions tons of pure sulfur per year, 10% of which is in the form of sulfuric acid. Around 17% of the total sulfur produced in the US comes from natural gas sweetening, while the rest comes from oil refineries and a very minor fraction from coke manufacturing. Currently, the principal process that is used for sulfur recovery is based on the Claus and SCOT technologies, which constitute more than 80% of the total sulfur recovery plants in service in the U.S. A typical flow sheet for these technologies is given in Fig. 9. The corresponding stream compositions are given in Table 12, and the capacity and flow rate information is given in Table 13.

The Claus/SCOT process removes species from sour streams that contain sulfur and converts them into elemental sulfur. The process is designed to treat gas streams containing more than 50 vol% H_2S, with CO_2 being the second largest species. The process starts with the Claus step, which produces elemental sulfur. This process is followed by the Shell-Claus offgas treating (SCOT) process, which converts all sulfur compounds in the gas leaving the Claus unit, e.g., SO_2, COS, CS_2, and elemental sulfur, into H_2S, which is then recycled back to the Claus step for further processing. The remaining gas is sent to an incinerator prior to exhausting to the atmosphere.

The Claus process consists of two steps. The first step, which is referred to as the thermal step, is basically an incineration step. It is where the sour gas becomes combined with air at high temperatures (1000-1400°C) to oxidize at least one third of the H_2S into SO_2 according to:

$$H_2S + 1.5O_2 \rightarrow SO_2 + H_2O \quad (5)$$

This reacted gas then goes to the second step that consists of a series of reactors and condensers, where H_2S and SO_2 react (200–350°C) to produce elemental sulfur according to:

$$2H_2S + SO_2 \rightarrow S + 2H_2O \quad (6)$$

The elemental sulfur is removed in the liquid state through the condensers.

The reactors consist of packed beds containing alumina as the principal catalyst; but, they may use as an option Co-Mo as the catalyst. At this step, all traces of NH_3 also react to form H_2 and N_2, and all traces of organic compounds combust into H_2O and CO_2. More than 95% of the sulfur compounds are removed in this step. Several improvements have been done to improve this process. For example, the superclaus process converts H_2S directly into elemental sulfur in one step. The gases produced during this step are mainly N_2, CO_2, and H_2O.

The SCOT process also consists of two steps. The first step consists of a reactor containing Co-Mo catalyst, where all the sulfur compounds react at about 250-300°C with H_2 to form H_2S. H_2 may already be present in the Claus tail gas. Otherwise, it is added upstream. This reactor is then followed by an absorption process that removes more than 99% of the H_2S from the processed gas, where the H_2S rich gas is sent back to the Claus step. Similar to the Claus process, the gases produced during the SCOT process are mainly N_2, CO_2, and H_2O.

Landfill and Coal Bed Methane Gases (464,465)

Landfills are scattered all over the US and the world. Each one covers anywhere from 10 to 1500 acres of land. They consist of layers 50 to 100 ft thick of solid human-generated wastes that are entombed beneath 5 ft of inert material that plays the role of reducing both gas permeation and rainfall water infiltration.

Landfill gas (LFG) is produced naturally from the anaerobic decomposition of the waste material. As a result, it contains relatively high concentrations of CH_4. This gas either slowly permeates the landfill cap into the environment, or it builds up pressure within the

landfill creating the potential for an explosion. Over the past few decades, pipes have been installed in most capped landfills to facilitate bringing the LFG to the surface for flaring or recovery as an energy source. For a typical LFG site, the flow rate is 2.5 million standard cubic feet of gas per day.

Typical flow sheets for landfill and coal bed methane gas production are given in Figs. 10a and 10b. The corresponding stream compositions are given in Table 12, and the capacity and flow rate information is given in Table 13. About 45 vol% of typical LFG is composed of CH_4. Another 45 vol% is composed of CO_2. The remaining 10 vol% is composed of a small amount of water vapor (saturated). N_2 and some toxic non-methane organic compounds, such as VOCs, and sulfur and chlorine bearing compounds are also present in a typical LFG.

In the forced extraction of LFG for energy recovery, the extraction lines are subjected to vacuum. This causes the infiltration of significant amounts of air into the landfill. As a result, significant amounts of N_2 become incorporated into the extracted gas mixture, which dilutes both the CH_4 and CO_2 constituents. Some, but not necessarily all, of the O_2 is bioprocessed near the surface before reaching the suction lines.

Coal bed methane gas represents not only a virtually untapped source of energy, but also another source of CO_2 emissions if tapped for this energy. However, the coal mine itself is being considered as a viable place to sequestor CO_2. In such a situation, the CO_2 emissions are offset by the CO_2 storage; and the storage of CO_2 comes with energy benefits because the mine produces coal bed methane gas that can be recovered during the storage process. Coal bed methane gas, much like landfill gas, contains N_2, O_2, CH_4, CO_2, and H_2O; but, the amounts of these gases in each case are quite different. Coal bed methane contains about the same amount of CH_4, but much more N_2 and O_2 and much less CO_2 than landfill gas (Table 12). The composition of coal bed methane gas can vary considerably, however, from coal mine to coal mine.

Fermentation to Produce Ethanol (466)

Ethanol manufacture from the fermentation of either cornstarch or ground whole corn is increasingly becoming a significant source of CO_2 emissions. During 2004, 3.4 billion gallons of ethanol were produced in the US, a nearly 21% increase from the 2.81 billion gallons produced the previous year. A typical flow sheet for the manufacture of ethanol through fermentation is given in Fig. 11. The corresponding stream compositions are given in Table 12, and capacity and flow rate information is given in Table 13.

Nearly 4000 tons of CO_2 are produced along with each million gallons of ethanol. In countries that promote the use of ethanol as a motor fuel, a growth trend is apparent and likely to continue. The ethanol produced worldwide by fermentation constitutes more than 90% of the manufactured ethanol destined for use as a motor fuel. In recent years it has accounted for around 1% of the US gasoline supply, which corresponds to the US using nearly 2 billion gallons of fuel ethanol annually. This is changing rapidly in the US, with its use on the rise.

The ethanol fermentation process is carried out in a batch mode at a temperature of around 35°C. Water is mixed with baking yeast and milled corn that contains between 150 and 250 g/L of starch. The reactants are converted into a juice that contains between 7 and 9 vol% percent ethanol. The offgas is mostly CO_2, with H_2O and ethanol being very minor components. After a series of purification steps, including odor removal and drying, much (but not all) of the CO_2 produced during ethanol manufacture is being sold for commercial use. Adsoption processes for trace contaminant and moisture removal, followed by condensation and liquefaction are the principal methods for the purification of the CO_2 generated from ethanol production.

EXPANDING THE DEFINITION OF CO_2 CAPTURE APPROACHES USED IN POWER PLANTS

In this section, the post combustion, pre-combustion, and oxyfuel combustion approaches that have traditionally been considered for the capture of CO_2 from fossil fuel power plants, are described in such a way as to make them general approaches that can be adopted for use with any CO_2 producing process. The post combustion approach consists of the removal of CO_2 from flue gas. Flue gas is typically low in both pressure and CO_2 concentration (1 atm, and 3 to 20 vol%, respectively). This post capture approach is the only economical approach to existing air-fueled power plants based on pulverized carbon or natural gas fuel sources.

In the pre-combustion approach, CO_2 is separated from the gas stream prior to its conversion into flue gas. This approach is applied to produce gases other than CO_2, such as CO and H_2 from a potentially CO_2 producing source. The pre-combustion approach is unique to the IGCC and NGCC power plant technologies. Nevertheless, the gas to be treated consists typically of synthesis or shifted gas at relatively high partial pressures of CO_2 (15 and 40 vol% at total pressures of over 20 atm).

In the oxyfuel combustion approach, N_2 is excluded from the combustion process to produce flue gas with elevated CO_2 concentrations. This methodology also eliminates the need for post combustion NO_x

removal. Also, in IGCC and NGCC power plant technologies controlled amounts of pure oxygen are added to achieve partial oxidation of the fuel during the initial gasification step. The oxyfuel combustion approach could also be applied to existing fossil fuel power plants, but the design and materials of construction may not be compatible with the use of higher concentrations of oxygen.

More broadly defined post combustion, pre-combustion, and oxy-fuel combustion concepts that can be applied to CO_2 separations in non-energy related processes are presented conceptually in Fig. 12. The post combustion approach involves the use of any CO_2 capture step where the gas stream has no energetic value. A typical gas may consist

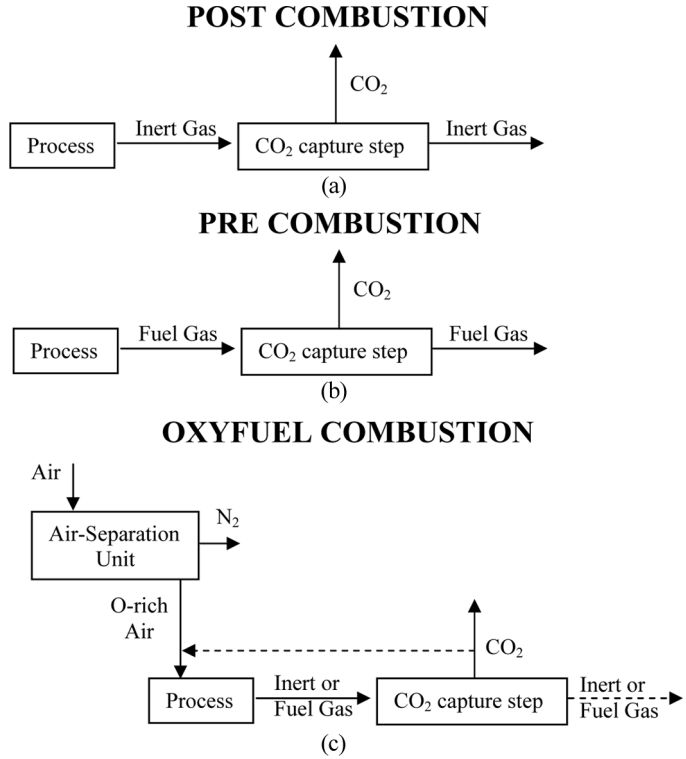

Figure 12. The three conventional approaches for CO_2 capture in the fossil fuel power plant industry are defined here in broader terms for use in any CO_2 producing industrial process. (Figs. 13 to 20). Post combustion refers to a CO_2 capture step from inert gas or one with no energetic value. Pre-combustion refers to a CO_2 capture step from a gas that has some value, such as a fuel. Oxyfuel combustion refers to those CO_2 capture steps that exploit the use of oxygen or an oxygen enriched stream for fuel.

primarily of flue gas produced during a combustion or flaring step. Examples of these kinds of gas streams include those resulting from metabolic combustion (i.e., fermentation), or reactions facilitated by the direct contact of a combustion step, such as autothermal reforming, or those in cement kilns and lime production.

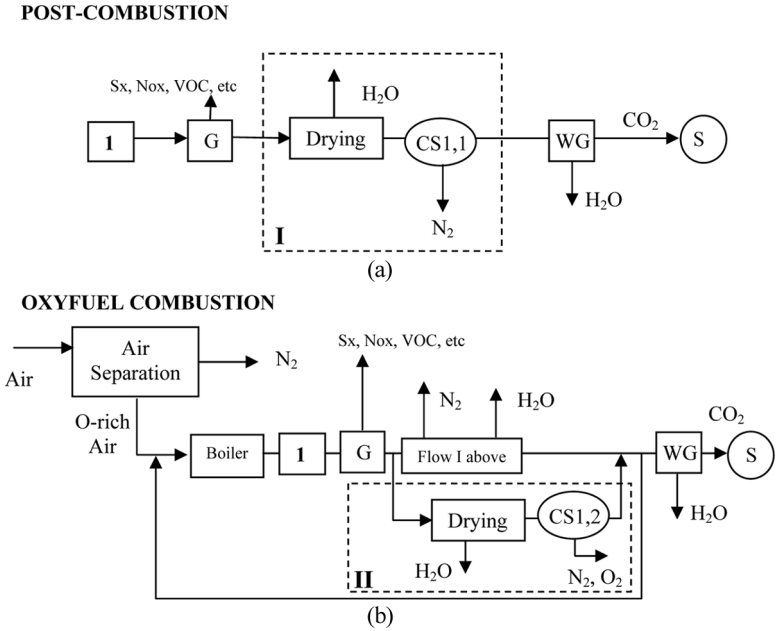

Figure 13. Post-combustion and oxyfuel-combustion approaches for the capture and concentration of CO_2 in combustion processes for stream 1 in Fig. 1. The short-hand notation used here appears as CS#,# or CS#−#,#. CS stands for a CO_2 separation step. The first number (#) corresponds to a figure number (or figure numbers as indicated by #−#). This number (or numbers) corresponds to one (or more) of the CO_2 producing flowsheets depicted in Figs. 1 to 11. The second number (#) after the comma represents the proposed CO_2 separation step that is indicated within the boxed region labeled with the corresponding Roman numeral. WG refers to a guard step particular for water, WGS refers to a water gas shift step, CS1,1 and CS1,2 refer to CO_2 separation steps appropriate to boxed flow sheets I and II, respectively, and S refers to the final CO_2 sequestration step. This fianl CO_2 stream is H_2O free but may contain small amounts CH_4, CO, O_2 and H_2. At the CO_2 separation steps, boxed flow sheets I and II contain CO_2 and N_2 as main gas components. Boxed flow sheet I is rich in N_2, while boxed flow sheet II is lean in this gas species. Depending on the CO_2 concentration, Fig 21 provides alternative processes for the CO_2 separation steps CS1,1 and CS1,2.

The pre-combustion approach consists of the use of any CO_2 capture step in a process where the gas stream has some value, energetic or otherwise. Examples of these kinds of gas streams are found during blast furnace operations in the steel industry that are typically rich in CO, the tail gas from a pressure swing adsorption unit of an ammonia production plant that are typically rich in H_2, or even natural gas before sweetening.

The oxyfuel combustion approach consists of using pure O_2 or O_2 enriched air as oxidants in reaction processes that produce CO_2 as a by-product. This approach offers the possibility for improving the economics of CO_2 production. Examples of where this approach can be used include in combustion processes and in the production of iron and steel, lime and cement, and NH_3.

Conceptual Flow Sheets for Additional Guidance

The flow sheets given in Figs. 1 to 11 for the most intense CO_2 producing processes were discussed at length in a preceeding section. They should be used for guidance to foster ideas for near and long term CO_2 production

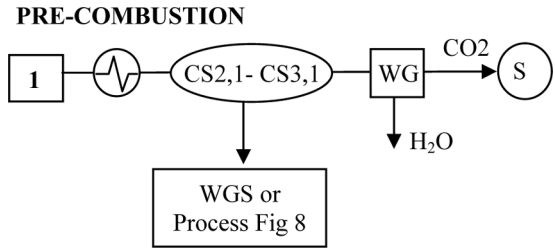

Figure 14. Pre-combustion approaches for the capture and concentration of CO_2 in the coal gasification industry for stream 1 in Figs. 2 and 3. The short-hand notation used here appears as CS#,# or CS#−#,#. CS stands for a CO_2 separation step. The first number (#) corresponds to a figure number (or figure numbers as indicated by #−#). This number (or numbers) corresponds to one (or more) of the CO_2 producing flowsheets depicted in Figs. 1 to 11. The second number (#) after the comma represents the proposed CO_2 separation step that is indicated within the boxed region labeled with the corresponding Roman numeral. WG refers to a guard step particular for water, WGS refers to a water gas shift step, CS2,1 and CS3,1 refer to a CO_2 separation step appropriate for the process in Figs. 5 and 6, respectively, and S refers to the final CO_2 sequestration step. This final CO_2 stream is H_2O free but may contain small amounts CH_4, CO and H_2. At the CO_2 separation steps, boxed flow sheets I and II contain CO_2, CO, H_2, and CH_4 as main gas components. Depending on the CO_2 concentration, Fig. 19 provides detailed alternative processes for the CO_2 separation steps CS2,1 and CS3,1.

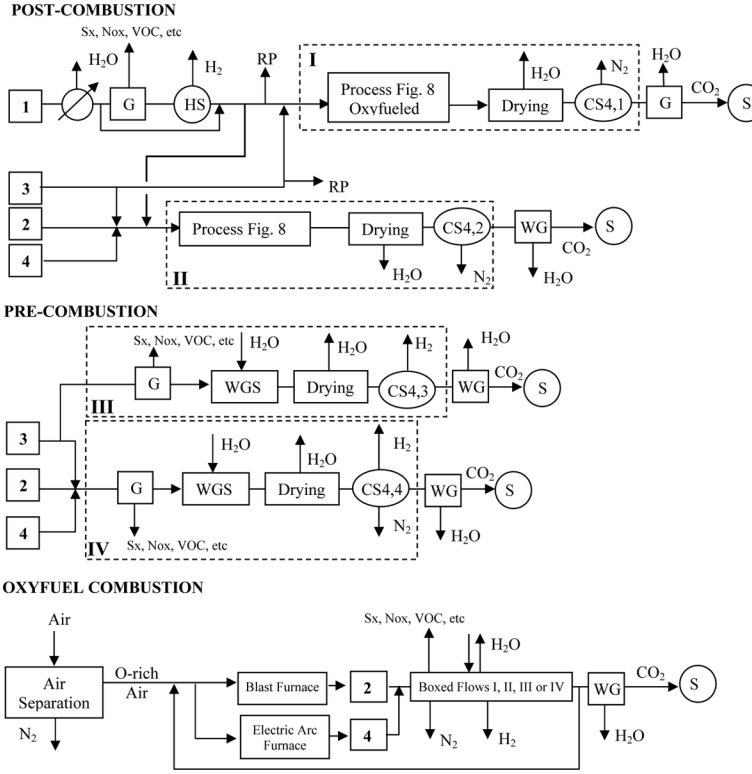

Figure 15. Post-combustion, pre-combustion and oxyfuel combustion approaches for capture and concentration of CO_2 in the stainless steel industry for the streams 1 through 4 defined in Fig. 4. The short-hand notation used here appears as CS#,# or CS#−#,#. CS stands for a CO_2 separation step. The first number (#) corresponds to a figure number (or figure numbers as indicated by #-#). This number (or numbers) corresponds to one (or more) of the CO_2 producing flowsheets depicted in Figs. 1 to 11. The second number (#) after the comma represents the proposed CO_2 separation step that is indicated within the boxed region labeled with the corresponding Roman numeral. G refers to a guard step, WG refers to a guard step particular for water, HS refers to a hydrogen separation step, WGS refers to a water gas shift step, CS4,1 through CS4,4 refer to CO_2 separation steps appropriate to boxed flow sheets I through IV, respectively, and S refers to the final CO_2 sequestration step. A stream labelled with CO_2 indicates that stream is ready for injection (i.e., sequestration). This stream is H_2O free but may contain small amounts of N_2, CH_4, O_2 and H_2. At the CO_2 separation steps, boxed flows I and II contain CO_2 and N_2 as main gas components, while boxed flows III and IV contain CO_2, N_2 and H_2 as the main gas components. Boxed flow sheets I and III are lean in N_2, while boxed flow sheets II and IV are rich in this gas species. Depending on the CO_2 concentration, Figs. 18 and 19 provide alternative processes for the CO_2 separation steps CS4,1 through CS4,4.

plant modifications with adsorption and membrane technologies. To further assist in this goal, new conceptual flow sheets have also been devised that are based on the post combustion, pre-combustion, and oxyfuel combustion approaches that have evolved over the years for the capture of CO_2 from fossil fuel power plants and that were introduced in the last section. They are given in Figs. 13 to 20. For each of the CO_2 producing processes discussed in this review a new flow sheet has been drawn that includes the incorporation of postcombustion,

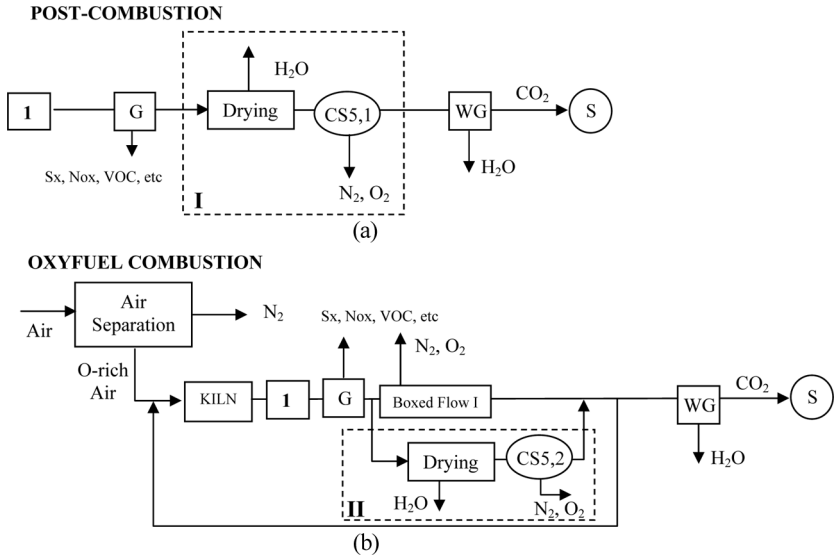

Figure 16. Post-combustion and oxyfuel-combustion approaches for capture and concentration of CO_2 in the cement and lime industry for stream 1 defined in Fig. 5. The short-hand notation used here appears as CS#,# or CS#−#,#. CS stands for a CO_2 separation step. The first number (#) corresponds to a figure number (or figure numbers as indicated by #−#). This number (or numbers) corresponds to one (or more) of the CO_2 producing flowsheets depicted in Figs. 1 to 11. The second number (#) after the comma represents the proposed CO_2 separation step that is indicated within the boxed region labeled with the corresponding Roman numeral. G refers to a guard step, WG refers to a guard step particular for water, CS5,1 and CS5,2 refer to CO_2 separation steps appropriate to boxed flow sheets I and II, respectively, and S refers to the final CO_2 sequestration step. This final CO_2 stream is H_2O free but may contain small amounts of N_2, CH_4, H_2S, O_2, and SO_2. At the CO_2 separation steps, boxed flow sheets I and II contain CO_2 and N_2 as main gas components. Boxed flow sheet I is rich in N_2, while boxed flow sheet II is lean in this gas species. Depending on the CO_2 concentration, Fig. 21 provides alternative processes for the CO_2 separation steps CS5,1 and CS5,2.

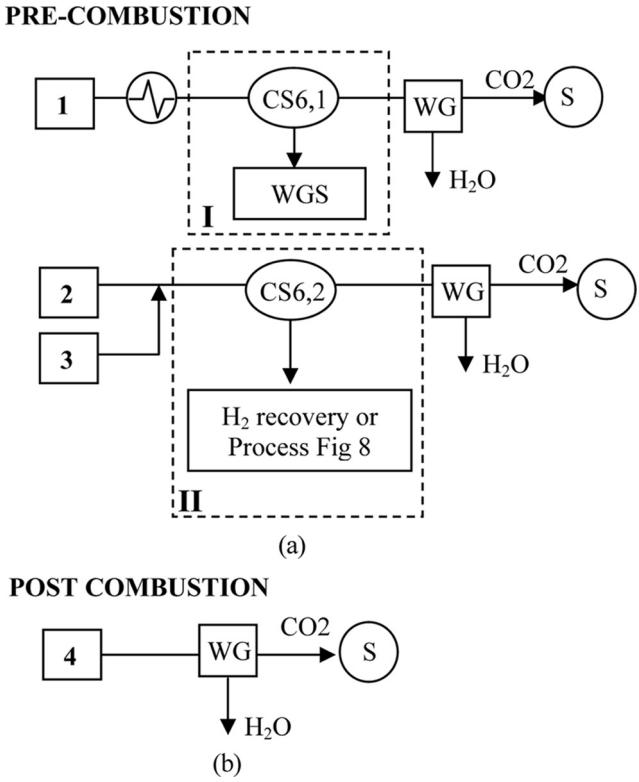

Figure 17. Pre-combustion and post-combustion approaches for capture and concentration of CO_2 in the ammonia manufacture industry for streams 1 through 4 in Fig. 6. The short-hand notation used here appears as CS#,# or CS#−#,#. CS stands for a CO_2 separation step. The first number (#) corresponds to a figure number (or figure numbers as indicated by #−#). This number (or numbers) corresponds to one (or more) of the CO_2 producing flowsheets depicted in Figs. 1 to 11. The second number (#) after the comma represents the proposed CO_2 separation step that is indicated within the boxed region labeled with the corresponding Roman numeral. WG refers to a guard step particular for water, WGS refers to a water gas shift step, CS6,1 and CS6,2 refer to CO_2 separation steps appropriate to boxed flow sheets I and II, respectively, and S refers to the final CO_2 sequestration step. This fianl CO_2 stream is H_2O free but may contain small amounts CH_4, CO and H_2. At the CO_2 separation steps, boxed flow sheets I and II contain CO_2, CO, H_2, and CH_4 as main gas components. Boxed flow sheet I is rich in CO and CH_4, while boxed flow sheet II is very lean in these gas species. Depending on the CO_2 concentration, Fig. 19 provides detailed alternative processes for the CO_2 separation steps CS6,1 and CS6,2. No particular action is taken over stream 4 other than a drying step.

pre-combustion, and/or oxyfuel combustion approaches. Within each of these new flow sheets, potential locations have been proposed where a CO_2 separations unit may be able to augment the performance of the current CO_2 producing plant.

At this point, the differentiation between these locations is not based on the type of separation process that may be applicable (i.e., adsorption, membrane, etc.); rather, it is based on the quality of the stream, i.e., the composition and CO_2 concentration in the stream. Hence, these proposed CO_2 separation processes for each of the indicated locations shown in Figs. 13 to 20 are identified in Figs. 21 to 23, where streams have been classified according to three main categories:

1. streams free of H_2 and sulfur bearing compounds,
2. streams containing significant H_2 and no sulfur bearing compounds, and
3. streams containing significant concentrations of sulfur bearing compounds.

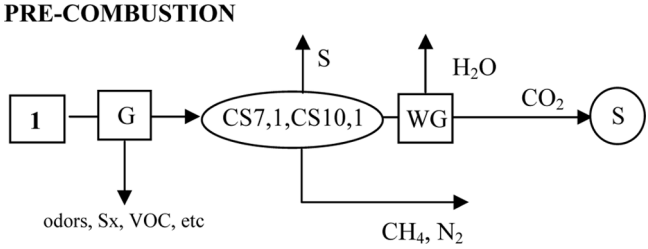

Figure 18. Pre-combustion approach for capture and concentration of CO_2 in the natural, coal and landfill gas industries for stream 1 defined in Figs. 7 and 10. The short-hand notation used here appears as CS#,# or CS#−#,#. CS stands for a CO_2 separation step. The first number (#) corresponds to a figure number (or figure numbers as indicated by #−#). This number (or numbers) corresponds to one (or more) of the CO_2 producing flowsheets depicted in Figs. 1 to 11. The second number (#) after the comma represents the proposed CO_2 separation step that is indicated within the boxed region labeled with the corresponding Roman numeral. G refers to a guard step, WG refers to a guard step particular for water, CS7,1 and CS10,1 refer to a CO_2 separation step appropriate for the process in Figs. 7 and 10, respectively, and S refers to the final CO_2 sequestration step. This final CO_2 stream is H_2O free but may contain small amounts of N_2, CH_4, and H_2S. At the CO_2 separation step, the stream contains CO_2, N_2 and H_2S as main gas components. Depending on the CO_2 and H_2S concentrations, Fig. 23 provides alternative processes for the CO_2 separation step CS7,1 and CS10,1.

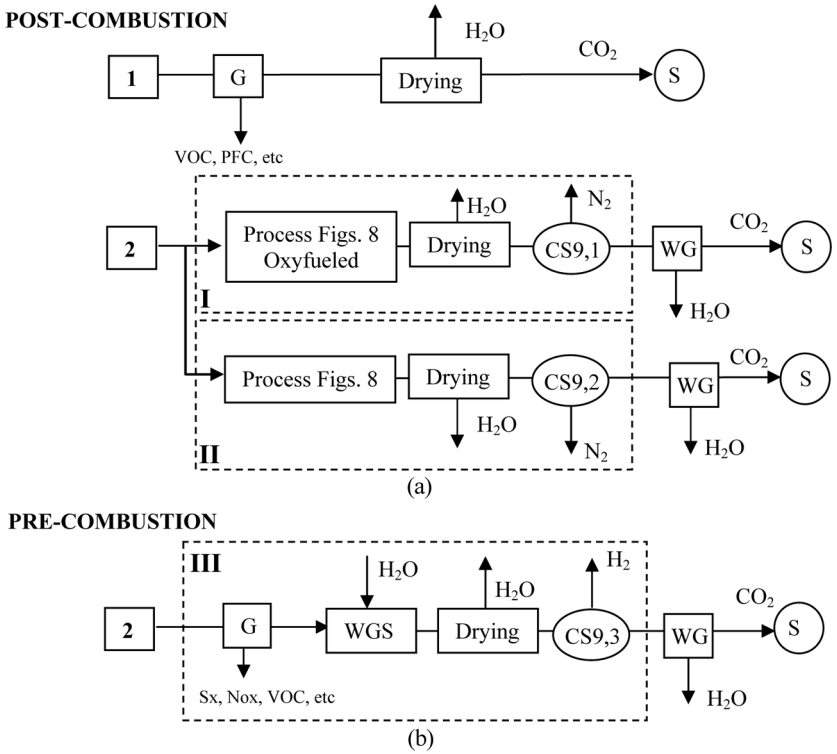

Figure 19. Post-combustion and pre-combustion approaches for capture and concentration of CO_2 in the aluminum industry for the streams 1 and 2 defined in Fig. 9. The short-hand notation used here appears as CS#,# or CS#−#,#. CS stands for a CO_2 separation step. The first number (#) corresponds to a figure number (or figure numbers as indicated by #−#). This number (or numbers) corresponds to one (or more) of the CO_2 producing flowsheets depicted in Figs. 1 to 11. The second number (#) after the comma represents the proposed CO_2 separation step that is indicated within the boxed region labeled with the corresponding Roman numeral. G refers to a guard step, WGS refers to a water gas shift step, WG refers to a guard step particular for water, CS9,1 through CS9,3 refer to CO_2 separation steps appropriate to boxed flow sheets I through III, respectively, and S refers to the final CO_2 seqestration step. This final CO_2 stream is H_2O free but may contain small amounts of N_2. At the CO_2 separation steps, boxed flow sheets I and II contain CO_2 and N_2 as main gas components, while boxed flow sheets III and IV contain CO_2, N_2 and H_2 as the main gas components. Boxed flow sheets I and III are lean in N_2, while boxed flow sheets II is rich in this gas species. Depending on the CO_2 concentration, Figs. 21 and 22 provide alternative processes for the CO_2 separation steps CS9,1 through CS9,3. No particular action is taken over stream 1 other than a drying step.

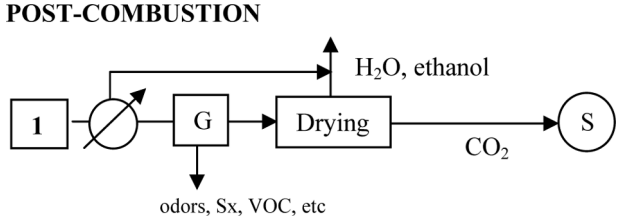

Figure 20. Post-combustion approach for capture and concentration of CO_2 in the ethanol production industry for stream 1 defined in Fig. 11. The short-hand notation used here appears as CS#,# or CS#−#,#. CS stands for a CO_2 separation step. The first number (#) corresponds to a figure number (or figure numbers as indicated by #−#). This number (or numbers) corresponds to one (or more) of the CO_2 producing flowsheets depicted in Figs. 1 to 11. The second number (#) after the comma represents the proposed CO_2 separation step that is indicated within the boxed region labeled with the corresponding Roman numeral. G refers to a guard step and S refers to the final CO_2 sequestration step. This final CO_2 stream is H_2O free but may contain small amounts of N_2. No particular action is taken over stream 1 other than a drying step.

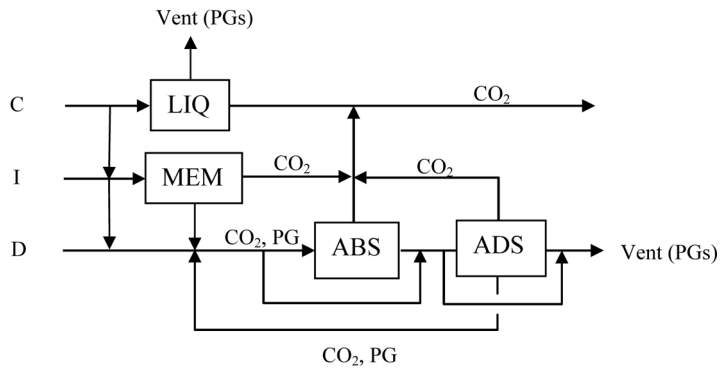

C: (>90% CO_2) CS1,2; CS4,1; CS5,2; CS9,1
I: (20-90% CO_2) CS1,1; CS4,1; CS4,2; CS5,1; CS9,1; CS9,2
D: (5-20% CO_2) CS4,2; CS9,2

Figure 21. Flow diagram representing a CO_2 separation and concentration step for streams in Figs. 13, 15, 16 and 19 that contain N_2, O_2, CO or CH_4 as permanent gases (PG) in addition to CO_2. The separation step may consist of one or more separation processes that include liquefaction (LIQ), membrane (MEM), absorption (ABS) and adsorption (ADS). The step flow diagram allows different accesses depending on whether the CO_2 content in the stream is concentrated (C), intermediate (I) or dilute (D).

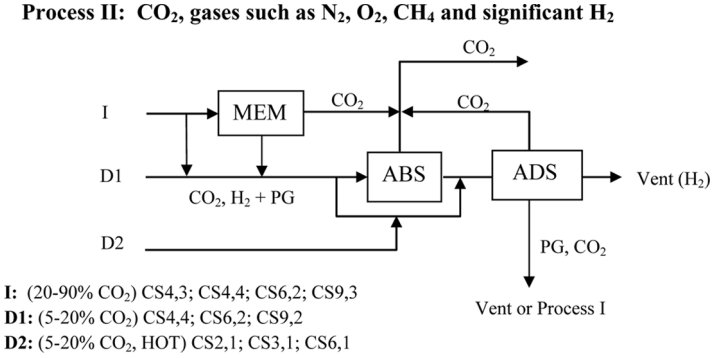

Figure 22. Flow diagram representing a CO_2 separation and concentration step for streams in Figs. 14, 15, 17 and 19 that contain N_2, O_2, CO or CH_4 as permanent gases (PG), as well as significant concentrations of H_2 in addition to CO_2. The separation step may consist of one or more separation processes that include membranes (MEM), absorption (ABS) and adsorption (ADS). The step flow diagram allows different accesses for the stream depending on whether its CO_2 content is intermediate (I), or dilute at room temperature (D1) or dilute at high temperatre (D2).

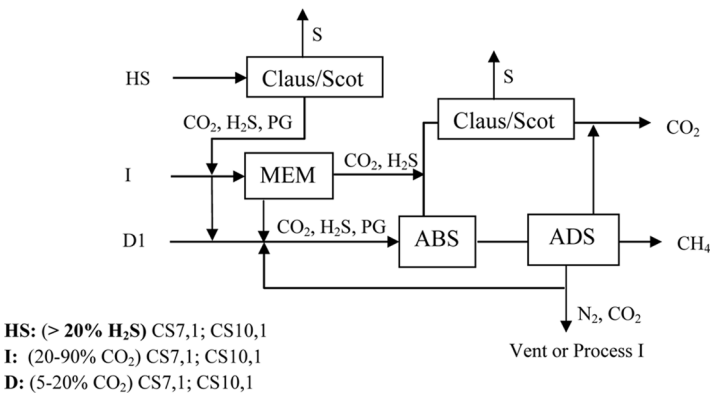

Figure 23. Flow diagram representing a CO_2 separation and concentration step for streams in Fig. 18 that contain N_2, O_2, CO or CH_4 as permanent gases (PG), as well as sulfur bearing compounds (e.g, H_2S, COS, etc.) in addition to CO_2. The separation step may consist of one or more separation processes that include a Claus/Scott step for sulfur removal, membranes (MEM), absorption (ABS) and adsorption (ADSA). The step flow diagram allows different accesses for the stream depending on whether its CO_2 content is intermediate (I) or dilute (D), or on whether its content of sulfur bearing compounds is elevated (HS).

Within each classification and according to the quality of the stream, one or more separation units (e.g., liquefaction, absorption, adsorption, or membrane) is suggested where they may be most advantageous.

Also stream compositions and conditions differ widely, depending on the process. For example, the removal of CO_2 from coal-fired power plants is very different from natural gas sweetening. In the former, the CO_2 is dilute, at low pressure, and dirty. In the latter, the CO_2 can be concentrated, at high pressure, and potentially with high sulfur content. The conditions of all the process streams are given in this review to ensure that these important design and development criteria are not overlooked. It is anticipated that these conceptual flowsheets, and corresponding stream differentiations, should be especially helpful to guide the near and far term developments of new adsorption and membrane processes for CO_2 separation or capture from industrial sources.

ACKNOWLEDGEMENTS

This study was carried out under a subcontract with the Oak Ridge National Laboratory (managed by UT-Battelle, LLC for the Department of Energy under contract DE-AC05-00OR22725) and sponsored by the U.S. Department of Energy's Office of Energy Efficiency and Renewable Energy, Industrial Technologies Program. The programmatic support of Dickson Ozokwelu, the Chemicals Industry of the Future team lead, who funded this effort, is greatly appreciated.

The authors would also like to thank members of the Chemical Industry Vision2020 Technology Partnership committee who contributed to this study: Francis Via, Fairfield Resources International, Inc.; Sharon Robinson, Oak Ridge National Laboratory; Charles G. Scouten, The Fusfeld Group; Linda Curran, BP; Timothy C. Frank, Patrick H. Au-Yeung and John G. Pendergast, Jr., Dow; Scott Barnicki, Eastman Chemical; Hans Wijmans, Membrane Technology and Research, Inc.; Krish R. Krishnamurthy and Stevan Jovanovic, BOC; Dante Bonaquist and Neil Stephenson, Praxair Inc.; Santi Kulprathipanja, UOP; Dilip Kalthod, Air Products and Chemicals, Inc.; Brendan Murray, Shell; and Greg Chambers, GE.

REFERENCES

1. Kohl, A.L.; Nielsen, R.B. (1997) *Gas Purification,* 4th ed., Gulf Publishing CompanyHouston, Texas.
2. Hydrocarbon Processing, (2004) *Gas Processes Handbook 2004*, Gulf Publishing Co.

3. Higman, C.; van der Burgt, M. (2003) Gasification, Elsevier.
4. Supp, E. (1990) *How to Produce Methanol from Coal*, Springer-Verlag.
5. Campbell, J.M. (1994) *Gas Conditioning and Processing*, Vol 3., Campbell Petroleum Series.
6. Ferguson, C.R.; Falsetti, J.S.; Volk, W.P. (1999) Refining Gasification: Petroleum Coke to fertilizer at Farmland's Coffeyville, KS Refinery. Report AM-99–13 presented at the NPRA 1999 Annual Meeting, San Antonio Texas.
7. Wills, J.; Shemaria, M.; Mitariten, M.J. (2004) Production of pipeline quality natural gas with Molecular GateTM CO_2 removal process, SPE Production and Facilities, February.
8. Izumi, J. (2004) Adsorption technology applications to the industries in Japan, Abstract and presentation at the 8th International Conference on Fundamentals of Adsorption, Sedona, AR, May (2004).
9. Wong, S.; Bioletti, R. (2002) Carbon dioxide separation technologies, Alberta Research Council.
10. Freemantle, M. (2005) Membranes for gas separation. *Chem. Eng. News*, *83*: 49.
11. Baker, R.W. (2004) Gas Separation in *Membrane Technology and Applications,* 2nd Edition.; Baker, R.W. Ed. John Wiley & Sons.
12. Baker, R.W. (2002) Future directions of membrane gas separation technology. *Ind. Eng. Chem. Res.*, *41* 1393–1411.
13. Basu, A.; Akhtar, J.; Rahman, M.H.; Islam, M.R. (2004) A review of separation of gases using membrane systems. *Petrol. Sci. Technol.*, *22* 1343–1368.
14. Shekhawat, D.; Luebke, D.R.; Pennline, H.W. (2003) A review of carbon dioxide selective membranes a topical report. DEO/NETL Report, 2003/1200.
15. Stookey, D.J. (2001) Gas separation membrane applications. In *Membrane Technology in the Chemical Industry*, Nunes, S.P.; Peinemann, K.V. Eds., Wiley-VCH Verlag GMbH.
16. Nunes, S.P.; Peinemann, K.V. (2001) Gas separation with membranes. In *Membrane technology in the chemical industry*, Nunes, S.P.; Peinemann, K.V., Ed., Wiley-VCH Verlag GMbH.
17. Fuderer, A.; Rudelstorfer, E. Selective adsorption process. US Patent, 3, 986,849, 1976.
18. Whysall, M.; Wagemans, L.J.M. Very large-scale pressure swing adsorption processes. USP 6,210,466 B1, 2001.
19. Baksh, M.S.A.; Terbot, C.E. Pressure-swing adsorption process for the production of hydrogen. US Patent, 6,503,299 B2, 2003.
20. Baksh, M.S.A.; Ackley, M.W.; Notaro, F. (2004) Process and apparatus for hydrogen purification. WO 2004/058630 A2.
21. Xu, J.; Weist, E.L. Jr. Six bed pressure swing adsorption process with four steps of pressure equalization. US Patent, 6,454,838 B1, 2002.
22. Xu, J.; Rarig, D.L.; Cook, T.A.; Hsu, K.-K.; Schoonover, M.; Agrawal, R. Pressure swing adsorption process with reduced pressure equalization time. US Patent 2003/0015091 A1, 2003.

23. Sircar, S.; Golden, T.C. (2000) Purification of hydrogen by pressure swing adsorption. *Sep. Sci. Tech.*, *35*: 667–687.
24. Waldron, W.E.; Sircar, S. (2000) Parametric study of a pressure swing adsorption process. *Adsorption*, *6*: 179–188.
25. Keefer, B.G. High-frequency rotary pressure swing adsorption. US Patent, *6*, 176,897 B1, 2001.
26. Keefer, B.G.; Doman, D.G. Flow regulated pressure swing adsorption system. US Patent, *6*, 063,191, 2000.
27. Keefer, B.G.; Doman, D.G. Flow regulated pressure swing adsorption system. US Patent, RE38,493, 2004.
28. Golden, C M.A.; Golden, T.C.; Battavio, O.J. Multilayered adsorbent system for gas separations by pressure swing adsorption. US Patent, 2003/0205131 A1, 2003a.
29. Golden, T.C.; Golden, C.M.A.; Zwilling, D.P. Self-supported structured adsorbent for gas separation. US Patent, 6,656,627 B1, 2003b.
30. Golden, T.C.; Weist, E.L. Activated carbon as sole adsorbent in rapid cycle hydrogen PSA. US Patent, 6,660,064, 2003.
31. Keefer, B.G.; Carel, A.; Sellars, B.; Shaw, I.; Larisch, B. Adsorbent laminate structures. US Patent, 6,692,626 B2, 2004.
32. Connor, D.J.; Doman, D.G.; Jeziorowski, L.; Keefer, B.G.; Larisch, B.; Mclean, C.R.; Shaw, I. Rotary pressure swing adsorption apparatus. US Patent, 6,406,523 B1, 2002.
33. Editorial staff. A fast PSA technology to be trialed at petroleum refinery. *Chemical and Engineering News*, *14*, September, 2006.
34. Reynolds, S.P.; Ebner, A.D.; Ritter, J.A. (2006a) Stripping PSA cycles for CO_2 recovery from flue gas at high temperature using a hydrotalcite-like adsorbent. *Ind. Eng. Chem. Res.*, *45*: 4278–4294.
35. Park, J-H.; Beum, H-T.; Kin, J-N.; Cho, S-H. (2002c) Numerical analysis on the power consumption of the PSA process for recovering CO_2 from flue gas. *Ind. Eng. Chem. Res.*, *41*: 4122–4131.
36. Ding, Y.; Alpay, E. (2001) High temperature recovery of CO_2 from flue gas using hydrotalcite adsorbent. *Proc. Safety Environ. Protection*, *79*: 45–52.
37. Will, J.; Shemaria, M. (2004) Production of pipeline quality natural gas with Molecular GateTM CO_2 removal process. *Production and Facilities*, *19*: 4–8.
38. Reinhold, H.E.; D-Amico, J.S.; Knaebel, K.S. Natural gas enrichment process. US Patent, 5,536,300, 1996.
39. Dolan, W.B.; Mitariten, M.J. Heavy hydrocarbon recovery from pressure swing adsorption unit tail gas. US Patent, 6,610,124 B1, 2003.
40. Knaebel, K.S.; Reinhold, H.E. (2003) Landfill gas: from rubbish to resource. *Adsorption*, *9*: 87–94.
41. Sircar, S.; Kumar, R.; Koch, W.R.; Van Sloun, J. Recovery of methane from land fill gas. US Patent, 4770676, 1988.
42. Cavenati, S.; Grande, C.A.; Rodrigues, A.E. (2005) Upgrade of methane from landfill gas by pressure swing adsorption. *Energy & Fuels*, *19*: 2545–2555.

43. Mitariten, M. (2002) Adsorption advances. *World Coal*, September.
44. Mitariten, M. (2004) Economic N_2 removal. *Hydrocarbon Engineering*, July.
45. Olajossy, A.; Gawdzik, A.; Budner, Z.; Dula, J. (2003) Methane separation from coal methane gas by vacuum pressure swing adsorption. *Trans. IChemE*, *81*: 474–482.
46. Jiang, L.; Fox, V.G.; Biegler, L.T. (2004) Simulation and optimal design of multiple-bed pressure swing adsorption systems. *AIChE Journal*, *50*: 2904–2917.
47. Warmuzinski, K.; Tanczyk, M. (1997) Multicomponent pressure swing adsorption. Part I. Modeling of large-scale PSA installations. *Chemical Engineering and Processing*, *36*: 89–99.
48. Tanczyk, M.; Warmuzinski, K. (1998) Multicomponent pressure swing adsorption. Part II. Experimental verification of the model. *Chemical Engineering and Processing*, *37*: 301–315.
49. Yang, J.; Ahn, H.; Lee, H.; Lee, C-H. (1998) Hydrogen recovery from coke oven gas using a layered-column PSA process. In *Fundamentals of Adsorption*, Francis, Meunier. Ed. Elsevier, Paris, France.
50. Ahn, H.; Yang, J.; Lee, C-H. (2001) Effects of feed composition of coke oven gas on a layered bed H_2 PSA process. *Adsorption*, *7*: 339–356.
51. Lee, C-H.; Yang, J.; Ahn, H. (1999) Effects of carbon-to-zeolite ratio on layered bed H_2 PSA for coke oven gas. *AIChE Journal*, *45*: 535–545.
52. Reynolds, S.P.; Ebner, A.D.; Ritter, J.A.; Knox, J.C.; LeVan, M.D. (2006c) Mathematical simulation of the sorbent-based atmosphere revitalization system for the crew exploration vehicle. In *Proceedings of the 36th International Conference on Environmental Systems*, SAE Aerospace.
53. Diagne, D.; Goto, M.; Hirose, T. (1995) Experimental-study of simultaneous removal and concentration of CO_2 by an improved pressure swing adsorption process. *Energy Conversion and Management*, *36*: 431–434.
54. Diagne, D.; Goto, M.; Hirose, T. (1994) New PSA process with intermediate feed inlet position and operated with dual refluxes: Application to carbon dioxide removal and enrichment. *J. Chem. Eng. Japan.*, *27*: 85–89.
55. Diagne, D.; Goto, M.; Hirose, T. (1995) Parametric studies on CO_2 separation and recovery by dual reflux PSA process consisting of both rectifying and stripping sections. *Ind. Eng. Chem. Res.*, *34*: 3083–3089.
56. Diagne, D.; Goto, M.; Hirose, T. (1996) Numerical analysis of a dual refluxed PSA process during simultaneous removal and concentration of carbon dioxide dilute gas from air. *J. Chem. Tech. Biotechnol.*, *65*: 29–38.
57. McIntyre, J.A.; Holland, C.E.; Ritter, J.A. (2002) High enrichment and recovery of dilute hydrocarbons by dual reflux pressure swing adsorption. *Ind. Eng. Chem. Res.*, *41*: 3499–3504.
58. Reynolds, S.P.; Ebner, A.D.; Ritter, J.A. (2006b) Enriching PSA cycle for the production of nitrogen from air. *Ind. Eng. Chem. Res.*, *45*: 3256–3264.
59. Wilson, P.H. Inverted Pressure Swing Adsorption Process. US Patent, 4,359,328, 1982.
60. Leavitt, F.W. Duplex adsorption process. US Patent, 5,085,674, 1992.

61. Zhong, G.; Baksh, M.S.A.; Notaro, F.; Leavitt, F.W. Pressure swing adsorption process for high recovery of high purity gas. US Patent, 6,500,235, 2002.
62. Dong, F.; Kodama, A.; Goto, M.; Hirose, T. (1999) A new concept in the design of PSA processes for the multicomponent gas mixtures. *Ind. Eng. Chem. Res.*, *38*: 233–239.
63. Vaporciyan, G.G.; Kadlec, H.R. (1987) Equilibrium–limited periodic separating reactors. *AIChE Journal*, *33*: 1334–1343.
64. Vaporciyan, G.G.; Kadlec, H.R. (1989) Periodic separating reactors: experiments and theory. *AIChE Journal*, *35*: 831–844.
65. Kadlec, H.R.; Vaporciyan, G.G. Periodic chemical processing system. US Patent, 5,254,368, 1993.
66. Hufton, J.R.; Sircar, S.; Baade, W.F.; Abrardo, J.M.; Anand, M. Integrated steam methane reforming process for producing carbon monoxide and hydrogen, US Patent 6,312,658 B1, 2001b.
67. Hufton, J.R.; Sircar, S.; Baade, W.F.; Abrardo, J.M.; Anand, M. Integrated steam methane reforming process for producing carbon monoxide, US Patent 6,328,945 B1, 2001a.
68. Sircar, S.; Hufton, J.R.; Nataraj, S. Process and apparatus for the production of hydrogen by steam reforming of hydrocarbon, US Patent 6,103,143, 2000.
69. Hufton, J.R.; Nataraj, S. Production of carbon monoxide, US Patent 6,592,836 B2, 2003.
70. Anand, M.; Sircar, S.; Carvill, B.T. Process for operating equilibrium controlled reactions, US Patent 6,303,092 B1, 2001.
71. Nataraj, S.; Carvill, B.T.; Hufton, J.R.; Mayorga, S.G.; Gaffney, T.R.; Brzozowski, J.R. Process for operating equilibrium controlled reactions, US Patent 6,315,973 B1, 2001.
72. Carvill, B.T.; Hufton, J.R.; Anand, M.; Sircar, S. (1996) Sorption-enhanced reaction process. *AIChE J.*, *42*: 2765–2772.
73. Hufton, J.R.; Mayorga, S.; Sircar, S. (1999) Sorption-enhanced reaction process for hydrogen production. *AIChE J.*, *45*: 248–256.
74. Waldron, W.E.; Hufton, J.R.; Sircar, S. (2001) Production of hydrogen by cyclic sorption enhanced reaction process. *AIChE J.*, *47*: 477–1479.
75. Ying, D.H.S.; Nataraj, S.; Hufton, J.R.; Xu, J.; Allam, R.J.; Dulley, S.J. Simultaneous shift-reactive and adsorptive process at moderate temperature to produce pure hydrogen, US Patent Appl. 20040081614 A1, 2004.
76. Hufton, J.R.;Allam, R.J.; Chiang, R. (2005) Development of a process for CO_2 capture from gas turbines using a sorption enhanced water gas shift reactor system. Proceedings of the 7th International Conference of Green House Gas Technology.
77. Han, C.; Harrison, D.P. (1994) Simultaneous shift reaction and carbon dioxide separation for the direct production of hydrogen. *Chemical Engineering Science*, *49*: 5875–5883.
78. Harrison, D.P.; Peng, Z. (2003) Low carbon monoxide hydrogen by sorption-enhanced reaction. *International Journal of Chemical Reactor Engineering*, *1*: A37.

79. Ortiz, A.L.; Harrison, D.P. (2001) Hydrogen production using sorption-enhanced reaction. *Ind. Eng. Chem. Res.*, *40*: 5102–5109.
80. Zou, Y.; Rodrigues, A.E. (2001) The separation enhanced reaction process (SERP) in the production of hydrogen from methane steam reforming. *Adsorption Science and Technology*, *19*: 655–671.
81. Xiu, G.H.; Li, P.; Rodrigues, A.E. (2002a) Sorption-enhanced reaction process with reactive regeneration. *Chemical Engineering Science*, *57*: 3893–3908.
82. Xiu, G-H.; Soares, J.L.; Li, P.; Rodrigues, A.E. (2002b) Simulation of five-step one-bed sorption-enhanced reaction process. *AIChE J.*, *48*: 2817–2832.
83. Xiu, G.H.; Li, P.; Rodrigues, A.E. (2003a) Adsorption-enhanced steam-methane reforming with intraparticle-diffusion limitations. *Chemical Engineering Journal*, *95*: 83–93.
84. Xiu, G.H.; Li, P.; Rodrigues, A.E. (2003b) New generalized strategy for improving sorption-enhanced reaction process. *Chemical Engineering Science*, *58*: 3425–3437.
85. Xiu, G.H.; Li, P.; Rodrigues, A.E. (2004) Subsection-controlling strategy for improving sorption-enhanced reaction process. *Chemical Engineering Research and Design*, *82*: 192–202.
86. Ding, Y.; Alpay, E. (2000) Adsorption-enhanced steam-methane reforming. *Chemical Engineering Science*, *55*: 3929–3940.
87. Ding, Y.; Alpay, E. (2000) Equilibria and kinetics of CO_2 adsorption on hydrotalcite adsorbent. *Chemical Engineering Science*, *55*: 3461–3474.
88. Yong, Z.; Mata, V.; Rodrigues, A.E. (2000) Adsorption of carbon dioxide on basic alumina at high temperatures. *Journal of Chemical and Engineering Data*, *45*: 1093–1095.
89. Easley, M.A.; Horn, W.E. Carbon dioxide adsorption of synthetic meixnerite, US Patent 5,882,622, 1999.
90. Mayorga, S.G.; Gaffney, T.R.; Brzozowski, J.R.; Weigel, S.J. Carbon dioxide adsorbents containing magnesium oxide suitable for use at high temperatures, US Patent 6,280,503 B1, 2001.
91. Yong, Z.; Mata, V.; Rodriguez, A.E. (2001) Adsorption of carbon dioxide onto hydrotalcite-like compounds (HTlcs) at high temperatures. *Ind. Eng. Chem. Res.*, *40*: 204–209.
92. Yong, Z.; Rodrigues, A.E. (2002) Hydrotalcite-like compounds as adsorbents for carbon dioxide. *Energy Conversion and Management*, *43*: 1865–1876.
93. Ebner, A.D.; Reynolds, S.P.; Ritter, J.A. (2006) Understanding the adsorption and desorption behavior of CO_2 on a K-promoted HTlc through non-equilibrium dynamic isotherms. *Ind. Eng. Chem. Res.*, *45*: 6387–6392.
94. Reynolds, S.P.; Ebner, A.D.; Ritter, J.A. (2005) New pressure swing adsorption cycles for carbon dioxide sequestration. *Adsorption*, *11*: 531–536.
95. Gaffney, T.R.; Golden, T.C.; Mayorga, S.G.; Brzozowski, J.R.; Taylor, F.W. Carbon dioxide pressure swing adsorption process using modified alumina adsorbents, US Patent 5,917,136, 1999.
96. Xiong, R.; Ida, J.; Lin, Y.S. (2003) Kinetics of carbon dioxide sorption on potassium-doped lithium zirconate. *Chem. Eng. Sci.*, *58*: 4377–4385.

97. Ida, J.; Lin, Y.S. (2003) Mechanism of high-temperature CO_2 sorption on lithium zirconate. *Environmental Science and Technology*, *37*: 1999–2004.
98. Ida, J-I.; Xiong, R.; Lin, Y.S. (2004) Synthesis and CO_2 sorption properties of pure and modified lithium zirconate. *Sep. Purification Tech.*, *36*: 41–51.
99. Nair, B.N.; Yamaguchi, T.; Kawamura, H.; Nakao, S.I.; Nakagawa, K. (2004) Processing of lithium zirconate for applications in carbon dioxide separation: structure and properties of the powders. *Journal of The American Ceramic Society*, *87*: 68–74.
100. Iyer, M.V.; Gupta, H.; Sakadjian, B.B.; Fan, L-S. (2004) Multicyclic study on the simultaneous carbonation and sulfation of high-reactivity CaO. *Ind. Eng. Chem. Res.*, *43*: 3939–3947.
101. Gupta, H.; Fan, L.S. (2002) Carbonation-calcination cycle using high reactivity calcium oxide for carbon dioxide separation from flue gas. *Ind. Eng. Chem. Res.*, *41*: 4035–4042.
102. Gupta, H.; Iyer, M.V.; Sakadjian, B.B.; Fan, L-S. (2004) Reactive separation of CO_2 using pressure pelletised limestone. *International Journal of Environmental Technology and Management*, *4*: 3–20.
103. Kuramoto, K.; Fujimoto, S.; Morita, A.; Shibano, S.; Suzuki, Y.; Hatano, H.; Lin, S-Y.; Harada, M.; Takarada, T. (2003) Repetitive carbonation-calcination reactions of Ca-based sorbents for efficient CO_2 sorption at elevated temperatures and pressures. *Ind. Eng. Chem. Res.*, *42*: 975–981.
104. Abanades, J.C. (2002) The maximum capture efficiency of CO_2 using a carbonation/calcination cycle of $CaO/CaCO_3$. *Chemical Engineering Journal*, *90*: 303–306.
105. Birbara, P.J.; Nalette, T.A. Regenerable supported amine-polyol sorbent. US Patent 5,376,614, 1994.
106. Birbara, P.J.; Filburn, T.P.; Nalette, T.A. Regenerable supported amine sorbent, USP 5,876,488, 1999.
107. Satyapal, S.; Filburn, T; Trela, J.; Strange, J. (2001) Performance and properties of a solid amine sorbent for carbon dioxide removal in space life support applications. *Energy and Fuels*, *15*: 250–255.
108. Xu, X.C.; Song, C.S.; Andresen, J.M. (2002) Novel polyethylenimine-modified mesoporous molecular sieve of MCM-41 type as high-capacity adsorbent for CO_2 capture. *Energy and Fuels*, *16*: 1463–1469.
109. Xu, X.C.; Song, C.S.; Andresen, J.M. (2003) Preparation and characterization of novel CO_2 "molecular basket" adsorbents based on polymer-modified mesoporous molecular sieve MCM-41. *Micropor. Mesopor. Mater.*, *62*: 29–45.
110. Xu, X.C.; Song, C.S.; Miller, B.G. (2005) Influence of moisture on CO_2 separation from gas mixture by a nanoporous adsorbent based on polyethylenimine-modified molecular sieve MCM-41. *Ind. Eng. Chem. Res.*, *44*: 8113–8119.
111. Robeson, L.M. (1999) Polymer membranes for gas separation. *Cur. Opinion Sol. St. Mater. Sci.*, *4*: 549–552.
112. Freeman, B.D. (1999) Basis of permeability/selectivity tradeoff relations in polymeric gas separation membranes. *Macromol.*, *32*: 375–380.

113. Stern, S.A. (1994) Polymers for gas separations – the next decade. *J. Mem. Sci.*, *94*: 1–65.
114. Dai, Y.; Guiver, M.D.; Robertson, G.P. (2004) Preparation and characterization of polysulfones containing both hexafluoroisopropylidene and trimethylsilyl groups as gas separation membrane materials. *Macromol.*, *37*: 1403–1410.
115. Dai, Y.; Guiver, M.D.; Robertson, G.P. (2003) Enhancement in the gas permeabilities of novel polysulfones with pendant 4-trimethylsilyl-a-hydroxylbenzyl substituents. *Macromol.*, *36*: 6807–6816.
116. Dai, Y.; Guiver, M.D.; Robertson, G.P. (2002) Modified polysulfones 5: Synthesis and characterization of tetramethyl polysulfones containing trimethylsilyl groups and their gas transport properties. *Polymer*, *43*: 5369–5378.
117. Lagunas-Fuentes, C.; Ruiz-Trevino, F.A. (2004) Syntheses and permselectivity properties of polysulfones based on bisphenol A and 1,1 Bi-2 naphthol. *J. Polym. Sci. B Polym. Phys.*, *42*: 226–231.
118. Ismail, A.F.; Dunkin, I.R.; Gallivan, S.L. (1999) Production of super selective polysulfone hollow fiber membranes for gas separation. *Polymer*, *40*: 6499–6506.
119. Ismail, A.F.; Ng, B.C.; Rahman, W.A. (2003) Effects of shear rate and forced convection residence time on asymmetric polysulfone membranes structure and gas separation performance. *Sep. Purif. Technol.*, *33*: 255–272.
120. Ismail, A.F.; Lorna, W. (2003) Suppression of plasticization in polysulfone membranes for gas separations by heat-treatment technique. *Sep. Purif. Technol.*, *30*: 37–46.
121. Choi, S.H.; Lee, M.K.; Oh, S.J. (2003a) Gas sorption and transport of ozone-treated polysulfone. *J. Mem. Sci.*, *221*: 37–46.
122. Bhardwaj, V.; Macintosh, A.; Sharpe, I.D. (2003) Polysulfone hollow fiber gas separation membranes filled with submicron particles. *Ann. NY Acad. Sci.*, *984*: 318–328.
123. Chung, T.S.; Shieh, J.J.; Lau, W.W.Y. (1999) Fabrication of multi-layer composite hollow fiber membranes for gas separation. *J. Mem. Sci.*, *152*: 211–225.
124. Guiver, M.D.; Le, T.H.N.; Robertson, G.P. Preparation of polysulfone-zeolite composite gas separation membranes. USP Appl. 2002062737, 2002.
125. Shao, L.; Chung, T.S.; Goh, S.H. (2004a) Transport properties of crosslinked polyimide membranes induced by different generations of diaminobutane (DAB) dendrimers. *J. Mem. Sci.*, *238*: 153–163.
126. Shao, L.; Chung, T.S.; Pramoda, K.P. (2005b) The evolution of physicochemical and transport properties of 6FDA-durene toward carbon membranes; from polymer, intermediate to carbon. *Micropor. Mesopor. Mater.*, *84*: 59–68.
127. Shao, L.; Chung, T.S.; Goh, S.H. (2005a) The effects of 1,3-cyclohexanebis-(methylamine) modification on gas transport and plasticization resistance of polyimide membranes. *J. Mem. Sci.*, *267*: 78–89.
128. Ren, J.H.; Wang, R.; Chung, T.S. (2003) The effects of chemical modifications on morphology and performance of 6FDA-ODA/ND: A hollow fiber membrane for CO_2/CH_4 separation. *J. Mem. Sci.*, *222*: 133–147.

129. Jeong, H.K.; Krych, W.; Ramanan, H. (2004) Fabrication of polymer/selective-flake nanocomposite membranes and their use in gas separation. *Chem. Mater.*, *16*: 3838–3845.
130. Xiao, Y.C.; Chung, T.S.; Chng, M.L. (2004) Surface characterization, modification chemistry, and separation performance of polyimide and polyamidoamine dendrimer composite films. *Langmuir*, *20*: 8230–8238.
131. Barsema, J.N.; Kapantaidakis, G.C.; van der Vegt, N.F.A. (2003b) Preparation and characterization of highly selective dense and hollow fiber asymmetric membranes based on BTDA-TDI/MDI co-polyimide. *J. Mem. Sci.*, *216*: 195–205.
132. Barsema, J.N.; Klijnstra, S.D.; Balster, J.H. (2004) Intermediate polymer to carbon gas separation membranes based on Matrimid PI. *J. Mem. Sci.*, *238*: 93–102.
133. Hibshman, C.; Mager, M.; Marand, E. (2004) Effects of feed pressure on fluorinated polyimide-organo silicate hybrid membranes. *J. Mem. Sci.*, *229*: 73–80.
134. Hibshman, C.; Cornelius, C.J.; Marand, E. (2003) The gas separation effects of annealing polyimide-organosilicate hybrid membranes. *J. Mem. Sci.*, *211*: 25–40.
135. Tin, P.S.; Chung, T.S.; Liu, Y. (2004a) Separation of CO_2/CH_4 through carbon molecular sieve membranes derived from P84 polyimide. *Carbon*, *42*: 3123–3131.
136. Qin, J.J.; Chung, T.S.; Cao, C. (2005) Effect of temperature on intrinsic permeation properties of 6FDA-Durene/1,3-phenylenediamine (mPDA) copolyimide and fabrication of its hollow fiber membranes for CO_2/CH_4 separation. *J. Mem. Sci.*, *250*: 95–103.
137. Xu, J.W.; Chng, M.L.; Chung, T.S. (2003) Permeability of polyimides derived from non-coplanar diamines and 4,4′-(hexafluoroisopropylidene)-diphthalic anhydride. *Polymer*, *44*: 4715–4721.
138. Chan, S.S., Chung, T.S.; Liu, Y. (2003) Gas and hydrocarbon (C-2 and C-3) transport properties of co-polyimides synthesized from 6FDA and 1,5-NDA (naphthalene)/Durene diamines. *J. Mem. Sci.*, *218*: 235–245.
139. Cao, C.; Chung, T.S.; Liu, Y. (2003) Chemical cross-linking modification of 6FDA-2,6-DAT hollow fiber membranes for natural gas separation. *J. Mem. Sci.*, *216*: 257–268.
140. Ayala, D.; Lozano, A.E.; de Abajo, J. (2003) Gas separation properties of aromatic polyimides. *J. Mem. Sci.*, *215*: 61–73.
141. Liu, Y.; Chng, M.L.; Chung, T.S. (2003a) Effects of amidation on gas permeation properties of polyimide membranes. *J. Mem. Sci.*, *214*: 83–92.
142. Liu, Y.; Chung, T.S.; Wang, R. (2003d) Chemical cross-linking modification of polyimide/poly(ether sulfone) dual-layer hollow-fiber membranes for gas separation. *Ind. Eng. Chem. Res.*, *42*: 1190–1195.
143. Lin, W.H.; Chung, T.S. (2000) The physical aging phenomenon of 6FDA-durene polyimide hollow fiber membranes. *J. Polym. Sci. B Polym. Phys.*, *38*: 765–775.
144. Lin, W.H.; Chung, T.S. (2001) Gas permeability, diffusivity, solubility, and aging characteristics of 6FDA-durene polyimide membranes. *J. Mem. Sci.*, *186*: 183–193.

145. Fuertes, A.B.; Nevskaia, D.M.; Centeno, T.A. (1999) Carbon composite membranes from Matrimid (R) and Kapton (R) polyimides for gas separation. *Micropor. Mesopor. Mater.*, *33*: 115–125.
146. Jois, Y.H.R.; Reale, J. Preparation of supported polyimide membranes for gas separations, USP 5928410, 1999.
147. Baker, R.W.; Wijmans, J.G.; He, Z.; Pinnau, I. Multiple-bed permselective membrane separation for rejection of nitrogen, carbon dioxide, water, and hydrogen sulfide from natural gas, USP 6565626, 2003.
148. Lee, S.J.; Kim, M.S.; Chung, J.G. (2004) Preparation of porous polycarbonate membranes using supercritical CO_2 with enhanced solubility. *J. Ind. Eng. Chem.*, *10*: 877–882.
149. Hacarlioglu, P.; Toppare, L.; Yilmaz, L. (2003) Effect of preparation parameters on performance of dense homogeneous polycarbonate gas separation membranes. *J. Appl. Polym. Sci.*, *90*: 776–785.
150. Pereira, B.; Admassu, W. (2001) Effects of chemical impurities on gas sorption in polymeric membranes. I. Polycarbonate and polysulfone. *Sep. Sci. Technol.*, *36*: 177–197.
151. Chen, S.H.; Huang, S.L.; Yu, K.C. (2000) Effect of CO_2 treated polycarbonate membranes on gas transport and sorption properties. *J. Mem. Sci.*, *172*: 105–112.
152. Dai, Y.; Guiver, M.D.; Robertson, G.P. (2005) Effect of hexafluoro-2-propanol substituents in polymers on gas permeability and fractional free volume. *Macromol.*, *38*: 9670–9678.
153. Bhole, Y.S.; Kharul, U.K.; Somani, S.P. (2005) Benzoylation of polyphenylene oxide: Characterization and gas permeability investigations. *Euro. Polym. J.*, *41*: 2461–2471.
154. Yoshimune, M.; Fujiwara, I.; Suda, H. (2005) Novel carbon molecular sieve membranes derived from poly(phenylene oxide) and its derivatives for gas separation. *Chem. Let.*, *34*: 958–959.
155. Li, J.T.; Wang, S.C.; Nagai, K. (1998) Effect of polyethyleneglycol (PEG) on gas permeabilities and permselectivities in its cellulose acetate (CA) blend membranes. *J. Mem. Sci.*, *138*: 143–152.
156. Li, J.T.; Nagai, K.; Nakagawa, T. (1995) Preparation of polyethyleneglycol (peg) and cellulose-acetate (ca) blend membranes and their gas permeabilities. *J. Appl. Polym. Sci.*, *58*: 1455–1463.
157. Hamad, F.; Khulbe, K.C.; Matsuura, T. (2005a) Comparison of gas separation performance and morphology of homogeneous and composite PPO membranes. *J. Mem. Sci.*, *256*: 29–37.
158. Hamad, F.; Matsuura, T. (2005b) Performance of gas separation membranes made from sulfonated brominated high molecular weight poly(2,4-dimethyl-1,6-phenyIene oxide). *J. Mem. Sci.*, *253*: 183–189.
159. Polotskaya, G.; Biryulin, Y., Pientka, Z. (2004) Transport properties of fullerene-polyphenylene oxide homogeneous membranes. *Full. Nanotube Carbon Nanos.*, *12*: 365–369.
160. Khulbe, K.C.; Hamad, F.; Feng, C. (2004) Characterization of the poly(phenylene oxide) dense membrane prepared at different temperatures. *Sep. Purif. Tech.*, *36*: 53–62.

161. Lie, J.A.; Hagg, M.B. (2005) Carbon membranes from cellulose and metal loaded cellulose. *Carbon*, *43*: 2600–2607.
162. Eckelt, J.; Wolf, B.A. (2005) Membranes directly prepared from solutions of unsubstituted cellulose. *Macromol. Chem. Phys.*, *206*: 227–232.
163. Jie, X.M.; Cao, Y.M.; Lin, B. (2004) Gas permeation performance of cellulose hollow fiber membranes made from the cellulose/N-methylmorpholine-N-oxide/H_2O system. *J. Appl. Polym. Sci.*, *91*: 1873–1880.
164. Nakabayashi, M.; Okabe, K.; Fujisawa, E.; Hirayama, Y.; Kazama, S.; Matsumiya, N.; Takagi, K.; Mano, H.; Haraya, K.; Kamizawa, C. (1995) Carbon-dioxide separation through water-swollen-gel membrane. *Energy Conversion and Management*, *36*: 419–422.
165. Riekerink, M.B.O.; Engbers, G.H.M.; Wessling, M. (2002) Tailoring the properties of asymmetric cellulose acetate membranes by gas plasma etching. *J. Col. Interf. Sci.*, *245*: 338–348.
166. Banerjee, S.; Maier, G.; Dannenberg, C. (2004) Gas permeabilities of novel poly(arylene ether)s with terphenyl unit in the main chain. *J. Mem. Sci.*, *229*: 63–71.
167. Hao, J.; Rice, P.A.; Stem, S.A. (2002) Upgrading low-quality natural gas with H_2S- and CO_2-selective polymer membranes Part I. Process design and economics of membrane stages without recycle streams. *J. Mem. Sci.*, *209*: 177–206.
168. Queiroz, D.P.; Pinho, M.N. (2002) Gas permeability of polypropylene oxide/polybutadiene bi-soft segment urethane/urea membranes. *Desal.*, *145*: 379–383.
169. Xu, Z.K.; Dannenberg, C.; Springer, J. (2002) Novel poly(arylene ether) as membranes for gas separation. *J. Mem. Sci.*, *205*: 23–31.
170. Park, H.B.; Kim, J.H.; Kim, J.K. (2002b) Morphology of a poly(imide siloxane) segmented copolymer/silica hybrid composite. *Macrom. Rapid Comm.*, *23*: 544–550.
171. Wang, Z.Y.; Moulinie, P.R.; Handa, Y.P. (1998) Gas transport properties of novel poly(arylene ether ketone)s containing dibenzoylbiphenyl and benzonaphthone moieties. *J. Polym. Sci. B Polym. Phys.*, *36*: 425–431.
172. Chatterjee, G.; Houde, A.A.; Stern, S.A. (1997) Poly(ether urethane) and poly(ether urethane urea) membranes with high H2S/CH4 selectivity. *J. Mem. Sci.*, *135*: 99–106.
173. Simmons, J.W. Block polyester-ether gas separation membranes, USP 6,860,920, 2005.
174. Lin, H.; Freeman, B.D. (2004) Gas solubility, diffusivity and permeability in poly(ethylene oxide). *J. Mem. Sci.*, *239*: 105–117.
175. Koros, W.J.; Mahajan, R. (2000) Pushing the limits on possibilities for large scale gas separation: Which strategies? *J. Mem. Sci.*, *175*: 181–196.
176. Koros, W.J.; Mahajan, R. (2001) Pushing the limits on possibilities for large scale gas separation: which strategies?. *J. Mem. Sci.*, *181*: 141–141.
177. Burns, R.L.; Koros, W.J. (2003) Structure-property relationships for poly(pyrrolone-imide) gas separation membranes. *Macromol.*, *36*: 2374–2381.
178. Budd, P.M.; McKeown, N.B.; Fritsch, D. (2005a) Free volume and intrinsic microporosity in polymers. *J. Mater. Chem*, *15*: 1977–1986.

179. Budd, P.M.; Msayib, K.J.; Tattershall, C.E. (2005b) Gas separation membranes from polymers of intrinsic microporosity. *J. Mem Sci.*, *251*: 263–269.
180. McKeown, N.B.; Budd, P.M.; Msayib, K.J. (2005) Polymers if intrinsic microporosity (PIMs). *Chem.- A Eur. J.*, *11*: 2610–2620.
181. Zimmerman, C.M.; Koros, W.J. (1999a) Comparison of gas transport and sorption in the ladder polymer BBL and some semi-ladder polymers. *Polymer*, *40*: 5655–5664.
182. Zimmerman, C.M.; Koros, W.J. (1999b) Entropic selectivity analysis of a series of polypyrrolones for gas separation membranes. *Macromol.*, *32*: 3341–3346.
183. Zimmerman, C.M.; Koros, W.J. (1999c) Polypyrrolones for membrane gas separations. I. Structural comparison of gas transport and sorption properties. *J. Polym. Sci. B Polym. Phys.*, *37*: 1235–1249.
184. Zimmerman, C.M.; Koros, W.J. (1999d) Polypyrrolones for membrane gas separations. II. Activation energies and heats of sorption. *J. Polym. Sci. B Polym. Phys.*, *37*: 1251–1265.
185. Chung, T.S.; Ren, J.H.; Wang, R. (2003) Development of asymmetric 6FDA-2,6DAT hollow fiber membranes for $CO_{(2)}/CH_4$ separation Part 2. Suppression of plasticization. *J. Mem. Sci.*, *214*: 57–69.
186. Bos, A.; Punt, I.G.M.; Wessling, M. (1998b) Suppression of CO_2-plasticization by semiinterpenetrating polymer network formation. *J. Polym. Sci. B-Polym. Phys.*, *36*: 1547–1556.
187. Bos, A.; Punt, I.G.M.; Wessling, M. (1998a) Plasticization-resistant glassy polyimide membranes for CO_2/CH_4 separations. *Sep. Purif. Technol*, *14*: 27–39.
188. Bos, A.; Punt, I.G.M.; Wessling, M. (1999) CO_2-induced plasticization phenomena in glassy polymers. *J. Mem. Sci.*, *155*: 67–78.
189. Bos, A.; Punt, I.; Strathmann, H. (2001) Suppression of gas separation membrane plasticization by homogeneous polymer blending. *AIChE J.*, *47*: 1088–1093.
190. Shao, L.; Chung, T.S.; Goh, S.H. (2005dc) Polyimide modification by a linear aliphatic diamine to enhance transport performance and plasticization resistance. *J. Mem. Sci.*, *256*: 46–56.
191. Wind, J.D.; Paul, D.R.; Koros, W.J. (2004) Natural gas permeation in polyimide membranes. *J. Mem Sci.*, *228*: 227–236.
192. Wind, J.D.; Sirard, S.M.; Paul, D.R. (2003a) Carbon dioxide-induced plasticization of polyimide membranes: Pseudo-equilibrium relationships of diffusion, sorption, and swelling. *Macromol.*, *36*: 6433–6441.
193. Wind, J.D.; Sirard, S.M.; Paul, D.R. (2003b) Relaxation dynamics of CO_2 diffusion, sorption, and polymer swelling for plasticized polyimide membranes. *Macromol.*, *36*: 6442–6448.
194. Wind, J.D.; Staudt-Bickel, C.; Paul, D.R. (2003c) Solid-state covalent crosslinking of polyimide membranes for carbon dioxide plasticization reduction. *Macromol.*, *36*: 1882–1888.
195. Wind, J.D.; Staudt-Bickel, C.; Paul, D.R. (2002) The effects of crosslinking chemistry on CO2 plasticization of polyimide gas separation membranes. *Ind. Eng. Chem. Res.*, *41*: 6139–6148.

196. Taubert, A.; Wind, J.D.; Paul, D.R. (2003) Novel polyimide ionomers: CO_2 plasticization, morphology, and ion distribution. *Polym.*, *44*: 1881–1892.
197. Krol, J.J.; Boerrigter, M.; Koops, G.H. (2001) Polyimide hollow fiber gas separation membranes: preparation and the suppression of plasticization in propane/propylene environments. *J. Mem. Sci.*, *184*: 275–286.
198. Staudt-Bickel, C.; Koros, W.J. (1999) Improvement of CO_2/CH_4 separation characteristics of polyimides by chemical crosslinking. *J. Mem. Sci.*, *155*: 145–154.
199. Kawakami, H.; Mikawa, M.; Nagaoka, S. (1996) Gas transport properties in thermally cured aromatic polyimide membranes. *J. Mem. Sci.*, *118*: 223–230.
200. Liu, Y.; Wang, R.; Chung, T.S. (2001) Chemical cross-linking modification of polyimide membranes for gas separation. *J. Mem. Sci.*, *189*: 231–239.
201. Hu, C.C.; Tu, C.Y.; Wang, Y.C. (2004) Effects of plasma treatment on CO_2 plasticization of poly(methyl methacrylate) gas-separation membranes. *J. Appl. Polym. Sci.*, *93*: 395–401.
202. Suzuki, T.; Yamada, Y. (2006) Characterization of 6FDA-based hyperbranched and linear polyimide-silica hybrid membranes by gas permeation and Xe-129 NMR measurements. *J. Polym. Sci. B Polym. Phys.*, *44*: 291–298.
203. Suzuki, T.; Yamada, Y. (2005) Physical and gas transport properties of novel hyperbranched polyimide-silica hybrid membranes. *Polym. Bull.*, *53*: 139–146.
204. Kim, J.H.; Lee, Y.M. (2001) Gas permeation properties of poly(amide-6-b-ethylene oxide)-silica hybrid membranes. *J. Mem. Sci.*, *193*: 209–225.
205. Tamaki, R.; Chujo, Y.; Kuraoka, K. (1999) Application of organic-inorganic polymer hybrids as selective gas permeation membranes. *J. Mater. Chem.*, *9*: 1741–1746.
206. Park, H.B.; Kim, J.K.; Nam, S.Y. (2003) Imide-siloxane block copolymer/silica hybrid membranes: preparation, characterization and gas separation properties. *J. Mem. Sci.*, *220*: 59–73.
207. Budd, P.M.; Ghanem, B.S.; Makhseed, S. (2004) Polymers of intrinsic microporosity (PIMs) robust, solution-processable, organic nanoporous materials. *Chem. Comm.*, *2*: 230–231.
208. Shida, Y.; Sakaguchi, T.; Shiotsuki, M. (2006) Synthesis and properties of membranes of poly(diphenylacetylenes) having fluorines and hydroxyl groups. *Macromol.*, *39*: 569–574.
209. Shida, Y.; Sakaguchi, T.; Shiotsuki, M. (2005) Synthesis and properties of poly(diphenylacetylenes) having hydroxyl groups. *Macromol.*, *38*: 4096–4102.
210. Sakaguchi, T.; Yumoto, K.; Shiotsuki, M. (2005) Synthesis of poly(diphenylacetylene) membranes by desilylation of various precursor polymers and their properties. *Macromol.*, *38*: 2704–2709.
211. Sakaguchi, T.; Kwak, G.; Masuda, T. (2002) Synthesis of poly(1-beta-naphthyl-2-phenylacetylene) membranes through desilylation and their properties. *Polym.*, *43*: 3937–3942.
212. Raharjo, R.D.; Lee, H.J.; Freeman, B.D. (2005) Pure gas and vapor permeation properties of poly[1-phenyl-2-[p-(trimethylsilyl)phenyl]acetylene]

(PTMSDPA) and its desilylated analog, poly[diphenylacetylene]. (*PDPA*), *Polym.*, *46*: 6316–6324.
213. Hill, A.J.; Pas, S.J.; Bastow, T.J. (2004) Influence of methanol conditioning and physical aging on carbon spin-lattice relaxation times of poly(1-trimethylsilyl-1-propyne). *J. Mem. Sci.*, *243*: 37–44.
214. Pinnau, I.; Toy, L.G. (1996) Transport of organic vapors through poly(1-trimethylsilyl-1-propyne). *J. Mem. Sci.*, *116*: 199–209.
215. Pinnau, I.; He, Z.J.; Morisato, A. (2004) Synthesis and gas permeation properties of poly(dialkylacetylenes) containing isopropyl-terminated side-chains. *J. Mem. Sci.*, *241*: 363–369.
216. Pinnau, I.; Morisato, A.; He, Z.J. (2004) Influence of side-chain length on the gas permeation properties of poly(2-alkylacetylenes). *Macromol.*, *37*: 2823–2828.
217. Merkel, T.C.; Bondar, V.; Nagai, K. (1999) Hydrocarbon and perfluorocarbon gas sorption in poly(dimethylsiloxane), poly(1-trimethylsilyl-1-propyne), and copolymers of tetrafluoroethylene and 2,2-bis(trifluoromethyl)-4,5-difluoro-1,3-dioxole. *Macromol.*, *32*: 370–374.
218. Merkel, T.C.; Bondar, V.; Nagai, K. (2000) Sorption and transport of hydrocarbon and perfluorocarbon gases in poly(1-trimethylsilyl-1-propyne). *J. Polym. Sci. B Polym. Phys.*, *38*: 273–296.
219. Merkel, T.C.; Gupta, R.P.; Turk, B.S. (2001) Mixed-gas permeation of syngas components in poly(dimethylsiloxane) and poly(1-trimethylsilyl-1-propyne) at elevated temperatures. *J. Mem. Sci.*, *191*: 85–94.
220. Merkel, T.C.; He, Z.J.; Pinnau, I. (2003) Sorption and transport in poly(2,2-bis(trifluoromethyl)-4,5-difluoro-1,3-dioxole-co-tetrafluoroethylene) containing nanoscale fumed silica. *Macromol.*, *36*: 8406–8414.
221. Nagai, K.; Freeman, B.D.; Hill, A.J. (2000) Effect of physical aging of poly(1-trimethylsilyl-1-propyne) films synthesized with $TaCl_5$ and $NbCl_5$ on gas permeability, fractional free volume, and positron annihilation lifetime spectroscopy parameters. *J. Polym. Sci. B Polym. Phys.*, *38*: 1222–1239.
222. Nagai, K.; Masuda, T.; Nakagawa, T. (2001) Poly[1-(trimethylsilyl)-1-propyne] and related polymers: synthesis, properties and functions. Prog. *Polym. Sci.*, *26*: 721–798.
223. Yampolskii, Y.P.; Korikov, A.P.; Shantarovich, V.P. (2001) Gas permeability and free volume of highly branched substituted acetylene polymers. *Macromol.*, *34*: 1788–1796.
224. Yampolskii, Y.P.; Motyakin, M.V.; Wasserman, A.M. (1999) Study of high permeability polymers by means of the spin probe technique. *Polymer*, *40*: 1745–1752.
225. Kwak, G.; Aoki, T.; Toy, L.G. (2000) Synthesis, characterization, and oxygen permeability of homo- and copolymers from p-[tris(trimethylsilyl)silyl]-phenylacetylene. *Polym. Bull.*, *45*: 215–221.
226. Higuchi, A.; Yoshida, T.; Imizu, T. (2000) Gas permeation of fullerene-dispersed poly(1-trimethylsilyl-1-propyne) membranes. *J. Polym. Sci. B Polym. Phys.*, *38*: 1749–1755.
227. Morisato, A.; Pinnau, I. (1996) Synthesis and gas permeation properties of poly(4-methyl-2-pentyne). *J. Mem. Sci.*, *121*: 243–250.

228. Morisato, A.; Shen, H.C.; Sankar, S.S. (1996) Polymer characterization and gas permeability of poly(1-trimethylsilyl-1-propyne) [PTMSP], poly(1-phenyl-1-propyne) [PPP], and PTMSP/PPP blends. *J. Polym. Sci. B Polym. Phys.*, *34*: 2209–2222.
229. Gomes, D.; Nunes, S.P.; Peinemann, K.V. (2005) Membranes for gas separation based on poly(1-trimethylsilyl-1-propyne)-silica nanocomposites. *J. Mem. Sci.*, *246*: 13–25.
230. He, Z.J.; Pinnau, I.; Morisato, A. (2002) Nanostructured poly(4-methyl-2-pentyne)/silica hybrid membranes for gas separation. *Desalination*, *146*: 11–15.
231. Camera-Roda, G. (1988) Performances of filled and unfilled PTMSP membranes in pervaporation. *Chem Eng. Comm.*, *163*: 3–22.
232. Lin, H.Q.; Van Wagner, E.; Raharjo, R. (2006a) High-performance polymer membranes for natural-gas sweetening. *Adv. Mater.*, *18*: 39–44.
233. Lin, H.; Van Wagner, E.; Freeman, B.D.; Toy, L.G.; Gupta, R.P. (2006) Plasticization-enhanced hydrogen purification using polymeric membranes. *Science*, *311*: 639–642.
234. Lin, H.Q.; Freeman, B.D. (2005) Gas and vapor solubility in cross-linked poly(ethylene glycol diacrylate). *Macromol.*, *38*: 8394–8407.
235. Lin, H.Q.; Freeman, B.D. (2005) Materials selection guidelines for membranes that remove CO_2 from gas mixtures. *J. Mol. Struct.*, *739*: 57–74.
236. Kalakkunnath, S.; Kalika, D.S.; Lin, H.Q. (2005) Segmental relaxation characteristics of cross-linked poly(ethylene oxide) copolymer networks. *Macromol.*, *38*: 9679–9687.
237. Orme, C.J.; Stewart, F.F. (2005) Mixed gas hydrogen sulfide permeability and separation using supported polyphosphazene membranes. *J. Mem. Sci.*, *253*: 243–249.
238. Orme, C.J.; Klaehn, J.R.; Stewart, F.F. (2004) Gas permeability and ideal selectivity of poly [bis-(phenoxy)phosphazene], poly [bis-(4-tert-butylphenoxy)phosphazene], and poly [bis-(3,5-di-tert-butylphenoxy)(1.2)(chloro)(0.8)phosphazene]. *J. Mem Sci.*, *238*: 47–55.
239. Patel, N.P.; Spontak, R.J. (2004) Gas-transport and thermal properties of a microphase-ordered poly(styrene-b-ethylene oxide-b-styrene) triblock copolymer and its blends with poly(ethylene glycol). *Macromol.*, *37*: 2829–2838.
240. Patel, N.P.; Aberg, C.M.; Sanchez, A.M. (2004) Morphological, mechanical and gas-transport characteristics of crosslinked poly(propylene glycol) homopolymers, nanocomposites and blends. *Polymer*, *45*: 5941–5950.
241. Patel, N.P.; Zielinski, J.M.; Samseth, J. (2004) Effects of pressure and nanoparticle functionality on CO_2-selective nanocomposites derived from crosslinked poly(ethylene glycol). *Macromol. Chem. Phys.*, *205*: 2409–2419.
242. Patel, N.P.; Hunt, M.A.; Lin-Gibson, S. (2005) Tunable CO_2 transport through mixed polyether membranes. *J. Mem. Sci.*, *251*: 51–57.
243. Patel, N.P.; Miller, A.C.; Spontak, R.J. (2004c) Highly CO_2-permeable and -selective membranes derived from crossfinked poly(ethylene glycol) and its nanocomposites. *Adv. Func. Mater.*, *14*: 699–707.
244. Patel, N.P.; Miller, A.C.; Spontak, R.J. (2003) Highly CO_2-permeable and selective polymer nanocomposite membranes. *Adv. Mater.*, *15*: 729–733.

245. Metz, S.J.; van de Ven, W.J.C.; Potreck, J. (2005) Transport of water vapor and inert gas mixtures through highly selective and highly permeable polymer membranes. *J. Mem. Sci.*, *251*: 29–41.
246. Metz, S.J.; Mulder, M.H.V.; Wessling, M. (2004) Gas-permeation properties of poly(ethylene oxide) poly(butylene terephthalate) block copolymers. *Macromol.*, *37*: 4590–4597.
247. Metz, S.J.; Potreck, J.; Mulder, M. (2002) Water vapor and gas transport through a poly(butylene terephthalate) poly(ethylene oxide) block copolymer. *Desal.*, *148*: 303–307.
248. Liu, L.; Chakma, A.; Feng, X. (2004) Preparation of hollow fiber poly(ether block amide)/polysulfone composite membranes for separation of carbon dioxide from nitrogen. *Chem. Eng. J.*, *105*: 43–51.
249. Balachandra, A.M.; Baker, G.L.; Bruening, M.L. (2003) Preparation of composite membranes by atom transfer radical polymerization initiated from a porous support. *J. Mem. Sci.*, *227*: 1–14.
250. Orme, C.J.; Stone, M.L.; Benson, M.T. (2003) Testing of polymer membranes for the selective permeability of hydrogen. *Sep. Sci. Technol.*, *38*: 3225–3238.
251. Kim, Y.K.; Lee, J.M.; Park, H.B. (2004) The gas separation properties of carbon molecular sieve membranes derived from polyimides having carboxylic acid groups. *J. Mem. Sci.*, *235*: 139–146.
252. Kim, J.H.; Ha, S.Y.; Nam, S.Y. et al. (2001) Selective permeation of CO_2 through pore-filled polyacrylonitrile membrane with poly(ethylene glycol). *J. Mem. Sci.*, *186*: 97–107.
253. Bondar, V.I.; Freeman, B.D.; Pinnau, I. (2000) Gas transport properties of poly(ether-b-amide) segmented block copolymers. *J. Polym. Sci. B Polym. Phys.*, *38*: 2051–2062.
254. Hirayama, Y.; Kase, Y.; Tanihara, R. et al. (1999) Permeation properties to CO_2 and N_2 of poly(ethylene oxide)-containing and crosslinked polymer films. *J. Mem. Sci.*, *160*: 87–99.
255. Kita, H.; Tabuchi, M.; Sakai, T. (2003) Polyether separation membrane US Patent App. 2003110947, 2003.
256. Laverty, B.W.; Chowdhury, G.; Vujosevic, R.; Deng, S.; Yao, B.; Matsuura, T. (1999) Manufacture of permeable gas separation materials having good mechanical strength and permselectivity. PCT Int. App. WO 9942204, 1999.
257. Senthilkumar, U.; Rajini, R.; Reddy, B.S.R. (2005) Gas permeation and sorption properties of non-ionic and cationic amino-hydroxy functionalized poly(dimethylsiloxane) membranes. *J. Mem. Sci.*, *254*: 169–177.
258. Senthilkumar, U.; Reddy, B.S.R. (2004) Structure-gas separation property relationships of non-ionic and cationic amino-hydroxy functionalized poly (dimethylsiloxane) membranes. *J. Mem. Sci.*, *232*: 73–83.
259. Queiroz, D.P.; de Pinho, M.N. (2005) Structural characteristics and gas permeation properties of polydimethylsiloxane/poly(propylene oxide) urethane/urea bi-soft segment membranes. *Polymer*, *46*: 2346–2353.

260. Prabhakar, R.S.; Merkel, T.C.; Freeman, B.D. (2005) Sorption and transport properties of propane and perfluoropropane in poly(dimethylsiloxane) and poly(1-trimethylsilyl-1-propyne). *Macromol.*, *38*: 1899–1910.
261. Pinnau, I.; He, Z.J. (2004) Pure- and mixed-gas permeation properties of polydimethylsiloxane for hydrocarbon/methane and hydrocarbon/hydrogen drogen separation. *J. Mem. Sci.*, *244*: 227–233.
262. Abdellah, L.; Boutevin, B.; Guida-Pietrasanta, F. (2003) Evaluation of photocrosslinkable fluorinated polydimethylsiloxanes as gas permeation membranes. *J. Mem. Sci.*, *217*: 295–298.
263. Kuraoka, K.; Chujo, Y.; Yazawa, T. (2001) Hydrocarbon separation via porous glass membranes surface-modified using organosilane compounds. *J. Mem. Sci.*, *182*: 139–149.
264. Matsuyama, H.; Teramoto, M.; Hirai, K. (1995) Effect of plasma treatment on CO_2 permeability and selectivity of poly(dimethylsiloxane) membrane. *J. Mem. Sci.*, *99*: 139–147.
265. Orme, C.J.; Harrup, M.K.; Luther, T.A. (2001) Characterization of gas transport in selected rubbery amorphous polyphosphazene membranes. *J. Mem Sci*, *186*: 249–256.
266. Nagai, K.; Freeman, B.D.; Cannon, A. (2000) Gas permeability of poly(bis-trifluoroethoxyphosphazene) and blends with adamantane amino/trifluoroethoxy (50/50) polyphosphazene. *J. Mem Sci.*, *172*: 167–176.
267. Barbi, V.; Funari, S.S.; Gehrke, R. (2003) SAXS and the gas transport in polyether-block-polyamide copolymer membranes. *Macromol.*, *36*: 749–758.
268. Yoshino, M.; Ito, K.; Kita, H. (2000) Effects of hard-segment polymers on CO_2/N_2 gas-separation properties of poly(ethylene oxide)-segmented copolymers. *J. Polym. Sci. B-Polym. Phys.*, *38*: 1707–1715.
269. Okamoto, K.; Fujii, M.; Okamyo, S. (1995) Gas permeation properties of poly(ether imide) segmented copolymers. *Macromol.*, *28*: 6950–6956.
270. Okamoto, K.; Umeo, N.; Okamyo, S. (1993) Selective permeation of carbon-dioxide over nitrogen through polyethyleneoxide-containing polyimide membranes. *Chem. Let.*, *2*: 225–228.
271. Kovvali, A.S.; Sirkar, K.K. (2003) Stable liquid membranes – Recent developments and future directions. *Ann. N. Y. Acad. Sci.*, *984*: 279–288.
272. Chen, H.; Kovvali, A.S.; Majumdar, S. (1999) Selective CO_2 separation from CO_2–N_2 mixtures by immobilized carbonate-glycerol membranes. *Ind. Eng. Chem. Res.*, *38*: 3489–3498.
273. Chen, H.; Kovvali, A.S.; Sirkar, K.K. (2000) Selective CO_2 separation from CO_2-N-2 mixtures by immobilized glycine-Na-glycerol membranes. *Ind. Eng. Chem. Res.*, *39*: 2447–2458.
274. Chen, H.; Obuskovic, G.; Majumdar, S. (2001) Immobilized glycerol-based liquid membranes in hollow fibers for selective CO_2 separation from CO_2-N_2 mixtures. *J. Mem Sci.*, *183*: 75–88.
275. Kovvali, A.S.; Sirkar, K.K. (2002) Carbon dioxide separation with novel solvents as liquid membranes. *Ind. Eng. Chem. Res.*, *41*: 2287–2295.

276. Kovvali, A.S.; Sirkar, K.K. (2001) Dendrimer liquid membranes: CO_2 separation from gas mixtures. *Industrial & Engineering Chemistry Research*, *40*: 2502–2511.
277. Quinn, R.; Appleby, J.B.; Pez, G.P. (2002) Hydrogen sulfide separation from gas streams using salt hydrate chemical absorbents and immobilized liquid membranes. *Sep. Sci. Technol.*, *37*: 627–638.
278. Quinn, R.; Laciak, D.V.; Pez, G.P. (1997) Polyelectrolyte-salt blend membranes for acid gas separations. *J. Mem Sci.*, *131*: 61–69.
279. Quinn, R.; Appleby, J.B.; Pez, G.P. (1995) New facilitated transport membranes for the separation of carbon-dioxide from hydrogen and methane. *J. Mem Sci.*, *104*: 139–146.
280. Quinn, R.; Laciak, D.V.; Appleby, J.B.; Pez, G.P. Polyelectrolyte membranes for the separation of acid gases. US Patent 5,336,298, 1993.
281. Quinn, R.; Laciak, D.V. (1997) Polyelectrolyte membranes for acid gas separations. *J. Mem Sci.*, *131*: 49–60.
282. Quinn, R. (1998) A repair technique for acid gas selective polyelectrolyte membranes. *J. Mem Sci.*, *139*: 97–102.
283. Matsuyama, H.; Teramoto, M.; Matsui, K. (2001) Preparation of poly(acrylic acid)/poly(vinyl alcohol) membrane for the facilitated transport of CO_2. *J. Appl. Pol. Sci.*, *81*: 936–942.
284. Way, J.D.; Noble, R.D.; Reed, D.L. (1987) Facilitated transport of CO_2 in ion-exchange membranes. *AIChE J.*, *33*: 480–487.
285. Noble, R.D.; Pellegrino, J.J.; Grosgogeat, E. (1988) CO_2 separation using facilitated transport ion-exchange membranes. *Sep. Sci. Technol.*, *23*: 1595–1609.
286. Eriksen, O.I.; Aksnes, E.; Dahl, I.M. (1993) Facilitated transport of ethene through nafion membranes 1. Water swollen membranes. *J. Mem Sci.*, *85*: 89–97.
287. Eriksen, O.I.; Aksnes, E.; Dahl, I.M. (1993) Facilitated transport of ethene through nafion membranes 2. glycerin treated, water swollen membranes. *J. Mem Sci.*, *85*: 99–106.
288. LeBlanc, O.H.; Ward, W.J.; Matson, S.L.; Kimura, S.G. (1980) Facilitated transport in ion-exchange membranes. *J. Mem Sci.*, *6*: 339–343.
289. Kim, M.J.; Park, Y.I.; Youm, K.H. (2004) Gas permeation through water-swollen polysaccharide/poly(vinvl alcohol) membranes. *J. Appl. Pol. Sci.*, *91*: 3225–3232.
290. Park, Y.I.; Lee, K.H. (2001) Preparation of water-swollen hydrogel membranes for gas separation. *J. Appl. Pol. Sci.*, *80*: 1785–1791.
291. Park, Y.I.; Lee, K.H. (1999) Preparation of water-swollen hydrogel membranes for the separation of carbon dioxide. *J. Ind. Eng. Chem.*, *5*: 235–239.
292. Kim, M.J.; Park, Y.I.; Youm, K.H. (2004) Facilitated transport of CO_2 through ethylenediamine-fixed cation-exchange polysaccharide membranes. *J. Mem Sci.*, *245*: 79–86.
293. Zhang, Y.; Wang, Z.; Wang, S.C. (2002) Novel fixed-carrier membranes for CO_2 separation. *J. Appl. Pol. Sci.*, *86*: 2222–2226.
294. Zhang, Y.; Wang, Z.; Wang, S.C. (2002) Selective permeation of CO_2 through new facilitated transport membranes. *Desalination*, *145*: 385–388.

295. Teramoto, M.; Kitada, S.; Ohnishi, N. (2004) Separation and concentration of CO_2 by capillary-type facilitated transport membrane module with permeation of carrier solution. *J. Mem Sci.*, *234*: 83–94.
296. Teramoto, M.; Ohnishi, N.; Takeuchi, N. (2003) Separation and enrichment of carbon dioxide by capillary membrane module with permeation of carrier solution. *Sep. Purif. Technol.*, *30*: 215–227.
297. Teramoto, M.; Takeuchi, N.; Maki, T. (2002) Facilitated transport of CO_2 through liquid membrane accompanied by permeation of carrier solution. *Sep. Purif. Technol.*, *27*: 25–31.
298. Lagorsse, S.; Campo, M.C.; Magalhaes, F.D. (2005) Water adsorption on carbon molecular sieve membranes: Experimental data and isotherm model. *Carbon*, *43*: 2769–2779.
299. Lagorsse, S.; Leite, A.; Magalhaes, F.D. (2005) Novel carbon molecular sieve honeycomb membrane module: configuration and membrane characterization. *Carbon*, *43*: 809–819.
300. Lagorsse, S.; Magalhaes, F.D.; Mendes, A. (2004) Carbon molecular sieve membranes - Sorption, kinetic and structural characterization. *J. Mem. Sci.*, *241*: 275–287.
301. Kim, Y.K.; Park, H.B.; Lee, Y.M. (2005) Preparation and characterization of carbon molecular sieve membranes derived from BTDA-ODA polyimide and their gas separation properties. *J. Mem. Sci.*, *255*: 265–273.
302. Kim, Y.K.; Park, H.B.; Lee, Y.M. (2005) Gas separation properties of carbon molecular sieve membranes derived from polyimide/polyvinylpyrrolidone blends: effect of the molecular weight of polyvinylpyrrolidone. *J. Mem. Sci.*, *251*: 159–167.
303. Kim, Y.K.; Park, H.B.; Lee, Y.M. (2004) Carbon molecular sieve membranes derived from thermally labile polymer containing blend polymers and their gas separation properties. *J. Mem. Sci.*, *243*: 9–17.
304. Park, H.B.; Lee, S.Y.; Lee, Y.M. (2005) Pyrolytic carbon membranes containing silica: morphological approach on gas transport behavior. *J. Mol. Struct.*, *739*: 179–190.
305. Park, H.B.; Jung, C.H.; Kim, Y.K. (2004) Pyrolytic carbon membranes containing silica derived from poly(imide siloxane) the effect of siloxane chain length on gas transport behavior and a study on the separation of mixed gases. *J. Mem. Sci.*, *235*: 87–98.
306. Park, H.B.; Kim, Y.K.; Lee, J.M. (2004) Relationship between chemical structure of aromatic polyimides and gas permeation properties of their carbon molecular sieve membranes. *J. Mem. Sci.*, *229*: 117–127.
307. Barsema, J.N.; van der Vegt, N.F.A.; Koops, G.H. (2005) Ag-functionalized carbon molecular-sieve membranes based on polyelectrolyte/polyimide blend precursors. *Adv. Funct. Mater.*, *15*: 69–75.
308. Barsema, J.N.; Balster, J.; Jordan, V. (2003) Functionalized carbon molecular sieve membranes containing Ag-nanoclusters. *J. Mem. Sci.*, *219*: 47–57.
309. Barsema, J.N.; van der Vegt, N.F.A.; Koops. G.H. (2002) Carbon molecular sieve membranes prepared from porous fiber precursor. *J. Mem. Sci.*, *205*: 239–246.

310. Tin, P.S.; Chung, T.S.; Hill, A.J. (2004) Advanced fabrication of carbon molecular sieve membranes by nonsolvent pretreatment of precursor polymers. *Ind. Eng. Chem. Res.*, *43*: 6476–6483.
311. Tin, P.S.; Chung, T.S. (2004) Novel approach to fabricate carbon molecular-sieve membranes based on consideration of interpenetrating networks. *Macrom. Rapid Comm.*, *25*: 1247–1250.
312. Vu, D.Q.; Koros, W.J.; Miller, S.J. (2003) Effect of condensable impurities in CO_2/CH_4 gas feeds on carbon molecular sieve hollow-fiber membranes. *Ind. Eng. Chem. Res.*, *42*: 1064–1075.
313. Fuertes, A.B.; Centeno, T.A. (1998) Carbon molecular sieve membranes from polyetherimide. *Micropor. Mesopor. Mater.*, *26*: 23–26.
314. Centeno, T.A.; Fuertes, A.B. (1999) Supported carbon molecular sieve membranes based on a phenolic resin. *J. Mem. Sci.*, *160*: 201–211.
315. Shin, D.W.; Hyun, S.H.; Cho, C.H. (2005) Synthesis and CO_2/N_2 gas permeation characteristics of ZSM-5 zeolite membranes. *Micropor. Mesopor. Mater.*, *85*: 313–323.
316. Li, S.G.; Martinek, J.G.; Falconer, J.L. (2005) High-pressure CO_2/CH_4 separation using SAPO-34 membranes. *Ind. Eng. Chem. Res.*, *44*: 3220–3228.
317. Li, S.G.; Alvarado, G.; Noble, R.D. (2005) Effects of impurities on CO_2/CH_4 separations through SAPO-34 membranes. *J. Mem. Sci.*, *25*: 159–66.
318. Li, S.G.; Falconer, J.L.; Noble, R.D. (2004) SAPO-34 membranes for CO_2/CH_4 separation. *J. Mem. Sci.*, *241*: 121–135.
319. Xomeritakis, G.; Tsai, C.Y.; Brinker, C.J. (2005) Microporous sol-gel derived aminosilicate membrane for enhanced carbon dioxide separation. *Sep. Purif. Technol.*, *42*: 249–257.
320. Moon, J.H.; Park, Y.J.; Kim, M.B. (2005) Permeation and separation of a carbon dioxide/nitrogen mixture in a methyltriethoxysillane templating silica/alpha-alumina composite membrane. *J. Mem. Sci.*, *250*: 195–205.
321. Gu, X.H.; Dong, J.H.; Nenoff, T.M. (2005) Synthesis of defect-free FAU-type zeolite membranes and separation for dry and moist CO_2/N_2 mixtures. *Ind. Eng. Chem. Res.*, *44*: 937–944.
322. Zhang, L.X.; Gilbert, K.E.; Baldwin, R.M. (2005) Preparation and testing of carbon/silicalite-1 composite membranes. *Chem. Eng. Comm.*, *191*: 665–681.
323. Bernal, M.P.; Coronas, J.; Menendez, M. (2004) Separation of CO_2/N_2 mixtures using MFI-type zeolite membranes. *AIChE J.*, *50*: 127–135.
324. Bernal, M.P.; Coronas, J.; Menendez, M. (2003) On the effect of morphological features on the properties of MFI zeolite membranes. *Micropor. Mesopor. Mater.*, *60*: 99–110.
325. Poshusta, J.C.; Noble, R.D.; Falconer, J.L. (2001) Characterization of SAPO-34 membranes by water adsorption. *J. Mem. Sci.*, *186*: 25–40.
326. Poshusta, J.C.; Tuan, V.A.; Pape, E.A. (2000) Separation of light gas mixtures using SAPO-34 membranes. *AIChE J.*, *46*: 779–789.
327. Poshusta, J.C.; Tuan, V.A.; Falconer, J.L. (1998) Synthesis and permeation properties of SAPO-34 tubular membranes. *Ind. Eng. Chem. Res.*, *37*: 3924–3929.

328. Kusakabe, K.; Kuroda, T.; Uchino, K. (1999) Gas permeation properties of ion-exchanged faujasite-type zeolite membranes. *AIChE J.*, *45*: 1220–1226.
329. Kusakabe, K.; Sakamoto, S.; Saie, T. (1999) Pore structure of silica membranes formed by a sol-gel technique using tetraethoxysilane and alkyltriethoxysilanes. *Sep. Purif. Technol.*, *16*: 139–146.
330. Kusakabe, K.; Kuroda, T.; Morooka, S. (1998) Separation of carbon dioxide from nitrogen using ion-exchanged faujasite-type zeolite membranes formed on porous support tubes. *J. Mem. Sci.*, *148*: 13–23.
331. van den Broeke, L.J.P.; Bakker, W.J.W.; Kapteijn, F. (1999) Binary permeation through a silicalite-1 membrane. *AIChE J.*, *45*: 976–985.
332. van den Broeke, L.J.P.; Bakker, W.J.W.; Kapteijn, F. (1999) Transport and separation properties of a silicalite-1 membrane-I. Operating conditions. *Chem. Eng. Sci.*, *54*: 245–258.
333. van den Broeke, L.J.P.; Kapteijn, F.; Moulijn, J.A. (1999) Transport and separation properties of a silicalite-1 membrane-II. Variable separation factor. *Chem. Eng. Sci.*, *54*: 259–269.
334. Masuda, T.; Fujikata, Y.; Nishida, T. (1998) The influence of acid sites on intracrystalline diffusivities within MFI-type zeolites. *Micropor. Mesopor. Mater.*, *23*: 157–167.
335. Lovallo, M.C.; Gouzinis, A.; Tsapatsis, M. (1998) Synthesis and characterization of oriented MFI membranes prepared by secondary growth. *AIChE J.*, *44*: 1903–1913.
336. Lovallo, M.C.; Tsapatsis, M. (1996) Preferentially oriented submicron silicalite membranes. *AIChE J.*, *42*: 3020–3029.
337. Morooka S.; Kuroda, T.; Kusakabe, K. (1998) Carbon dioxide separation from nitrogen using Y-type zeolite membranes. *Stud. Surf. Sci. Cat.*, *114*: 665–668.
338. Cooper, C.A.; Lin, Y.S. (2002) Microstructural and gas separation properties of CVD modified mesoporous gamma-alumina membranes. *J. Mem. Sci.*, *195*: 35–50.
339. Tsai, C.Y.; Tam, S.Y.; Lu, Y.F. (2000) Dual-layer asymmetric microporous silica membranes. *J. Mem. Sci.*, *169*: 255–268.
340. de Vos, R.M.; Maier, W.F.; Verwei, H. (1999) Hydrophobic silica membranes for gas separation. *J. Mem. Sci.*, *158*: 277–288.
341. de Vos, R.M.; Verweij, H. (1998) High-selectivity, high-flux silica membranes for gas separation. *Science*, *279*: 1710–1711.
342. de Vos, R.M.; Verweij, H. (1998) Improved performance of silica membranes for gas separation. *J. Mem. Sci.*, *143*: 37–51.
343. Sircar, S.; Rao, M.B.; Thaeron, C.M.A. (1999) Selective surface flow membrane for gas separation. *Sep. Sci. Technol.*, *34*: 2081–2093.
344. Sircar, S.; Waldron, W.E.; Rao, M.B. (1999) Hydrogen production by hybrid SMR-PSA-SSF membrane system. *Sep. Purif. Technol.*, *17*: 11–20.
345. Sircar, S.; Golden, T.C.; Rao, M.B. (1996) Activated carbon for gas separation and storage. *Carbon*, *34*: 1–12.

346. Thaeron, C.; Parrillo, D.J.; Sircar, S. (1999) Separation of hydrogen sulfide-methane mixtures by selective surface flow membrane. *Sep. Purif. Technol.*, *15*: 121–129.
347. Parrillo, D.J.; Thaeron, C.; Sircar, S. (1997) Separation of bulk hydrogen sulfide hydrogen mixtures by selective surface flow membrane. *AIChE J.*, *43*: 2239–2245.
348. Naheiri, T.; Ludwig, K.A.; Anand, M. (1997) Scale-up of selective surface flow membrane for gas separation. *Sep. Sci. Technol.*, *32*: 1589–1602.
349. Anand, M.; Langsam, M.; Rao, M.B. (1997) Multicomponent gas separation by selective surface flow (SSF) and poly-trimethylsilylpropyne (PTMSP) membranes. *J. Mem. Sci.*, *123*: 17–25.
350. Rao, M.B.; Sircar, S. (1996) Performance and pore characterization of nanoporous carbon membranes for gas separation. *J. Mem. Sci.*, *110*: 109–118.
351. Rao, M.B.; Sircar, S.; Abrardo, J.M.; Baade, W. F. (1994) Hydrogen recovery by adsorbent membranes. *Eur. Pat. Appl.*, EP582184.
352. Singh, R.P.; Way, J.D.; McCarley, K.C. (2004) Development of a model surface flow membrane by modification of porous vycor glass with a fluorosilane. *Ind. Eng. Chem. Res.*, *43*: 3033–3040.
353. Cui, Y.; Kita, H.; Okamoto, K.I. (2004) Zeolite T membrane: preparation, characterization, pervaporation of water/organic liquid mixtures and acid stability. *J. Mem. Sci.*, *236*: 17–27.
354. Cui, Y.; Kita, H.; Okamoto, K.I. (2004) Preparation and gas separation performance of zeolite T membrane. *J. Mater. Chem.*, *14*: 924–932.
355. Cui, Y.; Kita, H.; Okamoto, K.I. (2003) Preparation and gas separation properties of zeolite T membrane. *Chem. Comm.*, *17*: 2154–2155.
356. Tomita, T.; Nakayama, K.; Sakai, H. (2004) Gas separation characteristics of DDR type zeolite membrane. *Micropor. Mesopor. Mater.*, *68*: 71–75.
357. Centeno, T.A.; Vilas, J.L.; Fuertes, A.B. (2004) Effects of phenolic resin pyrolysis conditions on carbon membrane performance for gas separation. *J. Mem., Sci.*, *228*: 45–54.
358. Kalipcilar, H.; Bowen, T.C.; Noble, R.D. (2002) Synthesis and separation performance of SSZ-13 zeolite membranes on tubular supports. *Chem. Mater.*, *14*: 3458–3464.
359. McCarley, K.C.; Way, J.D. (2001) Development of a model surface flow membrane by modification of porous gamma-alumina with octadecyltrichlorosilane. *Sep. Purif. Technol.*, *25*: 195–210.
360. Robeson, L.M. (1991) Correlation of separation factor versus permeability for polymeric membranes. *J. Mem Sci.*, *62*: 165–185.
361. Kim, D.S.; Park, H.B.; Rhim, J.W. (2004) Preparation and characterization of crosslinked PVA/SiO2 hybrid membranes containing sulfonic acid groups for direct methanol fuel cell applications. *J. Mem. Sci.*, *240*: 37–48.
362. Kim, D.S.; Park, H.B.; Lee, Y.M. (2004) Preparation and characterization of PVDF/silica hybrid membranes containing sulfonic acid groups. *J. Appl. Polym. Sci.*, *93*: 209–218.

363. Kim, H.; Lim, C.; Hong, S.I. (2005) Gas permeation properties of organic-inorganic hybrid membranes prepared from hydroxyl-terminated polyether and 3-isocyanatopropyltriethoxysilane. *J. Sol-Gel Sci. Technol.*, *36*: 213–221.
364. Jose, N.M.; Prado, L.A.S.A.; Yoshida, I.V.P. (2004) Synthesis, characterization, and permeability evaluation of hybrid organic-inorganic films. *J. Polym. Sci. B Polym. Phys.*, *42*: 4281–4292.
365. Lum, D.S.; Shin, K.H.; Park, H.B. (2004) Preparation and characterization of sulfonated poly(phthalazinone ether sulfone ketone) (SPPESK)/Silica hybrid membranes for direct methanol fuel cell applications. *Macrom. Res.*, *12*: 413–421.
366. Dvornic, P.R.; Li, J.M.; de Leuze-Jallouli, A.M. (2002) Nanostructured dendrimer-based networks with hydrophilic polyamidoamine and hydrophobic organosilicon domains. *Macromol.*, *35*: 9323–9333.
367. West, G.D.; Diamond, G.G.; Holland, D. (2002) Gas transport mechanisms through sol-gel derived templated membranes. *J. Mem. Sci.*, *203*: 53–69.
368. Cornelius, C.J.; Marand, E. (2002) Hybrid silica-polyimide composite membranes: gas transport properties. *J. Mem. Sci.*, *202*: 97–118.
369. Cornelius, C.J.; Marand, E. (2002) Hybrid inorganic-organic materials based on a 6FDA-6FpDA-DABA polyimide and silica: physical characterization studies. *Polymer*, *43*: 2385–2400.
370. Cornelius, C., Hibshman, C.; Marand, E. (2001) Hybrid organic-inorganic membranes. *Sep. Purif. Technol.*, *25*: 181–193.
371. Chujo, Y.; Tamaki, R. (2001) New preparation methods for organic-inorganic polymer hybrids. *MRS Bull.*, *26*: 389–392.
372. Ruckenstein, E.; Yin, W.S. (2000) SiO_2-poly(amidoamine) dendrimer inorganic/organic hybrids. *J. Polym. Sci. A Polym. Chem.*, *38*: 1443–1449.
373. Joly, C.; Smaihi, M.; Porcar, L. (1999) Polyimide-silica composite materials: How does silica influence their microstructure and gas permeation properties?. *Chem. Mater.*, *11*: 2331–2338.
374. Joly, C.; Goizet, S.; Schrotter, J.C. (1997) Sol-gel polyimide-silica composite membrane: gas transport properties. *J. Mem. Sci.*, *130*: 63–74.
375. Tamaki, R.; Chujo, Y. (1998) Synthesis of poly(vinyl alcohol) silica gel polymer hybrids by in-situ hydrolysis method. *Appl. Organmet. Chem.*, *12*: 755–762.
376. Tamaki, R.; Naka, K.; Chujo, Y. (1998) Synthesis of poly(N,N-dimethylacrylamide) silica gel polymer hybrids by in situ polymerization method. *Polym. J.*, *30*: 60–65.
377. Smaihi, M.; Schrotter, J.C.; Lesimple, C. (1999) Gas separation properties of hybrid imide-siloxane copolymers with various silica contents. *J. Mem. Sci.*, *161*: 157–170.
378. Smaihi, M.; Jermoumi, T.; Marignan, J. (1996) Organic-inorganic gas separation membranes: Preparation and characterization. *J. Mem. Sci.*, *116*: 211–220.
379. Nunes, S.P.; Peinemann, K.V.; Ohlrogge, K. (1999) Membranes of poly(ether imide) and nanodispersed silica. *J. Mem. Sci.*, *157*: 219–226.

380. Matejka, L.; Plestil, J.; Dusek, K. (1998) Structure evolution in epoxy-silica hybrids: sol-gel process. *J. Non-Cryst. Sol.*, *226*: 114–121.
381. McCarthy, D.W.; Mark, J.E.; Schaefer, D.W. (1998) Synthesis, structure, and properties of hybrid organic-inorganic composites based on polysiloxanes. I. Poly(dimethylsiloxane) elastomers containing silica. *J. Polym. Sci. B Polym. Phys.*, *36*: 1167–1189.
382. Naito, M.; Nakahira, K.; Fukuda, Y. (1997) Process conditions on the preparation of supported microporous SiO_2 membranes by sol-gel modification techniques. *J. Mem. Sci.*, *129*: 263–269.
383. Moaddeb, M.; Koros, W.J. (1997) Gas transport properties of thin polymeric membranes in the presence of silicon dioxide particles. *J. Mem. Sci.*, *125*: 143–163.
384. Moaddeb, M.; Koros, W.J. (1996) Effects of colloidal silica incorporation on oxygen nitrogen separation properties of ceramic-supported 6FDA-IPDA thin films. *J. Mem. Sci.*, *111*: 283–290.
385. Kusakabe, K.; Ichiki, K.; Hayashi, J. (1996) Preparation and characterization of silica-polyimide composite membranes coated on porous tubes for CO_2 separation. *J. Mem. Sci.*, *115*: 65–75.
386. Raman, N.K.; Brinker, C.J. (1995) Organic template approach to molecular-sieving silica membranes. *J. Mem. Sci.*, *105*: 273–279.
387. Huang, H.H.; Orler, B.; Wilkees, G.L. (1987) Structure property behavior of new hybrid materials incorporating oligomeric species into sol-gel glasses. 3. Effect of acid content, tetraethoxysilane content, and molecular-weight of poly(dimethylsiloxane). *Macromol.*, *20*: 1322–1330.
388. Hu, Q.; Marand, E.; Dhingra, S. (1997) Poly(amide-imide)/TiO_2 nanocomposite gas separation membranes: Fabrication and characterization. *J. Mem. Sci.*, *135*: 65–79.
389. Moore, T.T.; Mahajan, R.; Vu, D.Q. (2004) Hybrid membrane materials comprising organic polymers with rigid dispersed phases. *AIChE J.*, *50*: 311–321.
390. Vu., D.; Koros, W.J.; Miller, S.J. (2003) Effect of condensable impurity in CO_2/CH_4 gas feeds on performance of mixed matrix membranes using carbon molecular sieves. *J. Mem. Sci.*, *221*: 233–239.
391. Vu, D.Q.; Koros, W.J.; Miller, S.J. (2003) Mixed matrix membranes using carbon molecular sieves-I. Preparation and experimental results. *J. Mem. Sci.*, *211*: 311–334.
392. Vu, D.Q.; Koros, W.J.; Miller, S.J. (2003) Mixed matrix membranes using carbon molecular sieves-II. Modeling permeation behavior. *J. Mem. Sci.*, *211*: 335–348.
393. Anson, M.; Marchese, J.; Garis, E. (2004) ABS copolymer-activated carbon mixed matrix membranes for CO_2/CH_4 separation. *J. Mem. Sci.*, *243*: 19–28.
394. Mahajan, R.; Burns, R.; Schaeffer, M. (2002) Challenges in forming successful mixed matrix membranes with rigid polymeric materials. *J. Appl. Polym. Sci.*, *86*: 881–890.
395. Mahajan, R.; Koros, W.J. (2000) Factors controlling successful formation of mixed-matrix gas separation materials. *Ind. Eng. Chem. Res.*, *39*: 2692–2696.

396. Kulprathipanja, S. (2003) Mixed matrix membrane development. *Ann. NY Acad. Sci.*, *984*: 361–369.
397. Kulprathipanja, S.; Neuzil, R.W.; Li, N.N. Separation of gases by means of mixed matrix membranes. USP 5,127,925, 1992.
398. Kulprathipanja, S.; Neuzil, R.W.; Li, N.N. Gas separation by means of mixed matrix membranes. USP 4,740,219, 1988.
399. Vankelecom, I.F.J.; VandenBroeck, S.; Merckx, E. (1996) Silylation to improve incorporation of zeolites in polyimide films. *J. Phys. Chem.*, *100*: 3753–3758.
400. Vankelecom, I.F.J.; Merckx, E.; Luts, M. (1995) Incorporation of zeolites in polyimide membranes. *J. Phys. Chem.*, *99*: 13187–13192.
401. Duval, J.M.; Kemperman, A.J.B.; Folkers, B. (1994) Preparation of zeolite filled glassy polymer membranes. *J. Appl. Polym. Sci.*, *54*: 409–418.
402. Duval, J.M.; Folkers, B.; Mulder, M.H.V. (1993) Adsorbent filled membranes for gas separation. 1. Improvement of the gas separation properties of polymeric membranes by incorporation of microporous adsorbents. *J. Mem. Sci.*, *80*: 189–198.
403. Suer, M.G.; Bac, N.; Yilmaz, L. (1994) Gas permeation characteristics of polymer-zeolite mixed matrix membranes. *J. Mem. Sci.*, *91*: 77–86.
404. Jia, M.D.; Peinemann, K.V.; Behling, R.D. (1994) Ceramic zeolite composite membranes-preparation, characterization and gas permeation. *J. Mem. Sci.*, *82*: 15–26.
405. Jia, M.D.; Peinemann, K.V.; Behling, R.D. (1992) Preparation and characterization of thin-film zeolite pdms composite membranes. *J. Mem. Sci.*, *73*: 119–128.
406. Jia, M.D.; Peinemann, K.V.; Behling, R.D. (1991) Molecular-sieving effect of the zeolite-filled silicone-rubber membranes in gas permeation. *J. Mem. Sci.*, *57*: 289–296.
407. Paul, D.R.; Kemp, D.R. (1973) The diffusion time lag in polymer membranes containing adsorptive fillers. *J. Polym Sci.*, *41*: 79–93.
408. Berry, M.B.; Libby, B.E.; Rose, K. (2000) Incorporation of zeolites into composite matrices. *Micropor. Mesopor. Mater.*, *39*: 205–217.
409. Gur, T.M. (1994) Permselectivity of zeolite filled polysulfone gas separation membranes. *J. Mem. Sci.*, *93*: 283–289.
410. Landry, C.J.T.; Coltrain, B.K.; Teegarden, D.M. (1996) Use of organic copolymers as compatibilizers for organic-inorganic composites. *Macromol.*, *29*: 4712–4721.
411. Zimmerman, C.M.; Singh, A.; Koros, W.J. (1997) Tailoring mixed matrix composite membranes for gas separations. *J. Mem. Sci.*, *137*: 145–154.
412. Rong, M.Z.; Zhang, M.Q.; Zheng, Y.X. (2001) Structure-property relationships of irradiation grafted nano-inorganic particle filled polypropylene composites. *Polymer*, *42*: 167–183.
413. Nunes, S.P.; Schultz, J.; Peinemann, K.V. (1996) Silicone membranes with silica nanoparticles. *J. Mater. Sci. Lett.*, *15*: 1139–1141.
414. Zhang, Q.; Cussler, E.L. (1985) Microporous hollow fibers for gas-absorption 1. Mass-transfer in the liquid. *J. Mem Sci.*, *23*: 321–332.

415. Zhang, Q.; Cussler, E.L. (1985) Microporous hollow fibers for gas-absorption 2. Mass-transfer across the membrane. *J. Mem Sci.*, *23*: 333–345.
416. Dindore, V.Y.; Brilman, D.W.F.; Versteeg, G.F. (2005) Modelling of cross-flow membrane contactors: physical mass transfer processes. *J. Mem. Sci.*, *251*: 209–222.
417. Dindore, V.Y.; Brilman, D.W.F.; Versteeg, G.F. (2005) Modelling of cross-flow membrane contactors: physical mass transfer processes. *J. Mem. Sci.*, *251*: 275–289.
418. Hoff, K.A.; Juliussen, O.; Falk-Pedersen, O. (2004) Modeling and experimental study of carbon dioxide absorption in aqueous alkanolamine solutions using a membrane contactor. *Ind. Eng. Chem. Res.*, *43*: 4908–4921.
419. Klaassen, R.; Jansen. A.E. (2001) The membrane contactor: Environmental applications and possibilities. *Environ. Prog.*, *20*: 37–43.
420. Klaassen, R.; Feron, P.H.M.; Jansen, A.E. (2005) Membrane contactors in industrial applications. *Chem. Eng. Res. Des.*, *83*: 234–246.
421. Dindore, V.Y.; Brilman, D.W.F.; Versteeg, G.E. (2005) Hollow fiber membrane contactor as a gas-liquid model contactor. *Chem. Eng. Sci.*, *60*: 467–479.
422. Dindore, V.Y.; Brilman, D.W.F.; Feron, P.H.M. (2004) CO_2 absorption at elevated pressures using a hollow fiber membrane contactor. *J. Mem. Sci.*, *235*: 99–109.
423. Kumar, P.S.; Hogendorn, J.A.; Feron, P.H.M. (2003) Approximate solution to predict the enhancement factor for the reactive absorption of a gas in a liquid flowing through a microporous membrane hollow fiber. *J. Mem. Sci.*, *213*: 231–245.
424. Kumar, P.S.; Hogendoorn, J.A.; Feron, P.H.M. (2002) New absorption liquids for the removal of CO_2 from dilute gas streams using membrane contactors. *Chem. Eng. Sci.*, *57*: 1639–1651.
425. Drioli, E.; Curcio, E.; Di Profio, G. (2005) State of the art and recent progresses in membrane contactors. *Chem. Eng. Res. Des.*, *83*: 223–233.
426. Bocquet, S.; Torres, A.; Sanchez, J. (2005) Modeling the mass transfer in solvent-extraction processes with hollow-fiber membranes. *AIChE J.*, *51*: 1067–1079.
427. Bothun, G.D.; Knutson, B.L.; Strobel, H.J. (2003) Mass transfer in hollow fiber membrane contactor extraction using compressed solvents. *J. Mem. Sci.*, *227*: 183–196.
428. Bothun, G.D.; Knutson, B.L.; Strobel, H.J. (2003) Compressed solvents for the extraction of fermentation products within a hollow fiber membrane contactor. *J. Supercrit. Fluids*, *25*: 119–134.
429. Dindore, V.Y.; Versteeg, G.F. (2005) Gas-liquid mass transfer in a cross-flow hollow fiber module: Analytical model and experimental validation. *Inter. J. Heat Mass Trans.*, *48*: 3352–3362.
430. Feron, P.H.M.; Jansen, A.E. (2002) CO_2 separation with polyolefin membrane contactors and dedicated absorption liquids: performances and prospects. *Sep. Purif. Technol.*, *27*: 231–242.
431. Gabelman, A.; Hwang, S.T.; Krantz, W.B. (2005) Dense gas extraction using a hollow fiber membrane contactor: experimental results versus model predictions. *J. Mem. Sci.*, *257*: 11–36.

432. Kang, M.S.; Moon, S.H.; Park, Y.I.; Lee, K.H. (2002) Development of carbon dioxide separation process using continuous hollow-fiber membrane contactor and water-splitting electrodialysis. *Separation Science and Technology*, *37*: 1789–1806.
433. Korikov, A.P.; Sirkar, K.K. (2005) Membrane gas permeance in gas-liquid membrane contactor systems for solutions containing a highly reactive absorbent. *J. Mem. Sci.*, *246*: 27–37.
434. Kosaraju, P.; Kovvali, A.S.; Korikov, A. (2005) Hollow fiber membrane contactor based CO2 absorption-stripping using novel solvents and membranes. *Ind. Eng. Chem. Res.*, *44*: 1250–1258.
435. Lu, J.G.; Wang, L.J.; Sun, X.Y. (2005) Absorption of CO_2 into aqueous solutions of methyldiethanolamine and activated methyldiethanolamine from a gas mixture in a hollow fiber contactor. *Ind. Eng. Chem. Res.*, *44*: 9230–9238.
436. Mavroudi, M.; Kaldis, S.P.; Sakellaropoulos, G.P. (2003) Reduction of CO_2 emissions by a membrane contacting process. *Fuel*, *82*: 2153–2159.
437. Nishikawa, N.; Ishibashi, M.; Ohta, H.; Akutsu, N.; Matsumoto, H.; Kanata, T.; Kitamura, H. (1995) CO_2 removal by hollow-fiber gas-liquid contactor. *Energy Conversion and Management*, *36*: 415–418.
438. Wang, R.; Zhang, H.Y.; Feron, P.H.M. (2005) Influence of membrane wetting on CO_2 capture in microporous hollow fiber membrane contactors. *Sep. Purif. Tech.*, *46*: 33–40.
439. Wang, R.; Li, D.F.; Liang, D.T. (2004) Modeling of CO_2 capture by three typical amine solutions in hollow fiber membrane contactors. *Chem. Eng. Process.*, *43*: 849–856.
440. Wang, R.; Li, D.F.; Zhou, C. (2004) Impact of DEA solutions with and without CO_2 loading on porous polypropylene membranes intended for use as contactors. *J. Mem. Sci.*, *229*: 147–157.
441. Yeon, S.H.; Lee, K.S.; Sea, B. (2005) Application of pilot-scale membrane contactor hybrid system for removal of carbon dioxide from flue gas. *J. Mem. Sci.*, *257*: 156–160.
442. Yeon, S.H.; Sea, B.; Park, Y.I. (2004) Absorption of carbon dioxide characterized by using the absorbent composed of piperazine and triethanolamine. *Sep. Sci. Technol.*, *39*: 3281–3300.
443. Yeon, S.H.; Sea, B.; Park, Y.I. (2003) Determination of mass transfer rates in PVDF and PTFE hollow fiber membranes for CO_2 absorption. *Sep. Sci. Technol.*, *38*: 271–293.
444. Zheng, J.M.; Xu, Y.Y.; Xu, Z.K. (2003) Shell side mass transfer characteristics in a parallel flow hollow fiber membrane module. *Sep. Sci. Technol.*, *38*: 1247–1267.
445. Li, J.L.; Chen, B.H. (2005) Review of CO_2 absorption using chemical solvents in hollow fiber membrane contactors. *Sep. Purif. Tech.*, *41*: 109–122.
446. EPA. (1997) *AP 42, Compilation of Air Pollutant Emission Factors, Vol. 1: Stationary Point and Area Sources.* 5th Ed. (http://www.epa.gov/ttn/chief/ap42/).

447. Nolan, P.S. (2000) Flue gas desulfurization technologies for coal-fired power plants,'' presented at the Coal Tech 2000 International Conference, Jakarta, Indonesia.
448. Alpert, S.B. (1991) Clean coal technology and advanced coal-based power plants. *Ann. Rev. Energy Environ.*, *16*: 1–23.
449. DOE. (2002) Inventory of Electric Utility Power Plants in the United States 2000, DOE/EIA-0095.
450. Merichem, *Cleaning Up the Gasification Gas* (http://www.gtp-merichem.com/news/releases/syngas.php).
451. NETL, (1998), *Destec Gasifier IGCC Base Cases*, PED-IGCC-98–003 (http://www.netl.doe.gov/technologies/coalpower/gasification/pubs/system-studies.html).
452. Bohm, M.C. (2006) Capture-ready power plants - Options, technologies and economics, Mark C, MS Thesis, Massachusetts Institute of Technology. (http://sequestration.mit.edu/pdf/Mark_Bohm_Thesis.pdf).
453. Platts, M. The coke oven by-product plant, American Iron and Steel Institute. (http://www.energymanagertraining.com/iron_steel/coke_oven_steel.htm).
454. Freitag, D.W.; Richerson, D.W. (1998) Opportunities for advanced ceramics to meet the needs of the industries of the future, DOE report DOE/ORO 2076.
455. Division of Pollution Prevention and Environmental Assistance, Primary Metals (http://www.p2pays.org/ref/01/text/00778/chapter1.htm).
456. Metallurgical Society, Virtual Tour (http://www.metsoc.org/virtualtour/default.asp).
457. Green Island Cement Holding limited site, Cement Process (http://www.gich.com.hk/Facilities/f_main.htm).
458. Worrell, E.; Price, L.; Martin, N.; Hendriks, C.; Meida, L.O. (2001) Carbon dioxide emissions from the global cement industry. *Annu. Rev. Energy Environ.*, *26*: 303–329.
459. Riter, J.A.; Ebner, A.D. (2007) State-of-the-art adsorption and membrane separation processes for hydrogen production in the chemical and petrochemical industries. *Sep. Sci. Tech.*, *42*: 1123–1193.
460. Pletcher, D.; Walsh, F.C. (1995) *Industrial Eletrochemistry,* 2nd Ed., Chapman and Hall, London.
461. Bruno, M.J. Aluminum Carbothermic Technology, DOE report Cooperative Agreement Number DE-FC36–00ID13900 (http://www.osti.gov/bridge/servlets/purl/838679-h1h8sh/838679.PDF).
462. EPA. (2000) Associated waste report, dehydration and sweetening wastes.
463. Ortloff Engineers Limited, Sulfur Recovery Process Information, http://www.ortloff.com/sulfur/sulfinfo.htm
464. EPA, Landfill Methane Outreach Program (LMOP). (http://www.epa.gov/landfill/overview.htm).
465. EPA, Coalbed Methane Outreach Program, (http://www.epa.gov/cmop/).
466. American Coalition for Ethanol. How is Ethanol Made? (http://www.ethanol.org/howethanol.html).

467. Hydrocarbon Processing: Gas Processes 2004 and Petrochemical Processes 2003, Gulf Publishing Co.
468. *Fuel Science and Technology Handbook*, (1998) 2nd edition. Speight JG Ed., Marcel Dekker, New York, Chapters 35 and 36.
469. Kohl, A.; Riesenfeld, F. (1985) *Gas Purification,* 4th edition, Gulf Publishing Company, Houston.
470. Rameshni, P. (2000) *State of the Art in Gas Treating*, Parsons Energy & Chemical Group, Inc. San Francisco.
471. Suzuki, T.; Sakoda, A.; Suzuki, M.; Izumi, J. (1997) Recovery of carbon dioxide from stack gas by piston-driven ultra-rapid PSA. *J. Chem. Eng. Japan*, *30*: 1026–1033.
472. Gomes, V.G.; Yee, K.W.K. (2002) Pressure swing adsorption for carbon dioxide sequestration from exhaust gases. *Separation and Purification Technology*, *28*: 161–171.
473. Ko, D.; Siriwardane, R.; Biegler, L.T. (2003) Optimization of a pressure swing adsorption process using zeolite 13X for CO_2 sequestration. *Ind. Eng. Chem. Res.*, *42*: 339–348.
474. Ko, D.; Siriwardane, R.; Biegler, L.T. (2005) Optimization of pressure swing adsorption and fractionated vacuum pressure swing adsorption processes for CO_2 capture. *Ind. Eng. Chem. Res.*, *44*: 8084–8094.
475. Na, B.-K.; Koo, K.-K.; Eum, H.-M.; Lee, H.; Song, H.-K. (2001) CO_2 recovery from flue gas by PSA process using activated carbon. *Korean J. Chem. Eng.*, *18*: 220–227.
476. Na, B.-K.; Lee, H.; Koo, K.-K.; Song, H.K. (2002) Effect of rinse and recycle methods on the pressure swing adsorption process to recover CO_2 from power plant flue gas using activated carbon. *Ind. Eng. Chem. Res.*, *41*: 5498–5503.
477. Choi, W.-K.; Kwon, T.-I.; Yeo, Y.-K.; Lee, H.; Song, H.-K.; Na, B.-K. (2003) Optimal operation of the pressure swing adsorption (PSA) process for CO_2 recovery. *Korean J. Chem. Eng.*, *20*: 617–623.
478. Chue, K.T.; Kim, J.N.; Yoo, Y.J.; Cho, S.H.; Yang, R.T. (1995) Comparison of activated carbon and zeolite 13X for CO_2 adsorption recovery from flue gas by pressure swing adsorption. *Ind. Eng. Chem. Res.*, *34*: 591–598.
479. Kikkinides, E.S.; Yang, R.T.; Cho, S.H. (1993) Concentration and recovery of CO_2 from flue gas by pressure swing adsorption. *Ind. Eng. Chem. Res.*, *32*: 2714–2720.
480. Chou, C.T.; Chen, C.Y. (2004) Carbon dioxide recovery by vacuum swing adsorption. Separ. *Purif. Technol.*, *39*: 51–65.
481. Rao, M.B.; Sircar, S.; Golden, T.C. (2001) Gas separation by adsorbent membranes. European Patent, EP0428052.
482. Syrtsova, D.A.; Kharitonov, A.P.; Teplyakov, V.V. (2004) Improving gas separation properties of polymeric membranes based on glassy polymers by gas phase fluorination. *Desal.*, *163*: 273–279.
483. Glugla, P.G.; Rickle, G.K.; Smith, B.L.; Bales, S.E. Interfacially polymerized polyester films for gas separation membranes and preparation thereof. USP 5,650,479, 1997.

484. Marek, M.; Brynda, E.; Pientka, Z. (1998) Gas separation properties of ultra-thin films based on fully cyclized polyimides. *Macrom. Rapid Comm.*, *19*: 53–57.
485. Pinnau, I.; Toy, L.G. (1996) Gas and vapor transport properties of amorphous perfluorinated copolymer membranes based on 2,2-bistrifluoromethyl-4,5-difluoro-1,3-dioxole/tetrafluoroethylene. *J. Mem. Sci.*, *109*: 125–133.
486. Yoshioka, T.; Nakanishi, E.; Tsuru, T. (2001) Experimental studies of gas permeation through microporous silica membranes. *AIChE J.*, *47*: 2052–2063.